Retrospective Theses and Dissertations

Iowa State University Capstones, Theses and Dissertations

1994

Emissions and combustion of fatty acid esters of soybean oil in a diesel engine

Yu Zhang
Iowa State University

Recommended Citation

Emissions and combustion of fatty acid esters of soybean oil in a diesel engine

by

Yu Zhang

A Thesis Submitted to the

Graduate Faculty in Partial Fulfillment of the

Requirements for the Degree of

MASTER OF SCIENCE

Department: Mechanical Engineering
Major: Mechanical Engineering

Iowa State University
Ames, Iowa

1994

TABLE OF CONTENTS

LIST OF FIGURES

LIST OF TABLES

1. INTRODUCTION

Internal combustion engines have undergone more than a century of development since Nicolaus A. Otto invented the first spark-ignition engine in 1876 and the German engineer Rudolf Diesel introduced the compression-ignition engine in 1892. Now, both types of engine play a dominant role in the field of energy conversion. The last 30 years have seen an explosive growth in engine research and development as the issues of air pollution, fuel cost and world-wide market competitiveness have become increasingly important. Based on its superiority in fuel economy and its low emissions of unburned hydrocarbons and carbon monoxide, the diesel engine has been a popular choice for heavy and medium-duty applications. However, due to decreasing petroleum reserves, unstable foreign supplies of petroleum, and the environmental consequences of exhaust products from internal combustion engines, a major thrust to develop alternate energy sources has become increasingly important.

Diesel engines usually exhaust much larger amounts of particulate matter (PM) than spark-ignition engines. About 90% of diesel particulate is in the size range from 0.0075 to 1.0 μm [1] and has a significant potential health impact due to the ability of particles to be inhaled and eventually trapped in the bronchial passages and alveoli of the lungs.

Over the past years, the Environmental Protection Agency (EPA) has issued more and more stringent diesel engine emission standards. Table 1.1 shows the EPA heavy-duty vehicle emission standards from 1988 to 1998 [2].

A number of studies have shown that organic seed oils, such as soybean, sunflower, peanut and their alkyl esters (called biodiesel), hold promise as fuel alternatives for diesel engines. The primary incentive for using biodiesel is that it is a nontoxic, biodegradable and renewable fuel that reduces the emission of harmful pollutants. Two areas where biodiesel has significant advantages over petroleum-based diesel fuel are its high cetane number and its particulate reduction potential.

Table 1.1   EPA heavy-duty diesel exhaust emission standards (GVW>8500 lbs)

Model year	Emissions (g/bhp-hr)			
	HC	NOx	Particulate	CO
1988	1.3	10.7	0.60	15.5
1991	1.3	6.0	0.25	15.5
1994	1.3	5.0	0.10[a]	15.5
1998	1.3	4.0	0.10	15.5

[a]Starting in 1996, new urban buses must have 0.05 g/bhp-hr
particulate emission standard.

One serious limitation to the use of vegetable oils and their esters as fuels is their high crystallization temperature. Many of the oils and esters will solidify at temperatures as high as -1.1 °C to 4.5 °C. One solution to this problem may be the use of iso-propyl esters instead of the more common methyl and ethyl esters. The chain branching of the iso-propyl ester has been shown to reduce the crystallization temperature of soybean oil ester by 11 °C compared with methyl ester [3].

A number of diesel emissions studies have been conducted with blends of methyl and ethyl esters of vegetable oils with diesel fuel. However, no data for the iso-propyl ester of vegetable oils has been found. The objective of this work was to test fuels with different blends of methyl and iso-propyl esters of soybean oil in No.2 diesel fuel, and to compare their emission levels with No.2 diesel fuel. This study also measured the emission level of a methyl ester of soybean oil that was treated using a special technique called "winterization" to provide better cold flow properties.

The major tasks for this project were:

1. Comparison of the emission levels of different blends of methyl and iso-propyl ester of soybean oil and No.2 diesel fuel with under steady state conditions.

2. Determining the proportion of solid carbon and soluble organic fraction in the particulates of the different fuel blends.

3. Performing heat release analysis based on measured cylinder pressure data to investigate the combustion phenomena of methyl and iso-propyl esters of soybean oil.

This thesis includes a literature review of diesel engine combustion and emissions and the properties of fuels produced from the esters of vegetable oils. The experimental set-up and test procedures also are discussed. Finally, the experimental results and conclusions will be presented.

2.   LITERATURE   REVIEW

In this chapter, diesel engine combustion and emission processes are described. This is followed by a discussion of renewable fuels and their emissions.

2.1   Combustion Processes in Diesel Engines

The combustion process in a diesel engine is an extremely complex phenomenon. It is an unsteady, heterogeneous, three-dimensional combustion process. It depends on many factors, such as the design of the engine's combustion chamber and fuel-injection system, the engine's operating conditions, and the characteristics of the fuel.

Combustion in a diesel engine proceeds in phases which involve both physical and chemical processes. Near the end of the compression stroke, liquid fuel is injected at high velocity into high temperature compressed air. The fuel breaks up into fine droplets, vaporizes, mixes with the high temperature and high pressure turbulent air and begins to undergo chemical reactions. There is a time period, called the ignition delay, during which the fuel undergoes heating, vaporization, mixing and pre-combustion reactions. After the delay period, usually a few degrees of crank rotation, spontaneous ignition will occur at regions where the mixture fuel-air ratio is close to stoichiometric. Because there are many locations in the mixture that are close to autoignition, when it finally occurs, the pressure and temperature in cylinder increase rapidly. The uncontrolled combustion and rapid pressure rise depend on the amount of fuel present in the combustion chamber, which in turn will be influenced by the length of the ignition delay and the amount of fuel injected during the delay period. The resulting compression of the unburned portion of the fuel-air mixture shortens the delay for that mixture. After the fuel and air which were mixed during the ignition delay have been consumed, the combustion rate is controlled by the rate at which the fuel mixes with the air. The heat-release rate may or may not reach a second peak in this phase.

Finally, the combustion will enter the final phase. The small fraction of fuel that has not

burned due to nonuniform mixing can continue to burn during expansion, but the final burn-out processes become slower as the gas temperature falls [4,5].

2.2   Diesel Engine Emissions

About 65 to 85% percent of engine emissions are associated with the engine exhaust gases. These pollutants are oxides of nitrogen (NO_x), carbon monoxide (CO), unburned hydrocarbons (HC), particulate matter (PM) which includes soot, or solid carbon, sulfates, condensed hydrocarbons, called the soluble organic fraction (SOF), and traces of alcohols, aldehydes, ketones, phenols, acids, esters, and ethers. The crankcase breather and fuel tank breather are the sources for the remainder of the engine emissions.

Although NO is the dominant oxide of nitrogen formed within the cylinder, most NO is converted to NO_2 in the atmosphere. The formation of NO is complex since it is dependent on a series of reactions, such as:

$$O_2 \Longleftrightarrow 2O$$

$$O + N_2 \Longleftrightarrow NO + N$$

$$N + O_2 \Longleftrightarrow NO + O$$

$$N + OH \Longleftrightarrow NO + H$$
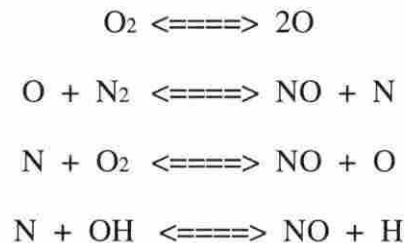
Most NO is formed by an endothermic reaction in the burned-gas regions of the cylinder. Chemical kinetics calculations show that formation of NO increases very strongly with increasing flame temperature. These calculations show that the highest concentration of NO is obtained for slightly lean mixtures and rapid combustion as these conditions combine the availability of oxygen with the highest flame temperature. Thus, the amount of NO in exhaust gas is sensitive to injection timing, the amount of suitable combustion fuel-air mixture and the rate of combustion. During the expansion stroke, the decreasing gas temperature freezes the reactions so that the concentrations that leave the engine are much higher than the equilibrium concentrations corresponding to the exhaust temperature. NO formation is also influenced by the flame speed. NO emissions tend to increase with reduced engine

speed [4, 5]. Some properties of the fuel will also have effects on the formation of NO, such as kinematic viscosity, cetane number and aromatic content [6, 7]. Moreover, because vegetable oils and their alcohol esters have oxygen atoms in their molecular structure, the emission of NO will generally to be higher than that from diesel fuel [8, 9].

Carbon monoxide (CO) emission is controlled primarily by the fuel/air ratio. Carbon monoxide production is greatest with fuel-rich mixtures, as there will be incomplete combustion. With lean mixtures, CO is always present due to dissociation, but the concentration decreases with reducing combustion temperature. Because diesel engines always operate well on the lean side of stoichometric, CO emission is always very low [4].

Unburned hydrocarbons are a consequence of incomplete combustion of the hydrocarbon fuel. Fuel composition can significantly influence the composition and magnitude of the organic emissions. Fuels containing high proportions of aromatics and olefins produce relatively higher concentrations of reactive hydrocarbons. Usually, there are two major causes of HC emissions from diesel engines under normal operating conditions: fuel mixed leaner than the lean combustion limit during the delay period; and under mixing of fuel which leaves the fuel injector nozzle at low velocity, late in the combustion process [4, 5, 10].

Particulate matter is defined by the Environmental Protection Agency (EPA) as any diesel exhaust substance that can be collected by filtering the diluted exhaust at or below 325 K [11]. Particulates consist principally of combustion generated carbonaceous material or soot. On their surfaces, some liquid phase emissions are adsorbed which are organic compounds (called soluble organic fraction, or SOF) and sulfate (primarily H_2SO_4 and some metal ion sulfates). The SOF is composed of unburned fuel and lubricating oil and their partial oxidation products. The term "smoke" is sometimes used to denote the solid carbon portion of the particulate. Smoke is visually apparent and usually measured with an optical technique such as opacity to light.

The carcinogenic effect related to diesel exhaust particles is now considered to have at least two components, one related to the inorganic "carbon core" (solid carbon soot or SOL)

and one to the adsorbed SOF. Several recent laboratory studies with rats have indicated that the SOL portion is probably essential for initiation of tumor formation [12, 13, 14, 15]. The associated SOF, particularly the polynuclear aromatic hydrocarbons (PAH) and the nitro-PAH, could also make a contribution to the overall carcinogenic effect [16].

Soot formation takes place in the fuel combustion environment at temperatures between 1000 and 2800 K, at pressures of 50 to 100 atm and with sufficient air overall to fully burn all the fuel. The time available for the formation of solid soot particles from the fuel is on the order of milliseconds.

The production of particulates in a diesel engine can be divided into two stages: particle generation and particle growth.

During the particle generation, or nucleation, process the first condensed phase material arises from the fuel molecules via their oxidation and/or pyrolysis products. These products include various unsaturated hydrocarbons, particularly acetylene and its higher analogues ($C_{2n}H_2$), and polycyclic aromatic hydrocarbons (PAH). These two types of molecules are considered the most likely precursors of soot in flames. Nucleation produces a large number of very small particles which represent almost negligible soot loading in the region of their formation.

Particle growth processes include surface growth, coagulation and aggregation. Surface growth involves the attachment of gas-phase species to the surface of particles and their incorporation into the particulate phase. Surface growth reactions lead to an increase in the amount of soot but the number of particles remains unchanged. Coagulation involves particle collisions and coalescence, which decreases the number of particles and increases their size with the amount of soot staying constant. Then the particles are aggregated into chains and clusters by collisions of larger particles. Figure 2.1 illustrates the relationship between these processes.

These stages of particle generation and growth constitute the soot formation process. In these processes, oxidation can occur whenever soot or soot precursors are in the presence of oxidizing species to form gaseous products such as CO and CO_2. The eventual emission of
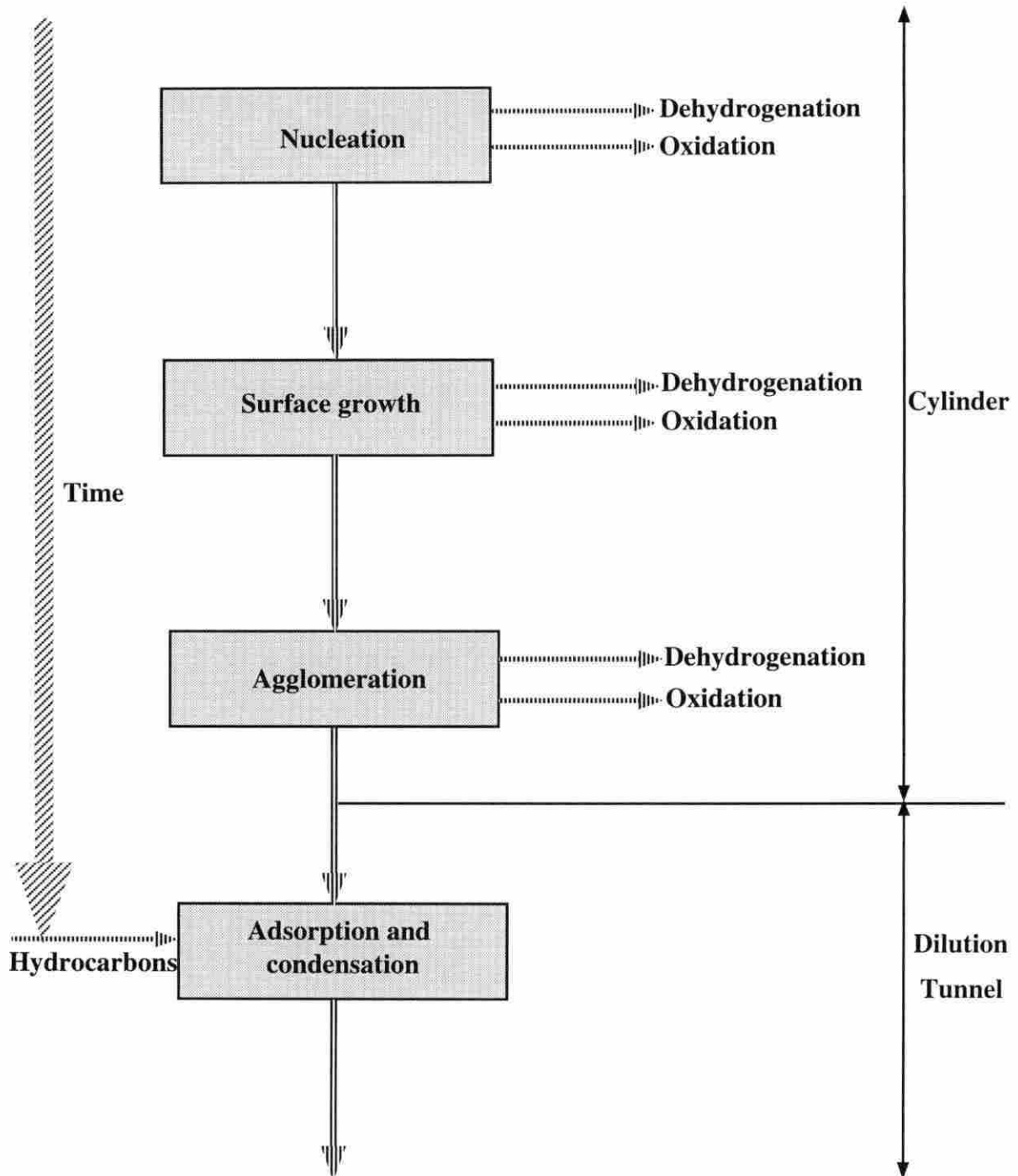
Figure 2.1   Processes of diesel particulate formation [4]

soot from the diesel engine will depend on the balance between the processes of formation and oxidation.

Adsorption and condensation of hydrocarbon are the final processes during particulate formation. They occur primarily after the burned gases have been exhausted from the engine, as these exhaust gases are diluted with air. During particulate emission measurement, the process occurs in a dilution tunnel that simulates the actual atmospheric dilution process. It can be seen that the nature and quantity of particulate emissions from a given source will be dependent, not only upon the source, but also upon the sample collection methods used. Among the important sampling considerations are the degree of exhaust gas dilution and mixing with ambient air before sampling, the sampling temperature, the sampling time, and the device used to remove the particulate matter from the exhaust gases. In order to compare sources of particulate emissions, it is critical that samples be collected as consistently as possible [4, 17, 18, 19].

The first step of a particulate analysis scheme generally is solvent extraction of the particulate matter. This results in the separation of the sample into soluble and insoluble fractions. The exact nature of this separation is dependent on the solvent and extraction conditions. A wide variety of solvents have been used for the extraction of particulate matter including methanol, hexane, cyclohexane, benzene, chloroform, methylene chloride and carbon disulfide. The criteria for the choice of a solvent include its extraction efficiency, purity, volatility, toxicity, cost and compatibility with subsequent analytical procedures [20, 21, 22].

For the extraction of PAH from airborne particulates, benzene and methanol have been shown to be more effective than most other commonly used solvents [20, 21]. Polar solvents such as methanol and methylene chloride are known to be more efficient extraction solvents for polar species than nonpolar solvents such as benzene and cyclohexane. Binary mixtures of polar and nonpolar solvents or alternatively separate extractions with each solvent type have been demonstrated to yield higher levels of soluble organic fraction from airborne particulates than single solvent extractions. The use of binary solvent extractions, particularly benzene and methanol, has become very popular [22, 23, 24, 25].

Methylene chloride has been shown to be an efficient general solvent for hydrocarbon extraction from particulate and was used as the extraction solvent for this study. Its selection over other available candidates was predicated by a desire to be consistent with EPA procedures for the analysis of diesel particulate matter [22, 26, 27, 28].

Typically 15 to 30 mass percent is extractable, though the range of observations is much larger (10 to 90 percent). Although most of the particulate emissions are formed through incomplete combustion of fuel hydrocarbons, engine oil may contribute significantly. The SOF of diesel particulate can be chemically characterized into eight fractions as shown in Table 2.1. Those fractions are generally labeled as: basic, acidic, paraffins, aromatics, transitional, oxygenates, ether insolubles, and hexane insoluble [29, 30]. The basic fraction contains aromatic or aliphatic species with basic functional groups such as $-NH_2$. Examples of these compounds are the benzacridenes. The acidic fraction contains aliphatic and aromatic species containing acidic functional groups such as -COOH or phenolic -OH groups. Benzoic acid and the phenols would be examples of this type of compound.

The paraffin fraction contains the aliphatic straight and branched chain alkanes; n-dodecane is an example of this type of compound. Unburned fuel would be a source for high levels of paraffins in diesel particulates. The aromatic portion of the particulate extract will contain those compounds that have aromatic structure and no functional groups that may be thought of as polar. Alkyl substances may be found with a variety of chain lengths expected. An example of the type of compound in this fraction is a polynuclear aromatic such as benzo(a)pyrene.

The transitional fraction consists of compounds that may be oxygenated but without acidic, basic or other polar functional groups. Those compounds can be aromatic or aliphatic and have a high probability of containing an ether type of functional group. The fraction labeled as oxygenates contains those oxygenated compounds that are not acidic or basic, but still have polar functional groups. Aromatic and aliphatic ketones and aldehydes fall into this class of compounds. Typical of these compounds might be quinone or α-napthoquinone.

Table 2.1   Fractions of SOF [29]

Characterization of SOF	Fractions of SOF
Basic	<1-2%
Acidic	3-15%
Paraffin	34-36%
Aromatic	3-14%
Transitional	<1-6%
Oxygenates	7-15%
Ether insolubles	6-25%
Hexane insolubles	1-3%

The insoluble fraction contains a wide variety of compounds that may include both organic and inorganic compounds. A number of different functional groups may be present in this fraction [29, 30].

2.3   Vegetable Oil Fuels

Interest in the development of alternative fuels has grown steadily during the past two decades. Researchers have found that vegetable oils and their alcohol esters have significant appeal as a substitute diesel fuel. Vegetable oils are naturally occurring esters found in numerous plant varieties. The difference of vegetable oils from typical diesel fuel is that the vegetable oils are composed of triglycerides with fatty acid chains of 16 to 22 carbons in length, while diesel fuel consists mostly of saturated hydrocarbons with carbon chain length

between 10 and 16. Saturated hydrocarbons contain only single bonds between carbon atoms. The chemical structure of a typical triglyceride is illustrated in Figure 2.2.

R_1, R_2 and R_3 in the structure of vegetable oil represent the hydrocarbon chain of the fatty acids, and may be of different chain length and have different numbers of double bonds present. Fatty acids comprise from 94% to 96% of the total mass of a triglyceride molecule.
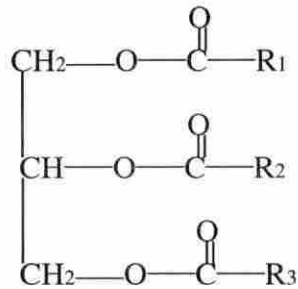
Figure 2.2 Chemical structure of vegetable oil

Therefore, the proportion of the acids determine the physiochemical properties of an oil, such as viscosity and calorific value. Table 2.2 shows the fatty acid compositions of some common vegetable oils [31]. The numbers following the name of the fatty acid indicate the total number of carbon atoms in the fatty acid and the number of double bonds. For example, oleic acid is designated 18:1, which means it has an 18 carbon chain with one double bond.

In most samples of vegetable oils, a small number of the fatty acid molecules have detached from the glycerin base and are known as "free fatty acids". The quantity of free fatty acids predominantly affects the flash point of a plant oil and to some extent its ignition characteristics. The degree of unsaturation (number of carbon-carbon double bonds) determines the oxidation stability as well as the melting temperature of the oils. The double bonds present in unsaturated oils are highly susceptible to attack by oxygen molecules and subsequent formation of chemically active hydroperoxides. However, unsaturated oils have much better cold flow properties than saturated oils [32]. The cetane number of vegetable

Table 2.2 Fatty acid compositions of some vegetable oils

(% by weight)

Fatty acid		Formula	Cotton seed	Peanut	Rape seed	Safflower	Soybean	Sunflower
Myristic	14:0	$C_{14}H_{28}O_2$	0.00	0.00	0.00	0.00	0.00	0.00
Palmitic	16:0	$C_{16}H_{32}O_2$	28.33	11.38	3.49	8.60	11.76	6.08
Stearic	18:0	$C_{18}H_{36}O_2$	0.89	2.39	0.85	1.93	3.15	3.26
Oleic	18:1	$C_{18}H_{34}O_2$	13.27	48.28	64.40	11.58	23.26	16.93
Linoleic	18:2	$C_{18}H_{30}O_2$	57.51	31.95	22.30	77.89	55.52	73.73
Linolenic	18:3	$C_{18}H_{28}O_2$	0.00	0.93	8.23	0.00	6.31	0.00
Arachidic	20:0	$C_{20}H_{40}O_2$	0.00	1.32	0.00	0.00	0.00	0.00
Behenic	22:0	$C_{22}H_{44}O_2$	0.00	2.52	0.00	0.00	0.00	0.00
Lignoceric	24:0	$C_{24}H_{48}O_2$	0.00	1.23	0.00	0.00	0.00	0.00

oils and their alcohol esters increases with increased chain length of the fatty acids, which generally tends to improve combustion and emissions. However, the viscosity also increases with increasing chain length. [31, 33].

The physical and chemical properties of vegetable oils are close enough to those of diesel fuel to operate unmodified engines for short periods of time. The volatility and viscosity do differ from diesel fuels, each having a negative impact on the oil's overall quality as an alternative fuel. Table 2.3 compares some of the fuel properties of vegetable oils and their alcohol esters with typical No.2 diesel fuel [31, 34].

Cetane number is one of the most important properties of diesel fuels. It indicates the readiness of a diesel fuel to ignite spontaneously under the temperature and pressure conditions in the combustion chamber of the engine. The higher the cetane number, the shorter the delay between injection and ignition. Shorter ignition delay is usually better for engine performance and emissions. The heating value is a measure of the energy available from a fuel when it is burned, and is the basis for calculating the thermal efficiency of an

Table 2.3   Fuel properties of vegetable oils and their alcohol esters

Fuel	Higher heating value MJ/kg	Cetane No.	Cloud point °C	Pour point °C	Viscosity cst @40°C
Peanut	39.5	41.8	12.8	-6.7	39.60
Soybean	39.6	37.9	-3.9	-12.2	32.60
Sunflower	39.6	37.1	7.2	-15.0	33.90
Methyl soybean	39.8	46.2	2.0	-1.0	4.08
Ethyl soybean	40.0	48.2	1.0	-4.0	4.41
Butyl soybean	40.7	51.7	-3.0	-7.0	5.21
Methyl sunflower	39.8	47.0	0.0	-	-
Methyl peanut	-	54.0	5.0	-	4.90
Methyl rapeseed	40.1	-	-3.3	-14.7	6.10
Ethyl rapeseed	41.4	-	-4.7	-18.7	6.75
No.2 diesel	45.3	47.0	-15.0	-33.0	2.70

engine using that fuel. Generally, the heating value of vegetable oils is slightly lower than diesel fuel. Viscosity of a fuel indicates its resistance to flow; the higher the viscosity, the greater the resistance to flow. Changes in fuel viscosity will alter the injector spray penetration rate, cone angle and drop-size distribution. These changes in spray quality will directly affect the quality of combustion. The higher viscosity of vegetable oils is their greatest shortcoming as a diesel fuel.

Previous studies on the use of unmodified vegetable oils have revealed their potential as an alternative to or extender for diesel fuel. Further enhancing their value from an environmental viewpoint, the vegetable oils are entirely renewable and biodegradable in the event of spills, and contain only trace amounts of sulfur. Low sulfur levels would significantly reduce the hazardous sulfate portion of diesel engine particulate emissions. However, the high viscosity and low volatility of unmodified vegetable oils cause injector spray pattern problems and result in poor combustion. In addition, this results in the formation of depos-

its in the combustion chamber, and the dilution of the lubricating oil with unburned fuel. Many tests have shown that short term performance indicators (power output, torque, brake thermal efficiency and emissions) of numerous vegetable oils are comparable to those of diesel fuel [35, 36, 37, 38, 39]. However, long term tests showed that unmodified vegetable oils produced severe engine deposits, injector coking and piston ring sticking [40, 41, 42, 43, 44].

A number of studies have shown that modification of the vegetable oils, typically through transesterification to form methyl, ethyl or butyl esters of vegetable oils can provide a significant reduction in the viscosity of the oils, and make them more suitable for use in a diesel engine without modifications [45, 46, 47]. Transesterification is the process of reacting a triglyceride (vegetable oil) with an excess of the stoichiometric amount of an alcohol in the presence of a catalyst (KOH, NaOH or $NaOCH_3$ etc.) at room temperature (30 to 70 °C) [47, 48] to produce glycerin and fatty esters. The chemical reaction is shown in Figure 2.3.

It is these fatty esters of vegetable oils which are now commonly called "biodiesel". With different alcohols, such as methanol, ethanol or butanol, the production of alcohol esters is methyl ester, ethyl ester or butyl ester. When a specific vegetable oil, such as soybean oil, is used to produce the ester, the product is methyl ester of soybean oil or methyl

$$
\begin{array}{llll}
CH_2COOR_1 & & CH_3COOR_1 & CH_2\text{---}OH \\
| & \quad Catalyst & | & | \\
CHCOOR_2 + 3\ CH_3OH \xrightarrow{\quad\quad} & CH_3COOR_2 & + & CH\text{---}OH \\
| & (NaOCH_3) & | & | \\
CH_2COOR_3 & & CH_3COOR_3 & CH_2\text{---}OH
\end{array}
$$

| Triglyceride (vegetable oil) | Alcohol | Mixture of fatty esters | Glycerin |
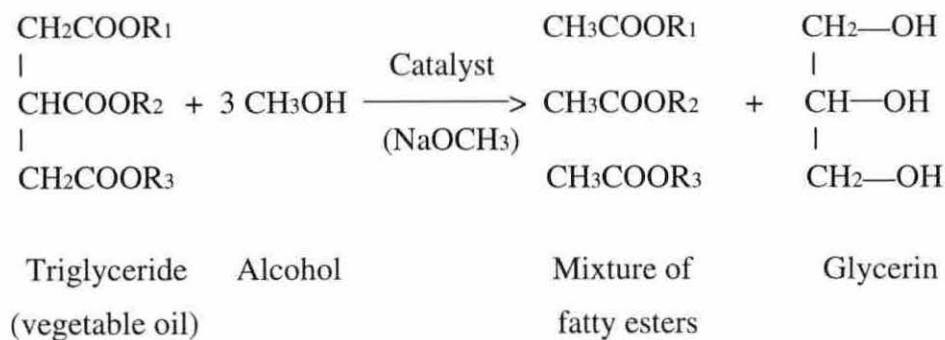
Figure 2.3   Chemical reaction of triglyceride with alcohol

soyate or sometimes "soydiesel". Successful transesterification processes for many different vegetable oils have been reported [46, 47, 48, 49, 50].

The alcohol esters have better fuel properties than those of unmodified vegetable oils [8, 34, 51]. They usually have lower viscosity, lower cloud and pour points, and about the same heating value. Table 2.2 also shows fuel properties of some vegetable oil esters.

Research evaluating the ester for sunflower, cottonseed, and rapeseed oils [52] reports that engine performance (based on thermal efficiency and brake horsepower) was equal to or exceeded that of diesel fuel. Although some reports of heavy carbon deposits have been associated with the use of methyl esters of sunflower oil [53], the primary operation-related concerns with esters include: dilution of the lubricating oil, relatively high cloud and pour points, material compatibility, and long-term storage implications [54].

2.4   Diesel Engine Emissions Fueled with Vegetable Oils and Their Alcohol Esters

Performance and emissions of diesel engines fueled with vegetable oils have been tested by many researchers. Vander Griend [47] observed that vegetable oil combustion does not proceed along the same lines as does diesel fuel. It displays the conventional stages of combustion very similar to diesel fuel, but offers some advantages over diesel by exhibiting lower peak pressures and a smoother diffusion burn. As such, the vegetable oils will respond differently and display a different sensitivity to combustion related parameters. As a result, research focusing on optimizing an engine for vegetable oil operation, especially in the case of emissions, may experience results far different from those for diesel fuel.

If an alternative fuel is to compete with an ordinary fuel, an important prerequisite is meeting today's exhaust emission standards with only minor modifications to the engine or exhaust system. Kaufman and Ziejewski [53] found that methyl and ethyl esters of sunflower oil have reduced smoke and exhaust gas temperature and the methyl esters of winter rapeseed oil, when evaluated as a supplement to diesel, have demonstrated smoke and exhaust gas temperature reduction in blends containing as little as 10% of the ester. All three esters provided lower particulate and NO_x emissions. Geyer et al. [52] reported that methyl

esters of cottonseed and sunflower oil have displayed significant reductions in particulate, but have contributed to higher exhaust gas temperature as well as higher NO_x emission.

Barsic and Humke [55] fueled a single cylinder, direct injection, naturally-aspirated diesel engine with peanut oil, sunflower oil and 50/50 blends of these oils with No.2 diesel fuel. The results showed that NO_x emissions using vegetable oils were not significantly different than when using diesel fuel. The increase in HC, CO and particulate emissions at maximum fuel delivery were due primarily to operation at higher equivalence ratios. Based on equal energy input, NO_x emission was similar for the vegetable oils and their blends with diesel fuel. HC emission for peanut oil, sunflower oil and their blends was 50% higher than for 100% diesel fuel. CO emission for vegetable oils was about twice that of diesel fuel for some operating modes and lower for others. The increase in CO emission as greater amounts of vegetable oil were blended with diesel fuel may be due to fuel property effects. Particulate emission exhibited some of the same trends as CO emission. There were generally higher emissions as more vegetable oil was substituted for diesel fuel.

Hemmerlein et al. [56] used six types of diesel engine to test the engine performance and emissions fueled with rapeseed oil. The results were that CO emission was up to 100% higher with rapeseed oil compared to diesel fuel. An increase in HC emission was also measured. The increase depended on the operating range of the engines and could increase by as much as 290% compared to diesel fuel, but the NO_x emission was up to 25% lower with rapeseed oil. Particulate emission was reduced by 30 to 50% with rapeseed oil in engines with divided combustion chambers. Direct injection engines showed higher particulate emission (90 to 140%) with rapeseed oil compared to diesel fuel.

The results discussed above indicate mixed results when using vegetable oils in diesel engines. A large amount of research has also been conducted on vegetable oil esters. Nearly every study performed to date has shown that alcohol esters of vegetable oils or their blends with typical No. 2 diesel fuel can be used as a substitute for diesel in short term tests. The presence of oxygen atoms in the biodiesel fuels assures more complete combustion in engines. This reduces the CO, HC and particulate matter (PM) in the exhaust gas when compared with No. 2 diesel fuel.

Schumacher et al. [9] used a Caterpillar 3408 and four International 574 farm tractors fueled with diesel/soydiesel blends to test the engine's performance and emissions. The results showed that engines fueled with 100% soydiesel did not lose a significant amount of maximum torque capacity, but developed approximately 5 to 7% less power than engines fueled with No. 2 diesel fuel. The engine's exhaust opacity readings declined as the concentration of soydiesel in the soydiesel/No. 2 diesel fuel blend increased. CO emission tended to decrease when engines were operated at peak torque as the percent soydiesel in the fuel mixture increased, but remained relatively constant at peak power. NO_x exhaust emissions tended to be lower when engines were fueled with 10-40% soydiesel/diesel blends compared to 100% diesel or 100% soydiesel. Kusy [46] found similar results when he fueled a direct injection engine in a John Deere 4640 tractor with ethyl ester of soybean oil.

Schumacher et al. [57] also used a 5.9 liter direct injection turbocharged Cummins diesel engine installed in a Dodge pickup to compare engine efficiency, wear, performance and emissions of 100% methyl ester of soybean oil with 100% diesel fuel. They found that the fuel efficiency was nearly identical to that obtained when the engine was fueled with diesel fuel. The engine did not appear to be wearing at an accelerated rate and no abnormal coking was noted on the injectors, on top of the pistons, or on the valve stems. The power of the engine fueled with 100% soydiesel was 5% less. CO emission stayed about the same, HC was reduced by 48%, particulate matter by 20%, but NO_x emission was increased by 13%. Based on performance tests with methyl ester of soybean oil in a Volkswagen 1.6 liter indirect injection diesel engine, Pischinger et al. [58] reported that the difference in power and torque between diesel fuel and methyl ester of soybean oil fuel varied only marginally while smoke emission levels were significantly lower for esters compared with diesel fuel.

Alfuso et al. [59] found that methyl ester of rapeseed oil caused a rise in NO_x emission, a decrease in HC and CO emissions, and a strong reduction in smoke. Particulate matter produced by the methyl ester in transient cycles was higher than that given by diesel fuel. Mittelbach et al. [60] noted that two different methyl ester fuels derived from rapeseed oil gave significantly lower total particulate matter and polynuclear HC emissions than No.2

diesel fuel. However, the methyl ester fuels produced higher levels of NO_x emission and aldehyde emissions than did No. 2 diesel fuel. Geyer et al. [52] reported that methyl esters of cottonseed and sunflower oil displayed significant reductions in particulates, but also had higher exhaust gas temperature as well as higher NO_x level.

The effects of methyl, ethyl and butyl esters of soybean oil on the performance and emissions of a John Deere 4239TF, direct injection, turbocharged diesel engine were investigated by Wagner et al. [8]. The performance of esters of soybean oil did not differ greatly from those of diesel fuel. The emissions of HC, CO and particulate matter were similar to diesel fuel. NO_x emission was higher for all the ester fuels. Smoke was definitely less visible under full rack conditions for the methyl and ethyl esters compared to diesel fuel, but was greater for the butyl ester.

In general, vegetable oils, their esters, and their blends with diesel fuel have lower carbon monoxide, unburned hydrocarbon, smoke and particulate emissions, but slightly higher oxides of nitrogen emissions than typical diesel fuel. The engine performance of these fuels is also similar to diesel fuel. They have great potential for reducing diesel engine emissions.

3. EXPERIMENTAL APPARATUS

This chapter will discuss the equipment that was used in this study. There are four sections in this chapter. First, an overview of the engine test setup is given. In the second section, the dilution tunnel, particulate sampling and analysis system are discussed. In section three, the fuels and fuel blends used for the project are described, and the data acquisition system is presented in the last section.

3.1 Engine Test Setup

The engine used in this experiment was a John Deere model 4276T four-cylinder, four-stroke, turbocharged diesel engine. The basic engine specifications are provided in Table 3.1. The combustion system of the engine is a bowl-in-piston, direct-injection, medium-swirl type. The engine was connected to a 150 HP General Electric model TLC2544 direct current dynamometer.

The atmospheric pressure was measured with a Datametrics Barocel pressure sensor. Boost pressure, exhaust back-pressure and engine lubricating oil pressure were measured with bourdon pressure gages. Table 3.2 lists the nineteen thermocouples that were installed at different locations around the engine and dilution tunnel system.

Table 3.1   Specifications of John Deere 4276T diesel engine

Bore	106.5 mm
Stroke	127.0 mm
Connecting rod length	202.9 mm
Compression ratio	16.8:1
Maximum power	57.1 kW @ 2100 rpm
Peak torque	305.0 Nm @ 1300 rpm
Firing order	1-3-4-2

Table 3.2   Thermocouples in the John Deere engine

No. of thermocouple	Location
1	Inlet air dry bulb temperature
2	Inlet air wet bulb temperature
3	Intake manifold temperature
4	Fuel temperature
5	Oil temperature
6	Coolant inlet temperature
7	Coolant outlet temperature
8	Exhaust manifold temperature
9	Exhaust temperature (shielded thermocouple)
10	Exhaust temperature (thermocouple shield)
11	Exhaust temperature (unshielded)
12	Not used
13	Building cooling water inlet temperature
14	Building cooling water outlet temperature
15	Static temperature of 1st dilution tunnel
16	Static temperature of 2nd dilution tunnel
17	Filter chamber temperature
18	Particulate sample temperature @ROOTS
19	Diluted exhaust temperature @sampling point 1
20	Diluted exhaust temperature @sampling point 2

A Kistler model 6061A pressure transducer was installed in the engine cylinder head to measure the combustion pressure. The pressure signal was amplified by a PCB charge amplifier, and recorded by a Zenith Z-386 computer through an Analog Devices RTI-860 data acquisition board. A computer program collected 24 engine cycles of pressure data with

0.25 degree resolution, and averaged the pressure data to save on floppy disk. The program also provided summary information about each of the 24 engine cycles. The calibration of the Kistler pressure transducer is presented in Appendix A.

The volume flow rate of air into the engine was determined using a Meriam laminar flow element with a Baratron differential pressure transducer to measure the pressure drop. The fuel mass flow rate was measured using a Toledo electronic scale with a stopwatch.

3.2   Emission Measurement Equipment

3.2.1   Dilution tunnel

Diesel engine particulate emission is measured with a special measurement system based on specifications contained in the Code of Federal Regulations [11]. A schematic of the measurement system is shown in Figure 3.1. It consists of a primary dilution tunnel, a heat exchanger, a positive displacement pump (PDP) and a constant volume sampler (CVS). During the test, the entire exhaust gas flow of the engine is supplied to the dilution tunnel. Tunnels of this type are termed "full-flow" dilution tunnels.

The dilution tunnel is intended to simulate the mixing of engine exhaust gas into the atmosphere, where some of the unburned hydrocarbon will be adsorbed and condensed onto the particulate surface. The total mass of adsorbed and condensed hydrocarbon is the soluble organic fraction (SOF) of the particulate.

In the particulate measurement system, the CVS system will draw a constant mass flow of diluted exhaust through the dilution tunnel. During transient tests, the flow rate and temperature of the engine exhaust entering the dilution tunnel will be highly variable. However, the large heat exchanger brings the diluted exhaust to an almost constant temperature. Since the pressure in the dilution tunnel does not vary significantly, the fact that the PDP is drawing a constant volume flow rate of constant-temperature, diluted exhaust means that the mass flow rate is also constant. If the mass flow is constant downstream, then it must

23
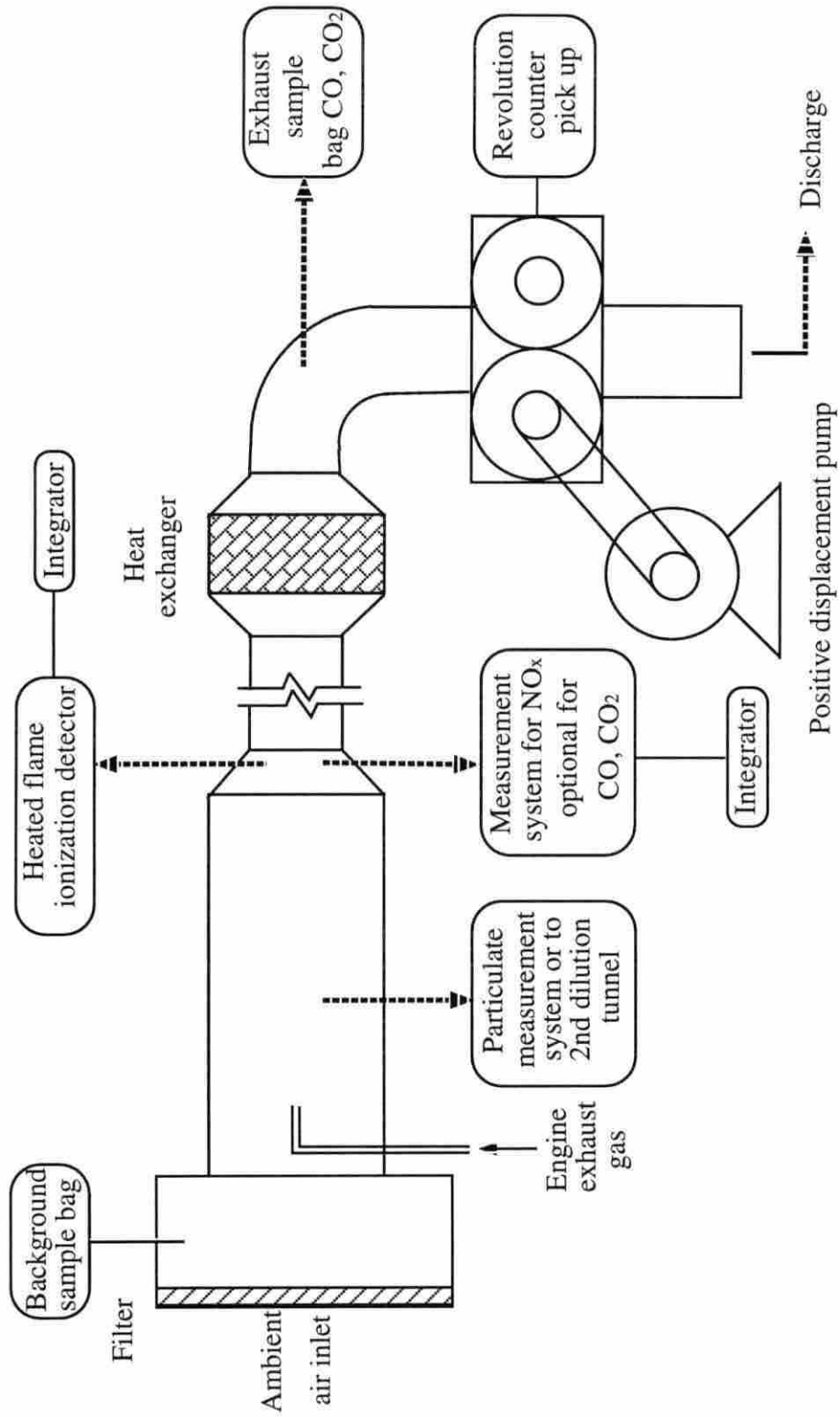
Figure 3.1   EPA specified exhaust emissions measurement system [65]

be constant upstream. This technique ensures that the exhaust measurements taken during a transient cycle are properly weighted with respect to the different conditions of the cycle.

It is clear that the PDP-CVS system is very expensive. Some researchers have simplified the EPA standard dilution tunnel and developed their own systems. There are many examples of successful simplified dilution tunnels [61, 62, 63, 64]. Some of them are full-flow dilution tunnels, and some draw a constant fraction of the total exhaust gas into the dilution tunnel. The dilution tunnel used in this study is a simplified full-flow dilution tunnel. Since the test objective was not to try to determine whether or not the engine met EPA emission standards, an EPA-type system was not essential. The details of the design and the validation tests can be found in B.C. Murray's M.S. thesis [65].

The particulate measurement system that was used for this study was a double dilution tunnel. Figure 3.2 shows a diagram of the primary and secondary dilution tunnels. The primary dilution tunnel was used to dilute the engine exhaust gas with compressed air, and the secondary tunnel was employed to mix a portion of the diluted exhaust gas with additional air.

The primary tunnel was built in 1989 of standard galvanized spiral tubing [65]. This material was not ideal since it did not have a perfectly smooth interior. A rough interior increases the potential for particulate deposition, and could cause problems with particulates being re-entrained into the stream during a later test. However, no abnormal phenomena were observed during this experiment.

The primary dilution tunnel was 0.305 meters in diameter [65]. The distance between the introduction of the engine exhaust gas and the particulate sample probe was 3.05 meters which corresponds to 10 tunnel diameters. This distance provided sufficient time for mixing of the engine exhaust gas with the dilution air before the diluted exhaust gas was extracted by the particulate sampling system. The choice of the diameter of the dilution tunnel allowed a proper Reynolds number to be produced to enhance the turbulent mixing. Tests conducted to ensure complete mixing of the exhaust gas with dilution air are discussed in Appendix D.

Figure 3.2   Dilution system of particulate measurement
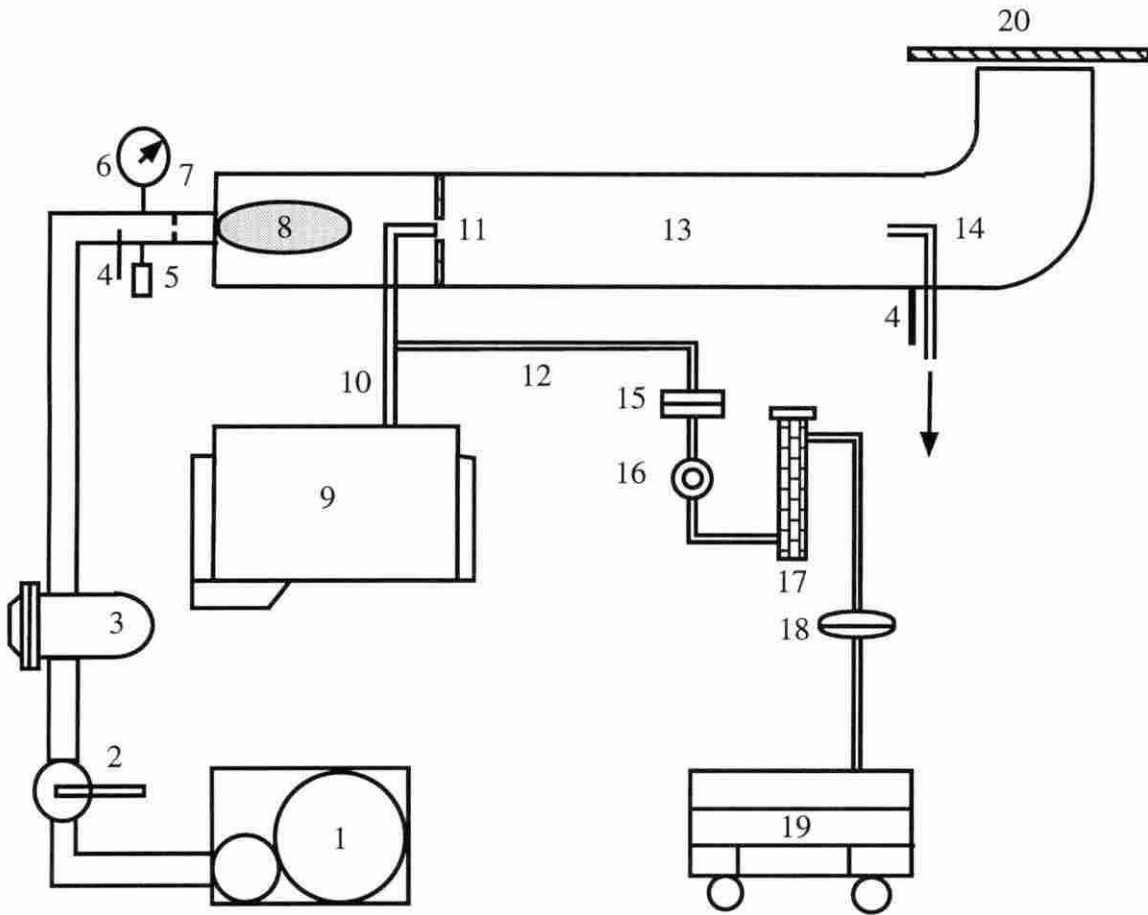
1. Centac II air compressor
2. Ball valve
3. Air filter
4. Thermocouple
5. Pressure transducer
6. Pressure gage
7. Orifice
8. Muffler
9. Diesel engine
10. Exhaust pipe

11. Mixing orifice
12. Gaseous emission sampling tube
13. Primary dilution tunnel
14. Particulate sampling probe
15. First filter
16. Sampling pump
17. Desiccant dryer
18. Secondary filter
19. Emission cart
20. Laboratory exhaust fan

A 90° elbow of 60 cm exhaust pipe introduced the engine exhaust gas into the primary dilution tunnel. The elbow, which faces downstream, was used to direct the exhaust gas into the center of the dilution tunnel to ensure even mixing of the exhaust gas with the dilution air. A 20 cm diameter orifice was installed in the dilution tunnel at the point of entry of the exhaust gas, which increased the flow velocity and turbulence of the dilution air. A high volume ceiling exhaust fan was located at the dilution tunnel exit. The fan was turned on to ventilate the laboratory whenever the dilution tunnel was operated.

3.2.2 Dilution air system

Dilution air was provided by an Ingersoll-Rand Centac II two-stage air compressor that developed an outlet gauge pressure of 620 kPa. The controller of the air compressor maintained the pressure within $\pm$ 7 kPa of the set point. The compressed air was introduced into the primary dilution tunnel through a 5 cm diameter pipe, and the flow rate of dilution air was controlled by a ball valve (shown in Figure 3.2). A standard in-line air filter and a smooth-edged orifice were also installed behind the valve. A Viatran model 141 pressure transducer and a thermocouple were located between the air filter and the orifice. The dilution air flow rate was determined by measuring the pressure and temperature of the compressed air on the upstream side of the orifice and using a calibration equation to determine the mass flow rate. The in-line air filter was installed to ensure that particles present in the dilution air did not enter the tunnel. A test conducted to determine the significance of particles in the dilution air is described in Appendix C.

An air-exhaust muffler was fitted to the end of the compressed air line to reduce the noise which was produced by the uncontrolled expansion of the dilution air when it entered the dilution tunnel. The dilution ratio of the tunnel could be varied widely. The definition of dilution ratio was the ratio of dilution-air mass flow rate to exhaust mass flow rate. The maximum dilution air flow rate that could be achieved was 0.744 kg/s. The flow rate of the engine exhaust was 0.058 kg/s for light-load at 1400 rpm to about 0.066 kg/s for full-load at 1400 rpm. Therefore, the dilution ratios for light-load and full-load at 1400 rpm were 12.76

and 11.16, respectively.

The secondary dilution air system could provide additional air to the diluted exhaust that came from the primary dilution tunnel. The flow rate of the secondary dilution air could be determined by measuring the pressure and temperature upstream of a choked orifice with a Viatran Model 141 pressure transducer and a thermocouple. Because the primary dilution tunnel was able to maintain the diluted exhaust gas temperature below that specified by the EPA, the secondary dilution air system was not operated during this experiment.

3.2.3 Particulate sampling system

Figure 3.3 shows a schematic diagram of the particulate sampling system. The particulate sampling system consists of ball valves, a filter holder, a sampling pump, a gas meter with a frequency counter, a by-pass valve, a vacuum gage and a vacuum pump. Ball valve 3 was opened when the experiment started, and closed at the end of the test to keep the diluted exhaust gas out of the system between tests. The secondary dilution tunnel which could increase the dilution ratio was located upstream of the filter holder. However, as mentioned above, there was no need to operate the secondary dilution tunnel for the tests conducted in this study. The filter holder was used to support a primary filter and a backup filter. The distance between these two filters was 8.9 cm, and a thermocouple was mounted between them to monitor the temperature in the filter holder during sampling. A second thermocouple was located at the inlet to the gas meter so the density of the sample flow could be computed.

The electronic counter, attached to the Roots sample flow meter, was capable of displaying the total amount of gas that had passed though the sampling system during the test as well as the instantaneous flow rate. The sampling pump had a by-pass line with a valve that was adjusted manually to keep the flow rate of particulate sample constant during the test. This was necessary because the sample flow rate would drop as the filters became loaded with particulate. The vacuum pump was used to test the system for leaks. The leak test des-
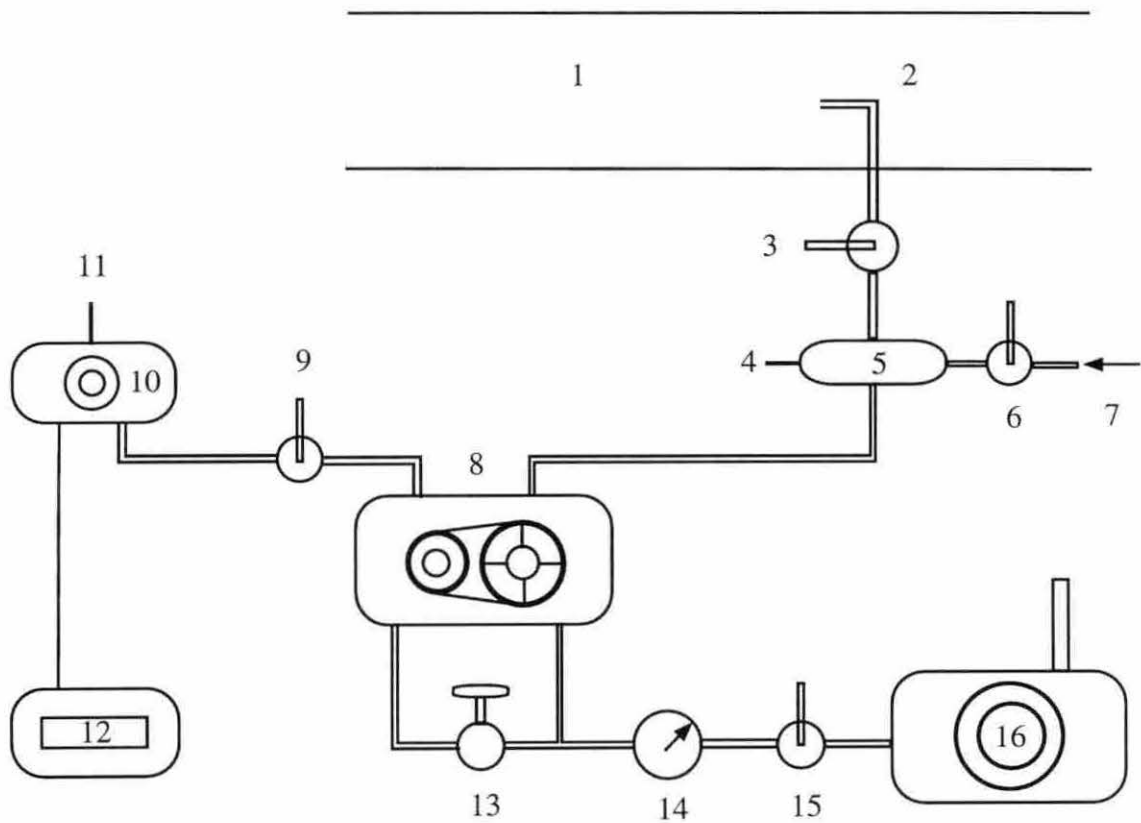
Figure 3.3   Particulate sampling system

1. Primary dilution tunnel
2. Particulate sampling probe
3. Ball valve 1
4. Thermocouple
5. Filter holder
6. Ball valve 2
7. Secondary dilution air
8. Sample pump
9. Ball valve 3
10. ROOTS meter
11. Thermocouple
12. Frequency counter
13. By-pass valve
14. Vacuum gage
15. Ball valve 4
16. Vacuum pump

cribed in Appendix E was conducted at the start of this project.

The filters used to collect the particulate sample in this project were 110 mm Pallflex T60A20 filters. The particulate sample volume flow rate was chosen to be 3.3×10^{-3} m^3/s (7 ft^3/min.) in order to collect at least 10 mg of particulate matter on the filters to minimize the impact of errors in filter weighing.

3.2.4   Particulate weighing chamber

A temperature and humidity controlled weighing chamber, 915x760x790 mm, was used to weigh and store the filters during the study. Compressed air was passed through an oil removal filter and diffused into the weighing chamber to control the humidity. The temperature in the chamber was maintained within $\pm$ 2 K of 298 K, and the relative humidity of the chamber was maintained within $\pm$ 3% of 30%.

A Mettler Model AE240 analytical balance with a reproducibility of 20 micrograms and a readability of 10 micrograms was placed inside the weighing chamber. There were also two shelves in the weighing chamber. One of them was covered with metal screen to ground any electrostatic charge on the filter surface. The effect of electrostatic charges on the weighing process is described in Appendix G.

3.2.5   Soluble hydrocarbon extractor and solvent

The particulate filters were Soxhlet extracted with methylene chloride in a fume hood. There were two Pyrex Soxhlet extractors using 125 ml flasks at the bottom, and Allihn type condensers at the top. During extraction, the particulate filter was contained in an 80x25 mm extraction thimble. Two Electromantle heaters heated the flasks and maintained a constant solvent temperature. The solvent used in this test was methylene chloride which is the most common solvent for this purpose [22, 29]. Appendix G discusses the solubility of methylene chloride with hydrocarbon fuels.

3.2.6 Equipment for measuring gaseous emissions

The gaseous emission sampling system is shown in Figure 3.2. A portion of the engine exhaust gas was drawn directly from the engine exhaust pipe with a vacuum pump. Two filters were located in the sampling system to remove solid particles from the sample gas to protect the equipment from damage. One of them was a 110 mm Whatman paper filter, the other was a 47 mm Gelman Sciences glass fiber filter. The sampling pump and a desiccant dryer were located between them. Although a vacuum pump was used to move the sample through the system, the pressure of the gaseous emission sampling system was above atmospheric for all test conditions. This was because the exhaust sample was drawn before the turbocharger where the pressure was above atmospheric. The lowest pressure corresponding to 20% of full load at 1400 rpm was about 8 kPa gauge, and the highest corresponding to 100% of full load at 1400 rpm was 13 kPa gauge. Therefore, there was no chance for air to leak into the sampling system to dilute the engine exhaust gas.

The concentrations of carbon monoxide and carbon dioxide in the engine exhaust gas were measured with two Beckman Model 864 infrared analyzers. The concentrations of nitric oxide and total oxides of nitrogen were determined with a Beckman Model 955 NO/NO_x analyzer. The unburned hydrocarbon in the exhaust gas was measured with a Beckman Model 402 heated flame ionization detector hydrocarbon analyzer, and the oxygen concentration was measured with a Beckman Model 7003 polarigraphic oxygen monitor.

The samples of exhaust gas to the hydrocarbon analyzer and to the NO/NO_x analyzer were kept at 450 K with a heated line as they were transported from the engine exhaust pipe to the analyzers. The heated exhaust gas was based on the wet sample without passing through the dryer, but the measurements of CO, CO_2 and O_2 were dry samples.

3.3   Fuels

Five fuels were selected as the base fuels for this study, methyl ester of soybean oil (termed MS), iso-propyl ester of soybean oil (IP), winterized methyl ester of soybean oil (WME), high sulfur No.2 diesel fuel (DH) and low sulfur No.2 diesel fuel (DL). Blends of those fuels were also tested as shown in Table 3.3. For convenience, abbreviations for the fuels are used in the thesis and are also listed in Table 3.3.

Table 3.3   Tested fuels

Fuels	Abbreviation
High sulfur No.2 commercial diesel	DH
20% ME soyate + 80% DH	20%MS+DH
50% ME soyate + 50% DH	50%MS+DH
70% ME soyate + 30% DH	70%MS+DH
Low sulfur No.2 commercial diesel	DL
20% IP soyate + 80% DL	20%IP+DL
50% IP soyate + 50% DL	50%IP+DL
20% ME soyate + 80% DL	20%MS+DL
50% ME soyate + 50% DL	50%MS+DL
20% WME soyate + 80% D L	20%WMS+DL
50% WME soyate + 50% DL	50% WMS+DL

Because of limited fuel storage capacity, it was not possible to use the same diesel fuel for all tests. The initial series of tests on methyl soyate were conducted on a diesel fuel containing 0.24% sulfur, which was designated "high sulfur" diesel fuel. After October 1, 1993, the EPA mandated that this fuel could no longer be used for on-highway applications.

After the first test of methyl soyate, low sulfur No.2 diesel fuel was purchased. Methyl ester of soybean oil was purchased from Interchem Environmental, Inc., and iso-propyl ester of soybean oil and winterized methyl ester of soybean oil were prepared by the Food Science Department at Iowa State University. The methyl ester was purchased from Interchem Environmental, Inc. in two batches, spaced about six months apart. However, subsequent testing has shown these two batches to be virtually identical so they will not be identified separately.

3.4   Data Acquisition System

An Analog Devices RTI-820 board was used to acquire the emission data from the emission analyzers. The RTI-820 board with a Zenith 386 computer scanned the emission signal channels every second, and the data were stored in the computer for analysis. The combustion pressure data were measured with a Kistler pressure transducer and acquired with an Analog Devices RTI-860 board. The pressure data were the average of the data of 24 engine cycles. The engine crankangle signal was measured with a BEI incremental shaft encoder.

4. EXPERIMENTAL PROCEDURES AND DATA ANALYSIS

This chapter will discuss the experimental procedures used in this study. The first section will discuss the production of the fuels. The engine test procedure and test schedule are described in sections two and three. The soluble hydrocarbon extraction is presented in the fourth section. The last section will discuss data analysis.

4.1   Preparation of Fuels

The iso-propyl ester of soybean oil and winterized methyl ester of soybean oil were produced in the Food Sciences Department of Iowa State University. Although this work was not the responsibility of the author of this thesis, it is an important part of the project and will be briefly discussed.

4.1.1   Preparation of iso-propyl ester of soybean oil

To encourage the transesterification reaction of soybean oil with iso-propyl alcohol, a catalyst must be present during the reaction. Fresh catalyst was produced for each batch of fuel produced. The catalyst was synthesized by putting 18.4 g of sodium into 400 ml of iso-propyl alcohol which produced about 400 ml of $(CH_3)_2CHONa$ for one batch of processing iso-propyl ester of soybean oil. The corresponding chemical reaction equation is

$$Na + CH_3\text{-}\underset{\overset{|}{OH}}{CH}\text{-}CH_3 \longrightarrow CH_3\text{-}\underset{\overset{|}{O\text{-}Na}}{CH}\text{-}CH_3 + 0.5H_2 \qquad (4\text{-}1)$$
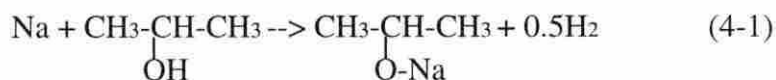
Then, 6 kg of soybean oil and 4.95 kg of iso-propyl alcohol (the mole ratio is 1:12) were mixed with the catalyst. After the mixture was stirred for 20 hours at room temperature, the products were allowed to separate into two phases. The top liquid was separated from the heavier material on the bottom. 4.2 g of acetic acid was added to the top liquid to lower its

pH value. The excess iso-propyl alcohol was removed from the iso-propyl ester by evaporation. To be more acceptable as fuel for a diesel engine, the crude iso-propyl ester was "winterized" by cooling it to about 275 K for three days so that some of the long chain, high-melting point, saturated iso-propyl esters would crystallize. The iso-propyl ester was then filtered through a 200 mesh sieve and was ready for washing. The first wash step was to add 1.6% $NaHCO_3$ in water. After that, the iso-propyl ester was washed with water [3].

4.1.2   Production of winterized methyl ester of soybean oil

A portion of the saturated (no double bonds) methyl esters will crystallize if it is cooled to sub-ambient temperatures. This causes problems when the ester is to be used as fuel because the fuel crystals may plug up the fuel filter. By separating the low-melting portions of the methyl ester of soybean oil, it may be possible to have better fuel properties than that of normal methyl ester of soybean oil.

All of the winterized methyl ester used in this project was prepared in two batches. For each batch, 33.5 kg of methyl ester of soybean oil and 79.3 kg of hexane were mixed and placed into a large metal drum. The mixture was progressively cooled to 251.65 K, 248.15 K and 244.75 K for 4-7 days at each temperature. At the cold temperatures, the saturated methyl esters crystallized and settled to the bottom. After each cooling, the upper liquid fraction was separated from the lower crystalline fraction by decanting, and the liquid portion was cooled again to the next lower temperature.   After the third crystallization, the hexane was removed by evaporation [3].

4.2   Steady-state Engine Test Procedures

The engine test procedures described below were largely dictated by the small amounts of fuel available for testing. There were four fuel groups and each of them included No.2 diesel fuel for the purpose of comparison. The first test was carried out at two different

engine conditions: 20% of the maximum torque at 1400 rpm, and 100% of the maximum torque at 1400 rpm. Three different blend proportions of methyl ester and high sulfur No.2 diesel fuel were used. Later tests of the iso-propyl ester, methyl ester (second test) and winterized methyl ester were only tested at one engine condition, 100% of full load at 1400 rpm. The engine conditions and fuels are shown in Table 4.1

At the beginning of each test day, all emission measurement equipment was calibrated with zero and span gases. The zero gas was usually compressed air, and the span gases were different for each analyzer. The filters were weighed with the Mettler micro-balance after having been allowed to equilibrate in the weighing chamber for 48 hours. The weighing procedure is described in Appendix F.

Before starting the engine, the primary dilution air was run through the dilution tunnel and the particulate sampling system for at least five minutes to keep the surfaces of the tunnel and the sampling system free of deposits that could remain from previous tests.

When the engine was started, the speed and load were set at 1400 rpm and 100% rated load. After the engine reached the equilibrium operating conditions as indicated by stable coolant and oil temperatures, the computer program used to collected the emission data was started. The program could also be used to calculate the approximate dilution ratio when the primary dilution air pressure and temperature, the pressure drop of the intake air laminar flow element and the intake air temperature were entered. After two particulate sample filters were placed in the filter holder shown in Figure 3.3, the particulate sample transfer valve was opened, and the sampling pump was started. A stopwatch was also started at this time, and the weight of the fuel-supply tank was recorded. The electronic counter shown in Figure 3.3 displayed the instantaneous particulate sample flow rate. The emission program automatically recorded emission analyzer readings and the engine inlet-air flow rate. During the test, the sampling pump bypass valve was manually adjusted to maintain the particulate sample flow rate within 3% of 0.1982 m^3/min. (7ft^3/min.). The data shown in Table 3.2, as well as the atmospheric pressure, the voltage of the pressure transducer in the dilution-air line and the engine coolant flow rate were also manually recorded.

Table 4.1   Fuel blends and engine test conditions

	1400 rpm 100% of full load	1400 rpm 20% of full load
Group one	DH 20%MS+DH 50%MS+DH 70%MS+DH	DH 20%MS+DH 50%MS+DH 70%MS+DH
Group two	DL 20%IP+DL 50%IP+DL	- - -
Group three	DL 20%MS+DL 50%MS+DL	- - -
Group four	DL 20%WMS+DL 50%WMS+DL	- - -

The steady state tests were 15 minutes in length. The length was chosen so that the particulate filters could accumulate a sample of at least 10 mg under the condition of 20% of full load. The measurement error of the Mettler micro-balance was $\pm$ 0.03 mg. Therefore, for samples of at least this size, the error in each weighing is no greater than $\pm$ 0.3%.

The gaseous emission data of CO, HC, CO_2 and O_2 were collected at one second intervals for 12 minutes. Since NO and NO_x could not be measured simultaneously, NO_x was

recorded for the first six minutes, and NO for the second six minutes. After the emission data were taken, another program was used to record the combustion pressure in the cylinder. This program could record 24 engine cycles of pressure data with data taken every quarter degree of engine crankangle. The average of these 24 engine cycles was saved in the computer for further analysis.

At the end of the tests, the particulate sampling pump was shut off, the sample line valve of diluted exhaust gas was turned off, and the test duration, the weight of the fuel-supply tank and the total volume of particulate sample gas that passed through the sampling system were recorded. The filters were removed from the filter holders and placed in the weighing chamber for stabilization. The engine was then brought to another steady state condition according to the test schedule. After the engine had run at the given condition for at least 30 minutes to reach steady state, a new pair of particulate sampling filters were placed into the filter holder and the entire test procedure repeated. When the fuel was changed, the engine was run for one hour to clear all previous fuel out of the engine fuel system. At the end of the test day, the emission analyzers were calibrated again to check for any shift in response.

The particulate sampling filters were weighed twice after equilibrating in the weighing chamber for 24 and 48 hours. The difference between the final weight and the weight before sampling was considered to be the particulate mass.

4.3   Test Schedule

At least three sets of data were collected for each engine condition and each fuel so that the repeatability of the tests could be investigated. The first test with methyl ester in high sulfur diesel fuel was carried out over three days under two different engine conditions, but the tests with iso-propyl ester, methyl ester (second test), and winterized methyl ester were each conducted during only one day at one engine condition due to the small amount of fuel that was available. Table 4.2 shows the test schedules for the six days of steady state tests. No.2 diesel fuel was used in each test as a reference fuel. The first three days of tests were

Table 4.2   Test Schedules

DAY ONE TEST

Speed rpm	Load % of full load	Fuel	Time Period	Comment
1400	100	DH	1 hour	warm up
1400	100	DH	15 min.	collecting data
1400	20	DH	30 min.	stabilization
1400	20	DH	15 min.	collecting data
1400	100	20%MS+DH	1 hour	clearing
1400	100	20%MS+DH	15 min.	collecting data
1400	20	20%MS+DH	30 min.	stabilization
1400	20	20%MS+DH	15 min.	collecting data
1400	100	50%MS+DH	1 hour	clearing
1400	100	50%MS+DH	15 min.	collecting data
1400	20	50%MS+DH	30 min.	stabilization
1400	20	50%MS+DH	15 min.	collecting data
1400	100	70%MS+DH	1 hour	clearing
1400	100	70%MS+DH	15 min.	collecting data
1400	20	70%MS+DH	30 min.	stabilization
1400	20	70%MS+DH	15 min.	collecting data

Table 4.2 (continued)

DAY TWO TEST

Speed rpm	Load % of full load	Fuel	Time Period	Comment
1400	20	70%MS+DH	1 hour	warm up
1400	20	70%MS+DH	15 min.	collecting data
1400	100	70%MS+DH	30 min.	stabilization
1400	100	70%MS+DH	15 min.	collecting data
1400	20	50%MS+DH	1 hour	clearing
1400	20	50%MS+DH	15 min.	collecting data
1400	100	50%MS+DH	30 min.	stabilization
1400	100	50%MS+DH	15 min.	collecting data
1400	20	20%MS+DH	30 min.	clearing
1400	20	20%MS+DH	15 min.	collecting data
1400	100	20%MS+DH	30 min.	stabilization
1400	100	20%MS+DH	15 min.	collecting data
1400	20	DH	30 min.	clearing
1400	20	DH	15 min.	collecting data
1400	100	DH	30 min.	stabilization
1400	100	DH	15 min.	collecting data

Table 4.2 (continued)

DAY THREE TEST

Speed rpm	Load % of full load	Fuel	Time Period	Comment
1400	100	DH	1 hour	warm up
1400	100	DH	15 min.	collecting data
1400	20	DH	30 min.	stabilization
1400	20	DH	15 min.	collecting data
1400	100	20%MS+DH	1 hour	clearing
1400	100	20%MS+DH	15 min.	collecting data
1400	20	20%MS+DH	30 min.	stabilization
1400	20	20%MS+DH	15 min.	collecting data
1400	100	50%MS+DH	1 hour	clearing
1400	100	50%MS+DH	15 min.	collecting data
1400	20	50%MS+DH	30 min.	stabilization
1400	20	50%MS+DH	15 min.	collecting data
1400	100	70%MS+DH	1 hour	clearing
1400	100	70%MS+DH	15 min.	collecting data
1400	20	70%MS+DH	30 min.	stabilization
1400	20	70%MS+DH	15 min.	collecting data

Table 4.2 (continued)

DAY FOUR TEST

Speed rpm	Load % of full load	Fuel	Time Period	Comment
1400	100	DL	1 hour	warm up
1400	100	DL	15 min.	collecting data
1400	100	20%IP+DL	45 min.	clearing
1400	100	20%IP+DL	15 min.	collecting data
1400	100	50%IP+DL	45 min.	clearing
1400	100	50%IP+DL	15 min.	collecting data
1400	100	DL	1 hour	warm up
1400	100	DL	15 min.	collecting data
1400	100	20%IP+DL	45 min.	clearing
1400	100	20%IP+DL	15 min.	collecting data
1400	100	50%IP+DL	45 min.	clearing
1400	100	50%IP+DL	15 min.	collecting data
1400	100	DL	1 hour	clearing
1400	100	DL	15 min.	collecting data
1400	100	20%IP+DL	45 min.	clearing
1400	100	20%IP+DL	15 min.	collecting data
1400	100	50%IP+DL	45 min.	clearing
1400	100	50%IP+DL	15 min.	collecting data

Table 4.2 (continued)

DAY FIVE TEST

Speed rpm	Load % of full load	Fuel	Time Period	Comment
1400	100	DL	1 hour	warm up
1400	100	DL	15 min.	collecting data
1400	100	20%MS+DL	1 hour	clearing
1400	100	20%MS+DL	15 min.	collecting data
1400	100	50%MS+DL	1 hour	clearing
1400	100	50%MS+DL	15 min.	collecting data
1400	100	DL	1 hour	warm up
1400	100	DL	15 min.	collecting data
1400	100	20%MS+DL	1 hour	clearing
1400	100	20%MS+DL	15 min.	collecting data
1400	100	50%MS+DL	1 hour	clearing
1400	100	50%MS+DL	15 min.	collecting data
1400	100	DL	1 hour	clearing
1400	100	DL	15 min.	collecting data
1400	100	20%MS+DL	1 hour	clearing
1400	100	20%MS+DL	15 min.	collecting data
1400	100	50%MS+DL	1 hour	clearing
1400	100	50%MS+DL	15 min.	collecting data

Table 4.2 (continued)

DAY SIX TEST

Speed rpm	Load % of full load	Fuel	Time Period	Comment
1400	100	DL	1 hour	warm up
1400	100	DL	15 min.	collecting data
1400	100	20%WMS+DL	30 min.	clearing
1400	100	20%WMS+DL	15 min.	collecting data
1400	100	50%WMS+DL	30 min.	clearing
1400	100	50%WMS+DL	15 min.	collecting data
1400	100	DL	1 hour	warm up
1400	100	DL	15 min.	collecting data
1400	100	20%WMS+DL	30 min.	clearing
1400	100	20%WMS+DL	15 min.	collecting data
1400	100	50%WMS+DL	30 min.	clearing
1400	100	50%WMS+DL	15 min.	collecting data
1400	100	DL	1 hour	clearing
1400	100	DL	15 min.	collecting data
1400	100	20%WMS+DL	30 min.	clearing
1400	100	20%WMS+DL	15 min.	collecting data
1400	100	50%WMS+DL	30 min.	clearing
1400	100	50%WMS+DL	15 min.	collecting data

based on different proportions of methyl ester to high sulfur No.2 diesel fuel under the same engine speed, but with two different loads, 100% and 20% of full load. Each day at the beginning of the test, the engine was run for one hour to warm up and stabilize.

As shown in Table 4.2, the day one tests were a variety of load and fuel combinations at 1400 rpm. Diesel fuel was supplied to the engine at 100% of full load for one hour to warm up the engine. After the engine reached steady state, a 15 minute period was used to collect the emission data. Then, the engine was changed to 20% of full load at the same speed and the engine was run for 30 minutes to stabilize and 15 minutes for the actual test. After these two test conditions, the fuel was changed. The fuel blend identified as 20%MS+DH was supplied to the engine, and the same conditions were repeated. Following that, the fuels were changed to the blend of 50%MS+DH, and 70%MS+DH. The schedule for day two tests used the same engine conditions and the same fuels, but the test order was reversed from the day one test. On day three, day one tests were repeated to check the reproducability of the tests.

On test days 4 to 6, low sulfur No.2 diesel fuel was used as the reference fuel. The fuels which were tested on day four were No.2 diesel (DL), 20%IP+DL and 50%IP+DL. Only one engine condition was used in this test, 1400 rpm and 100% of full load. The choice of test condition was based on the amount of fuel available, since only 8 gallons of iso-propyl ester were available. The shortage of fuel also dictated a shorter period of operation between fuels, but it is still believed to have been adequate to purge the system.

After the emission data of No.2 diesel fuel was recorded, the engine was run for 30 minutes at 1400 rpm and 100% of full load to shift to 20%IP+DL. Then, the particulate sample was taken for 15 minutes. For 50%IP+DL, the test followed the same procedure. After these three fuels were tested, the engine was fueled with No.2 diesel fuel for one hour and the same test procedure was repeated two more times in the same day.

To compare the effects of methyl ester and iso-propyl ester when blended with the same No.2 diesel fuel, the methyl ester was blended with the low sulfur No.2 diesel fuel, and tested following the same procedure as that of the iso-propyl ester described above.

The winterized methyl ester was tested on day six. Because of the small amount of winterized methyl ester available, the same test procedure described above for the iso-propyl ester was used.

4.4 Soluble Hydrocarbon Extraction

The particulates that were sampled from the engine exhaust gas were not only solid carbon and sulfate emissions, but also included adsorbed and condensed hydrocarbons commonly termed the "soluble organic fraction (SOF)". To characterize the amount of soluble material, the particulate filters were extracted with methylene chloride to determine the proportion of SOF in the particulates.

After the particulate-loaded filter was stabilized in the weighing chamber for 48 hours, it was put into an extraction thimble and the filter and thimble were weighed together. Then, the thimble was placed in a Pyrex Soxhlet extractor. 100 ml methylene chloride was poured into a flask at the bottom of the Soxhlot tube. After the power for the solvent heater was turned on, cooling water was passed through the top condenser. Each filter was extracted from 60 to 70 cycles (about 4 hours).

The thimble with the extracted filter was placed in a heated chamber for one hour after the last cycle was finished. The temperature in the chamber was kept about 315 K, which is just above the boiling point of methylene chloride to evaporate the solvent quickly and completely. The thimble and filter were then set in the weighing chamber for 48 hours. At the end of that period, they were weighed. The difference in the weight before extraction and after extraction was considered to be the mass of SOF.

4.5   Data Analysis

To compare the emission levels and fuel economy among these fuels, the data should be converted to the units of g/kW-hr, known as a "brake specific" basis. This requires the de-

velopment of a balanced chemical equation for the combustion reaction. This equation requires a chemically-correct expression for the fuel. This section will discuss how to determine the average "pseudo-molecular weight" of methyl and iso-propyl esters of soybean oil, the equivalent chemical formula, and the heating value of the fuel blends. Further, since the humidity of the inlet air has an effect on the amount of oxide of nitrogen formed during combustion [66], a humidity correction was applied to the measured oxide of nitrogen value to correct for variations in the inlet air humidity. Finally, heat release analysis was performed to investigate the combustion process. The details of the data-reduction calculation are presented in this section.

4.5.1 Calculation of molecular weight, equivalent chemical formula, and heating value

It is often helpful to define an equivalent fuel molecule for fuels containing mixtures of many different compounds. It is possible to use ASTM tests for molecular weight such as D2502 and D2503 to determine the apparent molecular weight of the mixtures. Then, using measured values of the weight percentage of carbon and hydrogen, an equivalent fuel molecule C_xH_y can be developed, that has the proper H/C ratio and apparent molecular weight.

Standard techniques for measuring molecular weight of hydrocarbon are not appropriate for esters. Therefore, a "pseudo-molecular weight" is calculated using the approach normally used for ideal gases, of calculating the molecular weight as the mole fraction-weighted average of the molecular weight of the constituents. The measured chemical composition of the commercial methyl ester of soybean oil and iso-propyl ester of soybean oil will be presented in Table 5.1. The average pseudo-molecular weight of both esters can be determined as:

$$\overline{M} = \sum_{i=1}^{n} y_i \times M_i \qquad (4\text{-}2)$$

where $\overline{M}$ = average pseudo-molecular weight of ester.

y$_i$ = mole fraction of component i in ester.

M_i = molecular weight of component i in ester.

n = the number of components in the ester.

The equivalent chemical formula of the esters can be written as $C_xH_yO_z$, where x, y and z represent equivalent carbon, hydrogen and oxygen atomic numbers in the ester. The values of x, y, and z can be calculated as follows:

$$x = \sum_{i=1}^{n} y_i \times N_{Ci} \tag{4-3}$$

$$y = \sum_{i=1}^{n} y_i \times N_{Hi} \tag{4-4}$$

$$z = \sum_{i=1}^{n} y_i \times N_{Oi} \tag{4-5}$$

where N_{Ci} = number of carbon atoms in component i.

N_{Hi} = number of hydrogen atoms in component i.

N_{Oi} = number of oxygen atoms in component i.

The chemical formula of diesel fuel can be calculated from the measured values of the average molecular weight and the hydrogen to carbon ratio. The results of tests from Phoenix Chemical Laboratory, Inc. will be shown in Table 5.2. The chemical formula of diesel fuel is usually written as C_xH_y. The carbon number, x, and hydrogen number, y, can be obtained by solving the linear equations:

$$12.01x + 1.009y = M_{diesel} \tag{4-6}$$

$$\frac{12.01x}{1.009y} = R_{C/H} \tag{4-7}$$

where M_{diesel} = average molecular weight of No.2 diesel fuel, and

$R_{C/H}$ = mass ratio of carbon to hydrogen in No.2 diesel fuel.

For fuel blends of ester and No.2 diesel fuel, its pseudo-molecular weight can be obtained as:

$$M_b = y_d M_{diesel} + y_e \overline{M} \tag{4-8}$$

where M_b = average pseudo-molecular weight of the fuel blends.

y_d = mole fraction of diesel in the fuel blend.

y_e = mole fraction of ester in the fuel blend.

$\overline{M}$ = average pseudo-molecular weight of ester.

After determining the molecular weight and chemical formula of the ester and diesel fuel, the equivalent chemical formula can be obtained in the same way as discussed above. The equivalent chemical formula of the fuel blend is written as $C_xH_yO_z$, where x, y and z represent the carbon, hydrogen and oxygen atom numbers, respectively.

$$x = y_d N_{Cd} + y_e N_{Ce}$$

$$y = y_d N_{Hd} + y_e N_{He} \tag{4-9}$$

$$z = y_d N_{Od} + y_e N_{Oe}$$

where y_d and y_e = mole fraction of diesel and ester in the fuel blend.

N_{Cd} and N_{Ce} = carbon atom numbers in diesel and ester.

N_{Hd} and N_{He} = hydrogen atom numbers in diesel and ester.

N_{Od} and N_{Oe} = oxygen atom numbers in diesel and ester.

The lower heating value of the fuel blend also is determined according to the mass fractions and lower heating value of the ester and diesel fuel in the blended fuels.

4.5.2 Humidity calculation and correction factor for oxides of nitrogen

The NOx humidity correction recommended by the Society of Automotive Engineers [67] requires the value of specific humidity of the inlet air (g H2O/kg of dry air).

The specific humidity, H, is found from the following equations:

$$H = \frac{621.10P_v}{P_b - P_v} \qquad (4\text{-}10)$$

where H = specific humidity (g H2O/kg of dry air).

P_b = observed barometric pressure (kPa).

P_v = partial pressure of water vapor (kPa).

The partial pressure of water vapor can be determined from Ferrel's equation [68]:

$$P_v = P_w - 1.80A \times P_b\left(T_d - T_w\right) \qquad (4\text{-}11)$$

where P_w = saturation pressure of water vapor at the wet bulb temperature (kPa).

T_d = dry bulb temperature (°C).

T_w = wet bulb temperature (°C).

A = experimentally derived constant, $A = 3.67\times10^{-4}(1 + 0.001152T_w)$

The saturation pressure of water vapor at the wet bulb temperature is:

$$P_w = 0.6048346 + 4.59058 \times 10^{-2}T_w + 1.2444 \times 10^{-3}T_w^2 + 3.52248 \times 10^{-5}T_w^3 +$$

$$9.32206 \times 10^{-8}T_w^4 + 4.18128 \times 10^{-9}T_w^5 \qquad (4\text{-}12)$$

which is a least-squares fit of Keenan and Keye's steam table [69].

The corrected oxides of nitrogen concentration can be calculated as [67]:

$$[NO]_{corr} = [NO]_{wet} \times \frac{1}{k} \qquad (4\text{-}13)$$

where $[NO]_{corr}$ = corrected NO concentration (ppm).

$[NO]_{wet}$ = measured NO concentration on a wet basis (ppm).

$k = 1+7A(H - 10.714) + 1.8B(T - 29.444)$.

$A = 0.044(F/A) - 0.0038$.

$B = -0.116(F/A)+0.0053$.

T = intake air temperature ($^\circ$C).

F/A = fuel-air ratio (dry basis).

H = specific humidity (g H_2O/kg of dry air).

4.5.3   Calculations of particulate emission level from measured values

The total mass of particulates emitted by the engine during the test period is found from the following equation:

$$m_p = m_s \times \frac{\dot{m}_{dilexh}}{\dot{m}_{sample}} \qquad (4\text{-}14)$$

where m_p = total particulate mass emitted during the test.

m_s = mass collected on the filters during the test.

$\dot{m}_{dil\ exh}$ = mass flow rate of diluted exhaust in the dilution tunnel.

m_{sample} = mass flow rate of diluted exhaust which passed through the particulate sampling system.

During the engine tests, the mass flow rate of the sample was held constant, and the sample temperature was measured just before the ROOTS flow meter. The sample flow rate was calculated as:

$$m_{sample} = \frac{P_s \times V_s}{R_s \times T_s}$$ (4-15)

where P_s = particulate sample pressure at the ROOTS meter. Here P_s was assumed to be equal to atmospheric pressure (negligible pressure drop across the ROOTS gas meter)

$\dot{V}s$ = volumetric flow rate of sample gas through the ROOTS meter.

R_s = gas constant of sample which is assumed to be the same as air.

T_s = sample temperature.

The mass flow rate of diluted exhaust gas in the dilution tunnel is calculated by the equation:

$$\dot{m}_{dil\ exh} = \dot{m}_{dil\ air} + \dot{m}_{in\ air} + \dot{m}f$$ (4-16)

where $\dot{m}_{dil\ air}$ = mass flow rate of dilution air which was determined by the dilution air system calibration equation in Appendix B.

$\dot{m}_{in\ air}$ = mass flow rate of engine intake air measured by the laminar flow element.

$\dot{m}f$ = fuel mass flow rate.

4.5.4   Heat release analysis

To investigate the combustion behavior of methyl and iso-propyl esters of soybean oil, a heat release analysis was performed. The theory behind the heat release combustion model used here can be found in Krieger and Borman [70]. The model simply computes an apparent fuel burning rate from experimental pressure data. This model assumes thermodynamic equilibrium at each instant in the engine cylinder during combustion which means that the entire cylinder contains a homogeneous mixture of air and combustion products at each instant. Phenomena such as temperature gradients, pressure waves, nonequilibrium composition, fuel vaporization, mixing and so on are ignored in this model.

The burning is assumed to take place incrementally as homogeneous combustion and acts as a uniformly distributed heat source. The equation of energy for the closed cylinder is written as:

$$\frac{d}{dt}(Mu) = -p\frac{dV}{dt} + \sum_i \dot{Q} + h_f\frac{dM}{dt} \qquad (4\text{-}17)$$

where M = total in cylinder fuel mass.

u = internal energy of fuel.

V = volume of cylinder.

P = pressure in cylinder.

h_f = enthalpy of fuel.

t = time.

$\dot{Q}$ = heat transfer rate between combustion gas and cylinder well.

It is convenient to use the following relationships to solve this equation

$$\frac{du}{dt} = \frac{\partial u}{\partial T} \frac{\partial T}{\partial t} + \frac{\partial u}{\partial p} \frac{\partial p}{\partial t} + \frac{\partial u}{\partial F} \frac{\partial F}{\partial t} \tag{4-18}$$

$$\frac{dR}{dt} = \frac{\partial R}{\partial T} \frac{\partial T}{\partial t} + \frac{\partial R}{\partial p} \frac{\partial p}{\partial t} + \frac{\partial R}{\partial F} \frac{\partial F}{\partial t} \tag{4-19}$$

where T = combustion gas temperature.

          F = equivalence ratio.

          R = gas constant.

The internal energy and gas constant can be calculated from equilibrium considerations as functions of temperature, pressure and equivalence ratio [71]. The equivalence ratio at any instant is given by

$$F = F_0 + (\frac{M}{M_0} - 1) \left(\frac{1+f_0}{f_s} \right) \tag{4-20}$$

$$\frac{dF}{dt} = \left(\frac{1+f_0}{f_s M_0} \right) \frac{dM}{dt} \tag{4-21}$$

where F_0 = initial equivalence ratio.

          f_0 = initial fuel-air ratio.

          f_s = stoichiometric fuel-air ratio.

M_0 = initial mass in the cylinder.

The equation of energy can thus be solved for the apparent fuel burning rate

$$\frac{1}{M}\frac{dM}{dt} = \frac{\frac{-RT}{V}\frac{dV}{dt} - \frac{\partial u}{\partial p}\frac{\partial p}{\partial t} + \frac{1}{M}\sum_i \dot{Q} - C(B)}{u - h_f + D\frac{\partial u}{\partial F} - C\left(1 + \frac{D}{R}\frac{\partial R}{\partial F}\right)} \qquad (4\text{-}22)$$

where $B = \frac{1}{p}\frac{dp}{dt} - \frac{1}{R}\frac{\partial R}{\partial p}\frac{dp}{dt} + \frac{1}{V}\frac{dV}{dt}$

$$C = T\frac{\partial u}{\partial T} \Big/ \left(1 + \frac{T}{R}\frac{\partial R}{\partial T}\right)$$

$$D = \frac{(1 + f_0)M}{f_s M_0}$$

These equations can be solved numerically to obtain the fuel burning rate as a function of crankangle provided the initial values of mass in the cylinder and equivalence ratio are specified with the cylinder pressure supplied from experimental data.

4.5.5 Statistical analysis

Statistical analyses were performed on the data for engine performance and emissions among each fuel group using multiway analysis of variance (ANOVA) and multiple comparison method. Least significant difference (LSD) was used to determine whether or not there was a significant difference between each pair of fuels within a fuel group. A significance level of 0.05 (95% confidence interval) was used for all ANOVA analyses.

5.   RESULTS AND DISCUSSION

The performance, combustion and emissions of a diesel engine fueled with methyl and iso-propyl esters of soybean oil are discussed in this chapter. Because fuel properties can affect engine emissions, the first section will discuss the changes in fuel properties caused by blending methyl and iso-propyl esters with diesel fuel. In sections two and three, engine performance and exhaust emissions of the tested fuels will be examined. Heat release analysis of the different fuels will be presented in the last section.

5.1   Fuel Properties

Table 5.1 shows the fatty acid compositions of the esters of soybean oil, and Table 5.2 and 5.3 are the results of fuel property tests from Phoenix Chemical Laboratory, Inc. Petroleum-based diesel fuels have very different chemical structures from methyl and iso-propyl esters of vegetable oils. Diesel fuel contains only carbon and hydrogen atoms. Most of these atoms are arranged in straight chain or branched chain structures called paraffin molecules. Some of the fuel also consists of circular rings of carbon atoms. These rings are called "cyclo-paraffins" if the carbons are connected by single carbon-carbon bonds. Some of the rings have a special type of bond connecting the carbons that is between a single and double bond and these molecules are called "aromatics". Diesel fuel can also have molecules containing double bonds, called "olefins", but the olefins are not present in large amounts since they make the diesel fuel prone to oxidation during storage.

Methyl and iso-propyl esters have a different chemical structure. The normal chemical structure of vegetable oils was shown in Figure 2.2. The fatty acids vary in their carbon chain length and in the number of double bonds. The large molecule size of the methyl or iso-propyl esters, the number of double bonds, the lack of aromatic compounds, the presence of oxygen in the molecules, and the low sulfur content suggest that some fuel properties will differ from those of diesel fuel.

Table 5.1   Compositions of the esters of soybean oil

(by weight)

Fatty acid	Methyl ester		Iso-propyl ester		Winterized methyl ester	
	Formula	%	Formula	%	Formula	%
Lauric 12:0	$C_{13}H_{26}O_2$	0.50	$C_{15}H_{30}O_2$	0.00	$C_{13}H_{26}O_2$	0.00
Myristic 14:0	$C_{15}H_{30}O_2$	0.50	$C_{17}H_{34}O_2$	0.00	$C_{15}H_{30}O_2$	0.00
Palmitic 16:0	$C_{17}H_{34}O_2$	12.00	$C_{19}H_{38}O_2$	10.98	$C_{17}H_{34}O_2$	4.13
Stearic 18:0	$C_{19}H_{38}O_2$	4.00	$C_{21}H_{42}O_2$	3.79	$C_{19}H_{38}O_2$	1.06
Oleic 18:1	$C_{19}H_{36}O_2$	25.00	$C_{21}H_{40}O_2$	20.35	$C_{19}H_{36}O_2$	22.41
Linoleic 18:2	$C_{19}H_{34}O_2$	52.00	$C_{21}H_{38}O_2$	55.89	$C_{19}H_{34}O_2$	62.23
Linolenic18:3	$C_{19}H_{32}O_2$	6.00	$C_{21}H_{36}O_2$	8.99	$C_{19}H_{32}O_2$	10.17

As shown in Table 5.1, palmitic (16:0) and stearic (18:0) are the two most common saturated fatty acids in the esters of soybean oil. The methyl ester of soybean oil also contained a small amount of lauric (12:0) and myristic (14:0) fatty acids. Linoleic (18:2) was the most common unsaturated fatty acid in those fuels. All of the esters of soybean oil contained some oleic (18:1) and linolenic (18:3) fatty acids. 14.65% (by wt.) of the methyl ester, 14.77% of the iso-propyl ester and 5.19% of the winterized methyl ester were made up of saturated fatty esters, . The lower amount of saturated species in the winterized methyl ester of soybean oil provided better cold flow properties. The results shown in Table 5.2 and 5.3 will be discussed as the individual fuel properties are compared later in this section.

The soybean oil esters do not contain any aromatic molecules. Thus, they have the effect of decreasing the concentration of aromatic compounds in the blended fuels. Lower concentrations of aromatics in fuels can have significant effects on engine emissions and combustion performance. The effects of the aromatic compounds in diesel fuel on emissions have been studied by several researchers. Ryan et al. [72], Ullman et al. [73] and McCarthy et al. [74] reported that particulate and NO_x emissions increased when the concentration of aromatics increased in diesel fuel. Tosaka et al. [75] also found particulate

Table 5.2   Pure fuel properties

Fuel	DH	DL	100%MS	100%IP	100%WMS
Cetane number	46.3	47.4	59.0	52.6	51.9
Average molecular weight	198.00	195.00	-	-	-
API Gravity @60 F	34.9	33.5	-	-	28.1
Carbon %	86.46	86.41	78.16	78.48	77.99
Hydrogen %	13.32	12.97	12.06	12.21	11.39
C/H ratio	6.491	6.662	6.481	6.428	-
Sulfur %	0.24	0.045	0.020	0.021	0.012
Ash %	0.000	0.001	-	-	-
HHV kJ/kg	45360.46	45330.22	39724.42	39982.61	39828.10
LHV kJ/kg	42534.30	42577.99	37165.29	37391.65	37411.04
Hydrocarbon types, FIA % (v/v)					
Paraffins	53.8	60.3	-	-	-
Olefins	2.5	0.5	-	-	-
Aromatics	43.7	39.2	-	-	-
Viscosity @40°C, cs	2.61	3.65	-	-	-
Distillation (ASTM D86)					
Initial boiling point K	455	452	-	-	-
5% recovery K	477	472	-	-	-
10% recovery K	488	483	-	-	-
20% recovery K	503.15	500	-	-	-
30% recovery K	515	512	-	-	-
40% recovery K	526.48	524	-	-	-
50% recovery K	538	535	-	-	-
60% recovery K	548	546	-	-	-
70% recovery K	560	558	-	-	-
80% recovery K	573	569	-	-	-
90% recovery K	589	588	-	-	-
95% recovery K	601	599	-	-	-
End point K	615	618	-	-	-
Recovery %	98.0	98.0	-	-	-
Residue %	1.9	1.9	-	-	-
Loss %	0.1	0.1	-	-	-

Table 5.3   Cetane number of tested fuels

Fuels	Cetane No.
DH	46.3
DL	47.4
20%MS+DH	51.1
50%MS+DH	54.2
70%MS+DH	57.2
100%MS	59.0
20%MS+DL	50.6
50%MS+DL	53.4
20%IP+DL	49.3
50%IP+DL	50.6
100%IP	52.6
20%WMS+DL	49.0
50%WMS+DL	48.9
100%WMS	51.9

emissions rose with increasing content of aromatics in diesel fuel.

As the concentrations of methyl or iso-propyl esters were changed, the properties of the fuel blends changed also. Table 5.4 shows the calculated fuel properties of molecular weight, heating value, and equivalent chemical formula for the fuel blends.

The concept of a pseudo-molecular weight, calculated based on the mole-fraction-weighted average of the molecular weights of the constituents was presented in Chapter 4. The pseudo-molecular weight of the fuel blends increased with increasing concentration of methyl or iso-propyl ester due to the long carbon chain species in those fuels. Pure winterized methyl ester had a heavier pseudo-molecular weight than methyl ester because some saturated compounds with lighter molecular weight, such as palmitic (methyl palmitate 16:0) and stearic (methyl stearate 18:0) had be removed. Comparing the percentage of carbon and hydrogen between the results from Phoenix Chemical Laboratory, Inc. and that calculated from gas chromatograph measurements of the composition, shows very little difference. The lower heating value of the fuel blends decreased with increasing content of methyl or iso-propyl ester due to the smaller lower heating value of the ester.

The cetane numbers of the fuel blends were measured by Phoenix Laboratory, Inc., and are shown in Table 5.3 and plotted in Figure 5.1. Cetane number is a measure of the ignition quality of the fuel. Ignition quality is dependent on a number of factors such as molecular weight, fuel structure (straight-chain vs. branched-chain), volatility and chemical structure (the numbers of double bonds). The cetane number of all fuel blends was improved with increasing concentration of the fatty esters of soybean oil. As will be discussed later, the engines experienced a decrease in ignition delay when the cetane number was increased. The longer the straight carbon chains and the lower the concentration of aromatic compounds in the fuel, the higher the cetane number. The pure methyl and iso-propyl esters of soybean oil and their mixtures with diesel fuel have these characteristics. However, the esters also contain carbon-carbon double bonds that are highly susceptible to attack by oxygen as well as weaker bonded radicals such as $-CH_3$ and $-CH(CH_3)_2$. There are two possible explanations for why the esters have higher cetane numbers. During reaction, double bonds need lower energy to react. Another reason is that the cleavage of the weakly bonded

Table 5.4   Calculated properties of fuels

Fuel	Formula	M.W.[1]	C% by wt.	H% by wt.	O% by wt.	LHV[2] MJ/kg	A/F$_{stoich.}$[3]
DH	$C_{14.29}H_{26.22}$	198.00[4]	86.46	13.32	0.00	42.53	14.52
100%MS	$C_{18.68}H_{34.46}O_2$	291.28	77.02	11.93	10.99	37.17	12.46
20%MS+DH	$C_{14.92}H_{27.42}O_{0.29}$	211.55	84.70	13.07	2.19	41.46	14.11
50%MS+DH	$C_{16.06}H_{29.55}O_{0.81}$	235.75	81.82	12.63	5.50	39.85	13.49
70%MS+DH	$C_{16.98}H_{31.27}O_{1.23}$	255.21	79.91	12.35	7.71	38.68	13.08
DL	$C_{14.03}H_{25.09}$	195.00[4]	86.41	12.97	0.00	42.58	14.45
20%MS+DL	$C_{14.71}H_{26.45}O_{0.29}$	208.99	84.53	12.76	2.22	41.50	14.05
50%MS+DL	$C_{15.90}H_{28.85}O_{0.81}$	233.61	81.74	12.45	5.55	39.87	13.45
100%IP	$C_{20.76}H_{38.37}O_2$	320.06	77.90	12.08	10.00	37.39	12.65
20%IP+DL	$C_{14.92}H_{26.85}O_{0.26}$	211.53	84.71	12.79	1.97	41.54	14.09
50%IP+DL	$C_{16.58}H_{30.12}O_{0.76}$	242.35	82.16	12.53	5.02	39.99	13.55
100%WMS	$C_{18.91}H_{34.28}O_2$	293.69	77.33	11.77	10.90	37.41	12.44
20%WMS+DL	$C_{14.72}H_{26.40}O_{0.28}$	209.05	84.57	12.73	2.14	41.54	14.05
50%WMS+DL	$C_{15.98}H_{28.76}O_{0.80}$	234.38	81.88	12.37	5.46	39.99	13.44

[1]Pseudo-molecular weight.

[2]Lower heating value.

[3]Stoichiometric air-fuel ratio.

[4]Actual molecular weight measured by Phoenix Chemical Laboratory.

alcohol radicals occurs easily. Both reasons may be reducing the ignition delay by lowering the self-ignition temperature of the fuels. The pure methyl ester of soybean oil had the highest cetane number, 59.0. 100% iso-propyl ester of soybean oil had a lower cetane number than methyl ester of soybean oil because of the branched-chain in the iso-propyl radical.

The proportion of oxygen in the fuel increased with increasing concentration of soybean oil esters. The presence of oxygen in the fuel probably contributes to the observed reduction in particulate emissions and other products of incomplete combustion such as carbon
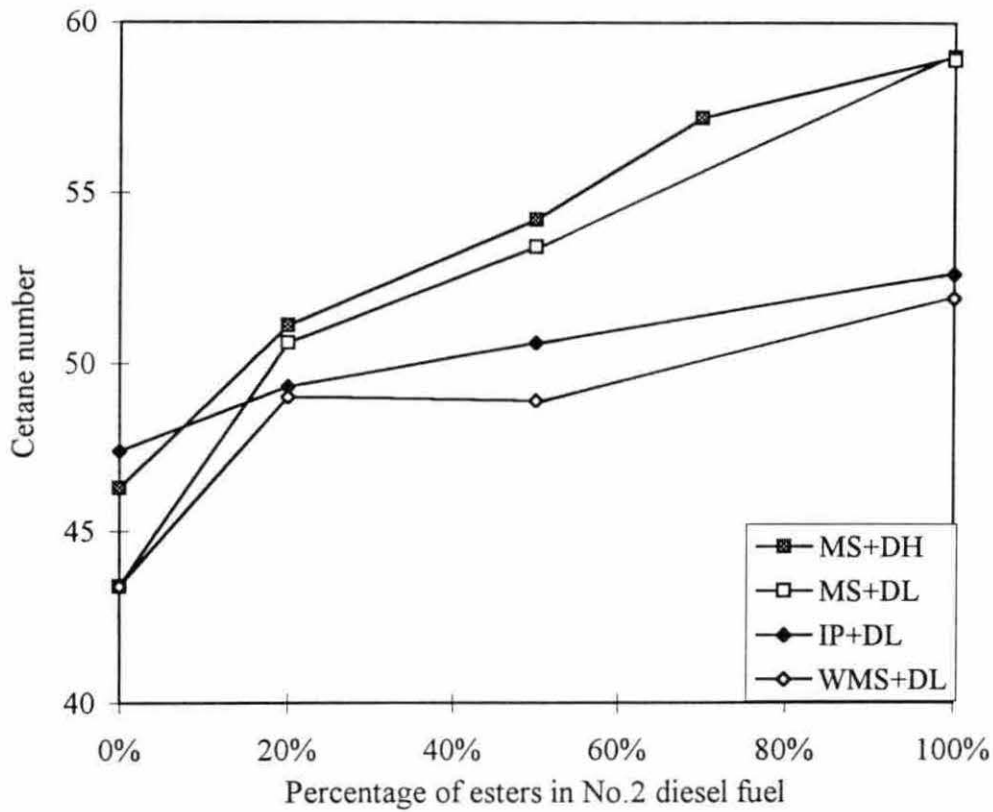
Figure 5.1   Cetane number of fuels

monoxide and unburned hydrocarbon.

The lower heating value of methyl, iso-propyl and winterized methyl esters of soybean oil was approximately 12.7%, 12.2% and 12.1% (based on mass) lower than No.2 diesel fuel, respectively. The lower heating value of the iso-propyl ester is slightly greater than the methyl ester (0.6%). This is due to the molecule of iso-propyl ester having two more carbon atoms and four more hydrogen atoms than the methyl ester.

5.2   Engine Performance

This section will discuss the impact of the soybean oil esters on the engine's power and fuel consumption. The tested fuels were divided into four groups distinguished by the three different ester fuels and with methyl ester being compared with both high and low sulfur diesel fuels. Each fuel group included the diesel fuel itself as a reference fuel. Table 5.5 presents engine performance results that are the average of three tests for each fuel. They were analyzed statistically. The alphabetical superscripts shown in Table 5.5 indicate whether the change in that quantity is different from the other values by a statistically significant amount at the 95% level of significance. For example, the values of bsfc for DH and 20%MS+DH are different, but the fact that both have a superscript of "a" indicates the change is not statistically significant. For 50%MS+DH, the Bsfc has a superscript of "b" so it is considered to be different from the reference fuel or any fuel with a different superscript. Since the energy per unit mass of the fuel blends was lower than No.2 diesel fuel, the brake power decreased and the brake specific fuel consumption increased. Figures 5.2 and 5.3 show the relationship of engine brake power and engine brake thermal efficiency for different blend fuels at the steady state test condition of 1400 rpm and 100% of full load.

Among the same fuel group, all of the 50% fuel blends had a significant drop in brake power compared with No.2 diesel fuel, and with all of the 20% blend fuels. All of the 20% blend fuels except 20%IP+DL had a significant decrease of brake power compared with No.2 diesel fuel. The maximum change in brake power at 1400 rpm and 100% of full load was 7.9% between DL and 50%IP+DL.

Fuel blends except 20%IP+DL gave a slightly higher brake thermal efficiency than No.2 diesel fuel. The largest increase of brake thermal efficiency was 0.9% between 20%MS+DH and DH. 20%IP+DL gave a 0.9% lower brake thermal efficiency. However, the differences were still not statistically significant.

The brake specific fuel consumption (bsfc) of the ester blends was higher than for No.2 diesel fuel. The measured bsfc's of the tested fuels are shown in Figure 5.4. Since the thermal efficiency was essentially constant for all of the ester blends, most of the increase in

Table 5.5   Results of engine performance under 1400 rpm and 100% of full load[1]

Group	Fuel	Bsfc g/kW hr	Brake power kW	Thermal efficiency %
One	DH	227.9^a	42.69^a	37.15^a
	20%MS+DH	231.6^a	42.12^b	37.50^a
	50%MS+DH	242.7^b	41.12^c	37.22^a
	70%MS+DH	249.0^c	40.42^d	37.29^a
Two	DL	226.4^a	42.97^a	37.35^a
	20%IP+DL	234.2^b	41.64^a	37.41^a
	50%IP+DL	240.6^c	39.59^b	37.42^a
Three	DL	226.4^a	42.87^a	37.35^a
	20%MS+DL	231.9^b	42.36^b	37.41^a
	50%MS+DL	241.2^c	41.23^c	37.43^a
Four	DL^2	228.3^a	43.30^a	37.04^a
	20%WMS+DL^2	233.7^b	42.61^b	37.08^a
	50%WMS+DL^2	242.8^c	41.52^c	37.07^a

[1]In the same fuel group, after ANOVA, values within a column with different superscript letters are significantly different (probability<0.05).

[2]Test after drive shaft changed.
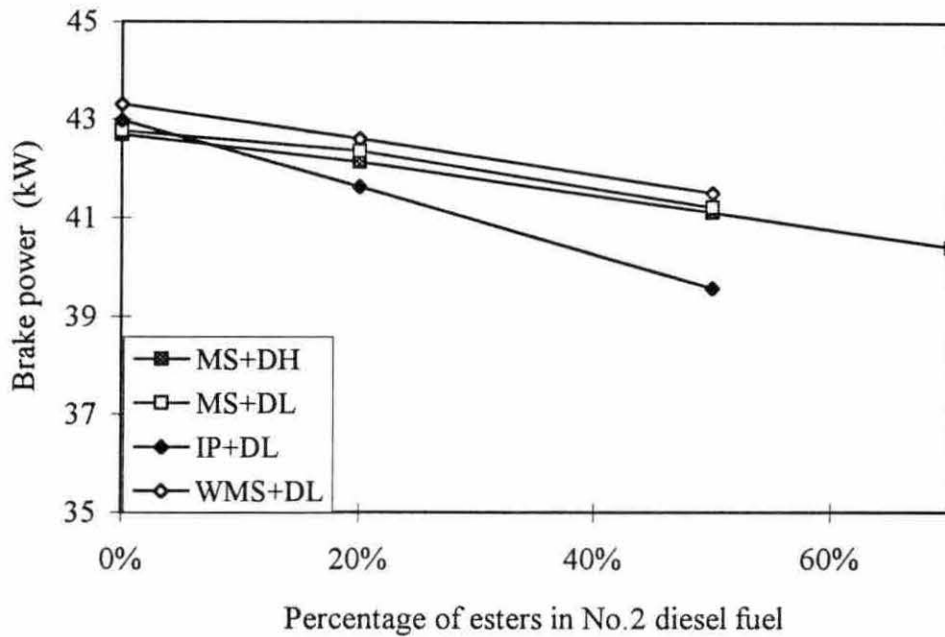
Figure 5.2   Brake power for different fuel blends at 100% load
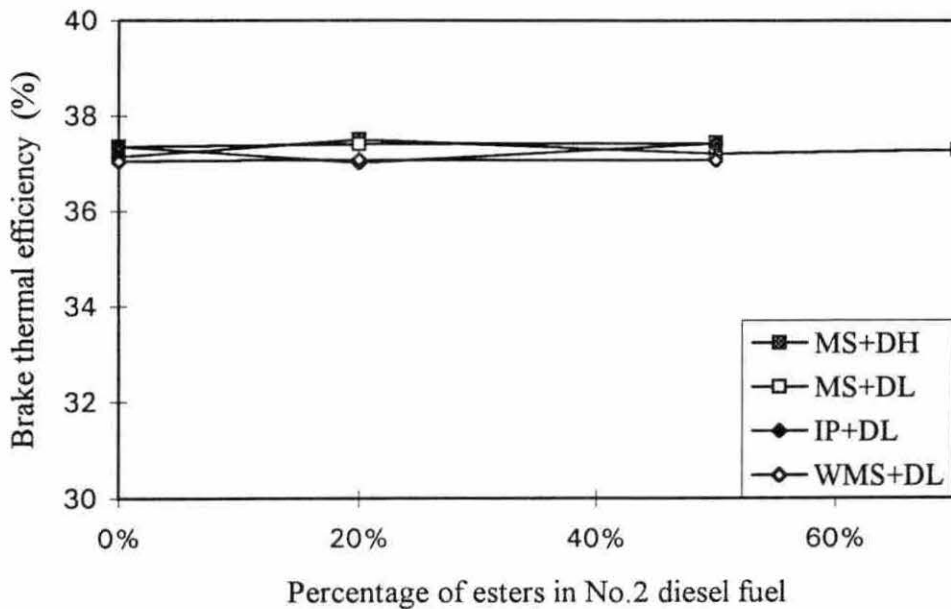
Figure 5.3   Engine brake thermal efficiency for different fuel blends at 100% load
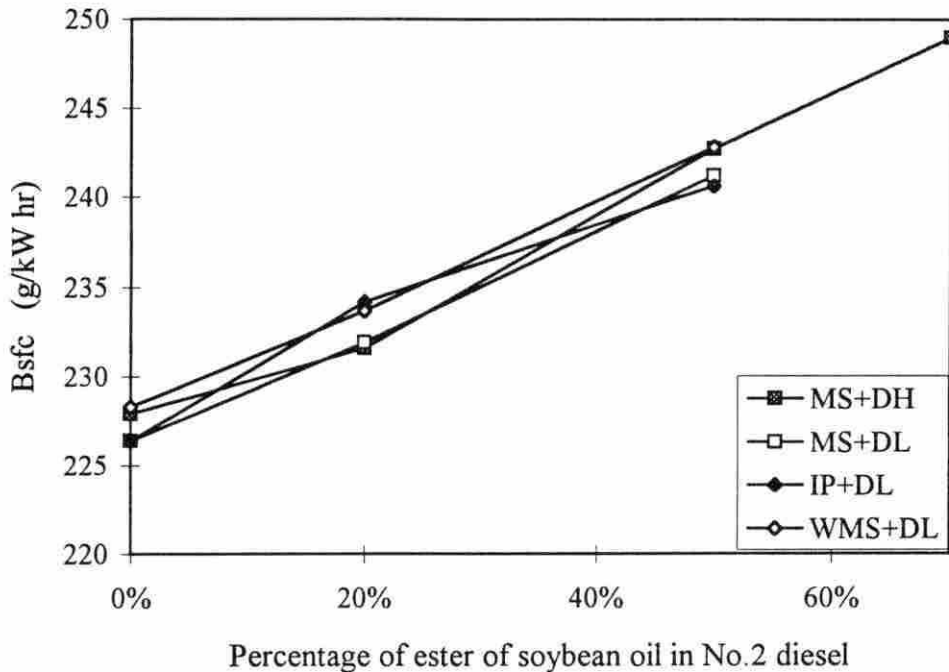
Figure 5.4   Brake specific fuel consumption for different fuel blends at 100% load

bsfc can be attributed to the decrease in power discussed above. The highest increase of bsfc is 9.3% for the fuel 70%MS+DH. This was because the proportion of lower energy density fuel, methyl ester of soybean oil, was a maximum in this fuel blend. All fuel blends with 50% ester increased in bsfc significantly compared with No.2 diesel fuel. The 20% fuel blends also had a significant increase of bsfc for 20%MS+DH. For fuel blends with the same concentration of methyl or iso-propyl ester of soybean oil, the bsfc's were very close.

As mentioned above, the lower heating value of the ordinary winterized methyl ester of soybean oil was about 12.7% and 12.1% lower than No.2 diesel fuel, respectively, and the iso-propyl ester was about 12.2% lower. This is probably the most important reason why the fuel consumption was higher and the brake power was lower than for No.2 diesel fuel.

A decrease in power and an increase in brake specific fuel consumption when the diesel engine was fueled with esters of soybean oil has been observed by other researchers. Wagner et al. [8] fueled a diesel engine with methyl, ethyl and butyl esters of soybean oil, and reported that brake specific fuel consumption was 12% higher for all the esters than for the reference fuel, but the thermal efficiency was very similar among those tested fuels.

5.3   Emissions of the Diesel Engine Fueled with Fuel Blends

All emission data were collected under steady state test conditions of 1400 rpm. Two load conditions were considered: 100% of full load and 20% of full load. All measurements were replicated three times. Table 5.6 shows the average of emission results under the given test conditions.

Between the test of MS+DL and WMS+DL, there was a period of more than one month due to a mechanical problem associated with the drive shaft connecting the engine and dynamometer. The drive shaft was changed before the tests were continued. A shift in the engine's baseline emissions was observed in the tests following this change. The particulate emissions increased substantially compared with the previous test. After the last test, all four fuel injectors of the diesel engine were removed and inspected. Carbon deposits were found around each of the four orifices of the injectors as shown in Figure 5.5. The deposit build-up may have affected the fuel spray, the formation of droplets and the air-fuel mixture, causing poorer quality combustion. The change in combustion characteristics could lead to some of the observed changes in emissions and engine performance. This phenomenon was observed by other researchers when they tested unmodified vegetable oils in diesel engines [40, 43, 44, 76, 77]. However, no reports have been found on the formation of carbon deposits on injector nozzles when the esters of vegetable oils were tested. Another possible reason for the changes is that soot deposits on the surface of the dilution tunnel from previous tests fell off during the test. Another problem may have been that the seal on the air filter in the compressed air line was poor due to excessive installation torque. Particles in the dilution air supply could have entered the dilution tunnel. Changing the drive shaft

Table 5.6   Emissions of tested fuels under 1400 rpm, 100% of full load[1]

Fuel	Brake specific emissions g/kW hr						
	CO	HC	NO	NO_x	PM^2	SOL^3	SOF^4 %
Group one							
DH	2.3636^a	0.9700^a	11.3069^a	20.3711^a	0.5359^a	0.4742^a	11.5265^a
20%MS+DH	2.2380^{ab}	0.9408^a	11.2454^a	20.5026^a	0.4619^b	0.3946^b	14.6059^b
50%MS+DH	1.9845^{ab}	0.8762^b	11.1923^a	20.3983^a	0.4031^c	0.2986^c	25.8643^c
70%MS+DH	1.8718^b	0.8225^c	11.6411^a	20.9390^a	0.3994^c	0.2701^c	32.3434^d
Group two							
DL	1.8114^a	0.7769^a	11.4548^a	21.6089^a	0.4314^a	0.3654^a	15.3115^a
20%IP+DL	1.7341^a	0.5977^b	12.2883^b	23.3870^b	0.3503^b	0.2851^b	18.6161^a
50%IP+DL	1.6314^a	0.5517^b	12.4181^b	24.2174^c	0.3106^b	0.1633^c	47.3233^b
Group three							
DL	1.9731^a	0.6299^a	11.3639^a	20.9404^a	0.4331^a	0.3666^a	15.4272^a
20%MS+DL	1.8095^a	0.6475^a	11.3525^a	21.3401^a	0.3914^b	0.3200^b	18.2423^a
50%MS+DL	1.4731^b	0.5836^a	11.3718^a	21.6902^a	0.3371^c	0.2375^c	29.4806^b
Group four							
DL^5	2.5827^a	0.8849^a	11.6175^a	20.1502^a	0.5444^a	0.4766^a	12.2012^a
$20\%WMS+DL^5$	2.4377^{ab}	0.8051^b	11.4983^a	21.3648^b	0.4843^b	0.4028^b	16.5219^b
$50\%WMS+DL^5$	2.2861^b	0.6980^c	11.4031^a	22.2658^b	0.4495^b	0.2971^c	33.7353^c

[1]In the same fuel group, after ANOVA, values within a column with different superscript letters are significantly different (probability<0.05).

[2]Total particulate emissions.

[3]Solid carbon emissions.

[4]Soluble organic fraction.

[5]Test after drive shaft changed.
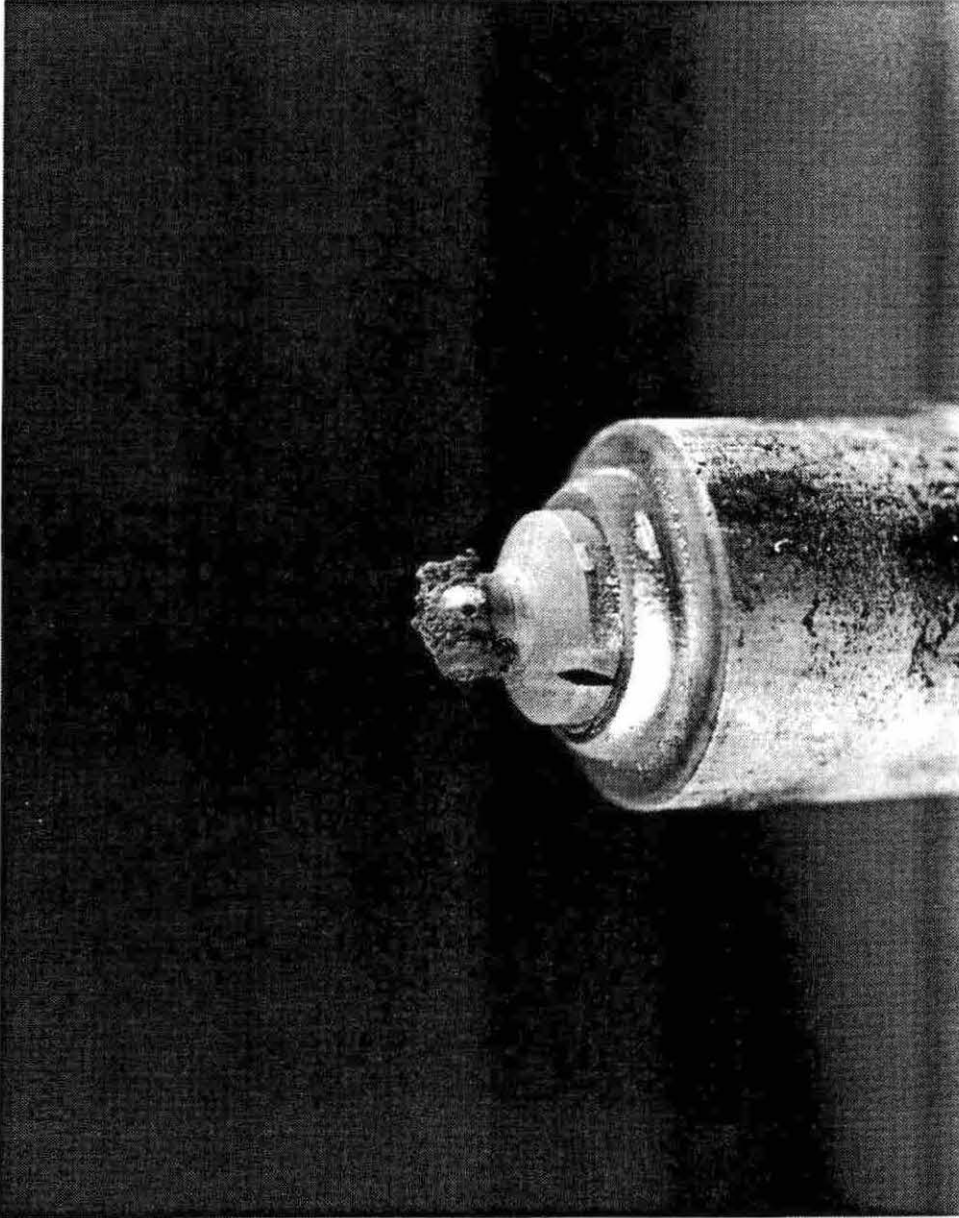
Figure 5.5   Carbon deposits on injector nozzles

was another possible reason for the experiment errors because the engine brake power and fuel consumption increased slightly for the same fuel. All of these potential error sources are being investigated.

5.3.1 Carbon monoxide emissions

Carbon monoxide (CO) is a natural intermediate product of hydrocarbon combustion. CO emissions are caused by the primary CO oxidation reaction $CO + OH \longrightarrow CO_2 + H$ becoming too slow and freezing the CO concentrations well above the equilibrium level. The brake specific carbon monoxide emissions for the fuel blends are plotted in Figure 5.6. CO emission for all fuel blends was significantly lower than No.2 diesel. 50%MS+DL had the largest reduction of CO emission which was 25.3%. Esters may reduce CO by reducing the amount of CO formed in rich zones due to their oxygen content lowering the overall fuel-air ratio.
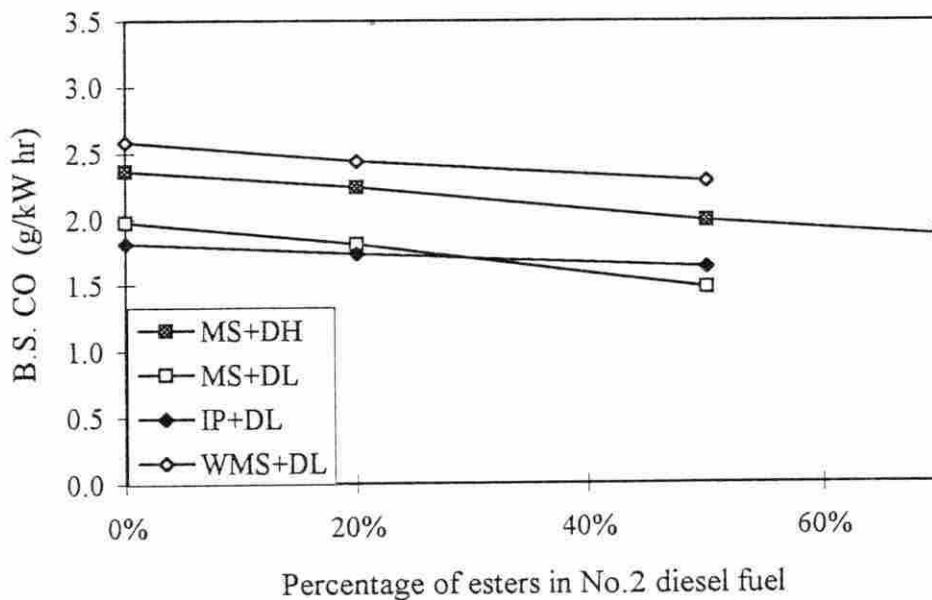
Figure 5.6   CO emissions for different fuel blends at 100% load

5.3.2   Unburned hydrocarbon emissions

Figure 5.7 shows the brake specific unburned hydrocarbon (HC) emissions with different fuel blends. In every case except one, the ester blends significantly lowered HC emissions. The maximum reduction in HC emissions was 29.0% by fuel 50%IP+DL. In fuel group two, the results were mixed. 50%MS+DL had 7.4% lower HC emissions, but 20%MS+DL gave a 2.8% increase compared with No.2 diesel fuel. However, neither of these changes were statistically significant.
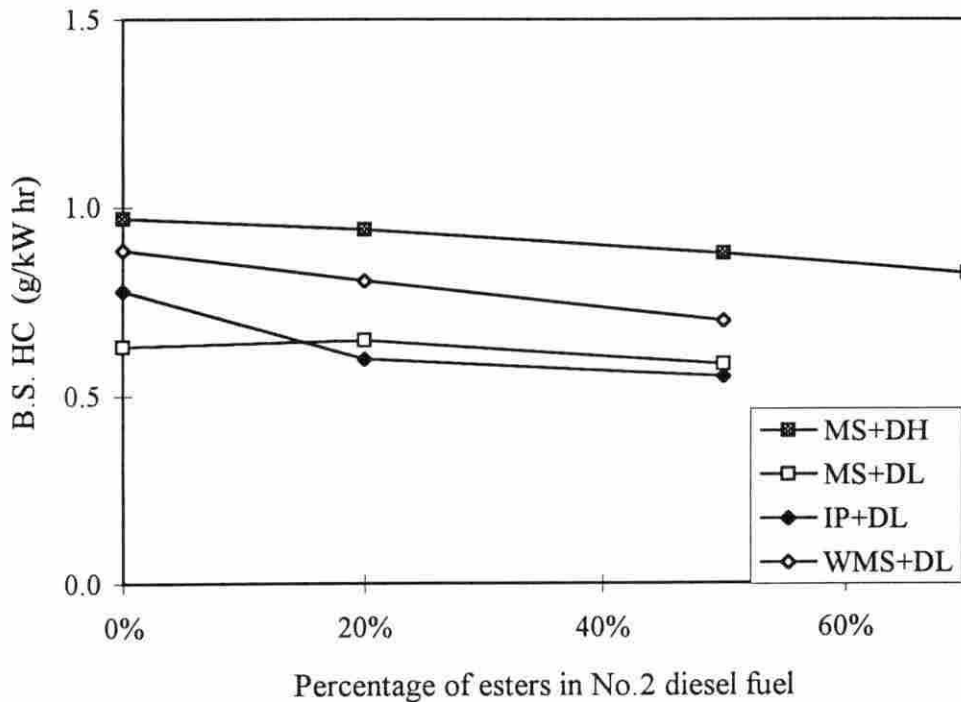
Figure 5.7   HC emissions for different fuel blends at 100% load

5.3.3   Oxides of nitrogen emissions

Figure 5.8 shows the results of brake specific NO_x emission. Although emission of oxides of nitrogen was slightly higher than No.2 diesel fuel in fuel groups one and two, the increases in NO_x emission were small. NO_x emission of the 20% and 50% blend fuels in the other two fuel groups increased significantly. 50%IP+DL had 12.1% higher NO_x than No.2 diesel fuel which was the largest increase among the tested fuels. The fuel blends with methyl ester had the lowest increase of NO_x emission which was below 4.0%. Wagner et al. [8] observed increases in NO_x emissions that were significantly greater for all esters than found in this study. Schumacher et al. [57] reported that NO_x emissions tended to be lower when a diesel engine was fueled with 10-40% blends of methyl ester and No.2 diesel fuel. But 50% fuel blends increased NO_x emissions under 100% of full load and at different engine speeds. NO_x level generally increases under conditions of high temperature and lean operation where oxygen is present. Although the combustion temperature of the fuel blends was probably lower than for No.2 diesel fuel, due to the lower energy content of the ester, more oxygen was available in the reaction zone during combustion which caused the NO_x level to rise.

5.3.4   Particulate emissions

Brake specific particulate emissions are shown in Figure 5.9. The largest reduction of particulate emissions was 28.0% which was produced by fuel 50%IP+DL. All fuel blends significantly improved particulate emissions compared to their No.2 diesel baselines. The 50% blend fuels decreased particulate emissions at least 17.4% and the 20% blend fuels decreased particulate emission at least 9.6%. 20%IP+DL and 50%IP+DL had the best effects on decreasing particulate emissions. 20%WMS+DL was better on particulate reduction than 20%MS+DL, but 50%WMS+DL gave a better reduction than 20%MS+DL.

The total particulate emissions consisted of soluble organic fraction and solid carbon.

Figure 5.8   NOx emissions for different fuel blends at 100% load
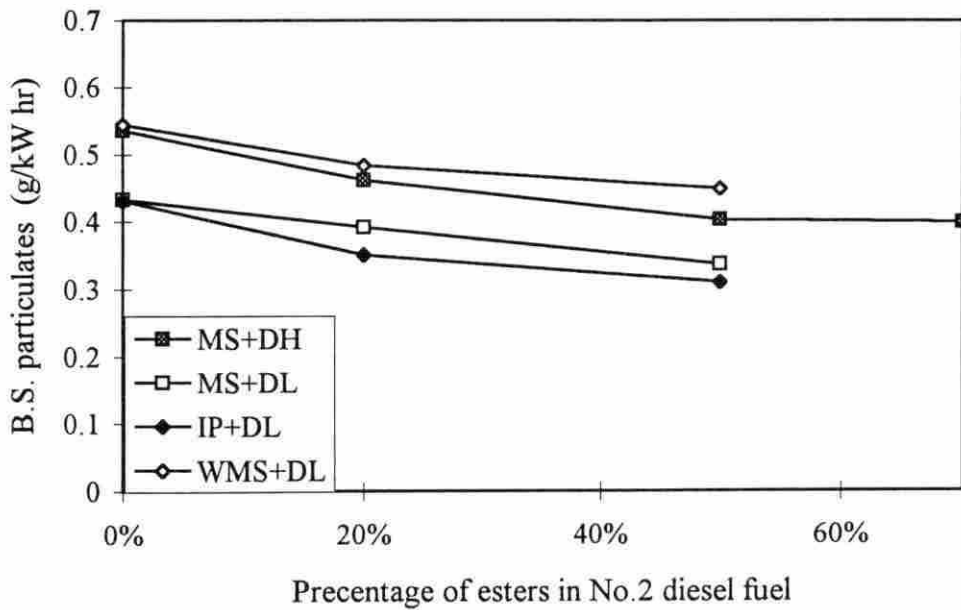
Figure 5.9   Particulate emissions for different fuel blends at 100% load

To determine the proportion of each in the particulate, all primary filters were Soxhlet extracted with methylene chloride for 60-70 cycles (about four hours). The brake specific solid carbon emissions are shown in Figure 5.10.

The carbon emissions had the same trend as the particulate emissions. The largest reduction of carbon was from the fuel 50%IP+DL which was 55.3% lower than No.2 diesel fuel. All carbon emission levels of the fuel blends were significantly decreased compared with No.2 diesel fuel. 20%IP+DL also was the lowest carbon emission fuel among the 20% blend fuels and was 22.0% lower than No.2 diesel fuel.

The percentage of soluble organic fraction in the particulates is shown in Figure 5.11. The soluble organic fraction increased with increasing proportion of esters in the fuel blends. 50%IP+DL had the highest SOF which was 47.3%. 20%IP+DL also had the highest SOF among the 20% fuel blends which was 18.6%. The increase of SOF for 50%IP+DL was 209.1% compared with No.2 diesel fuel. The increases of SOF for MS+DL were the lowest for the same percentage fuel blends. The content increase in SOF for the ester fuels was probably due to the long carbon chain molecules in the esters of soybean oil. The unburned esters of soybean oil, which had lower volatility than No.2 diesel fuel, were easier to condense and adsorb onto the soot surfaces during the dilution process.

5.3.5   Light load emissions

Only MS+DH was tested under the conditions of 1400 rpm and 20% of full load. The emission data that were collected at this light load condition revealed some different characteristics from that at 100% of full load. Table 5.7 shows the average results of three replications of the tests and the statistical analysis.

At light load, fuel blends of methyl ester also showed a slight reduction in CO emission. The brake specific CO emission is plotted in Figure 5.12. 50%MS+DH cut down 7.9% of CO emission which was the largest decrease of CO emission among those blend fuels. However, the CO emission increased compared with the 20% and 50% fuel blends when
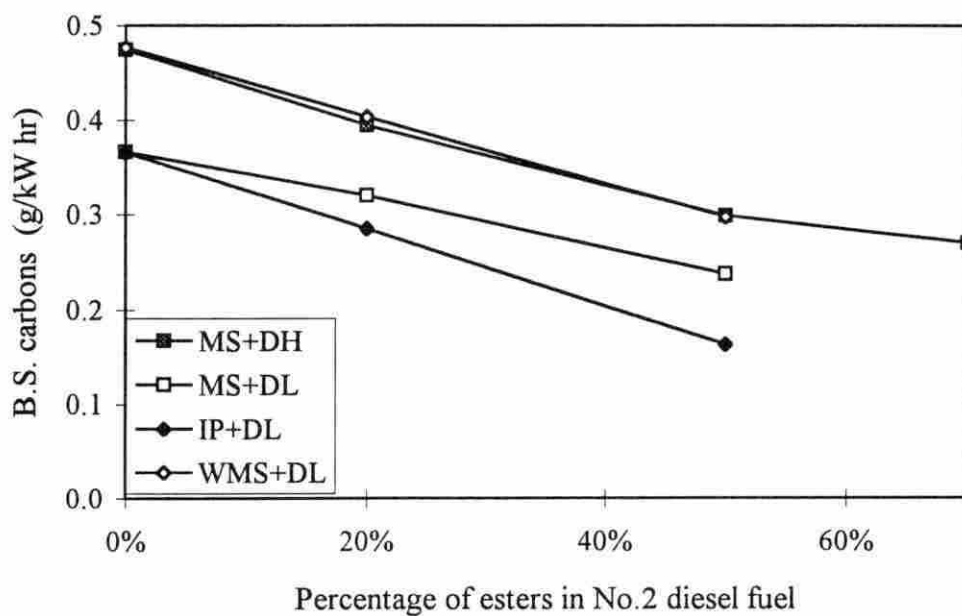
Figure 5.10   Solid carbon emissions for different fuel blends at 100% load
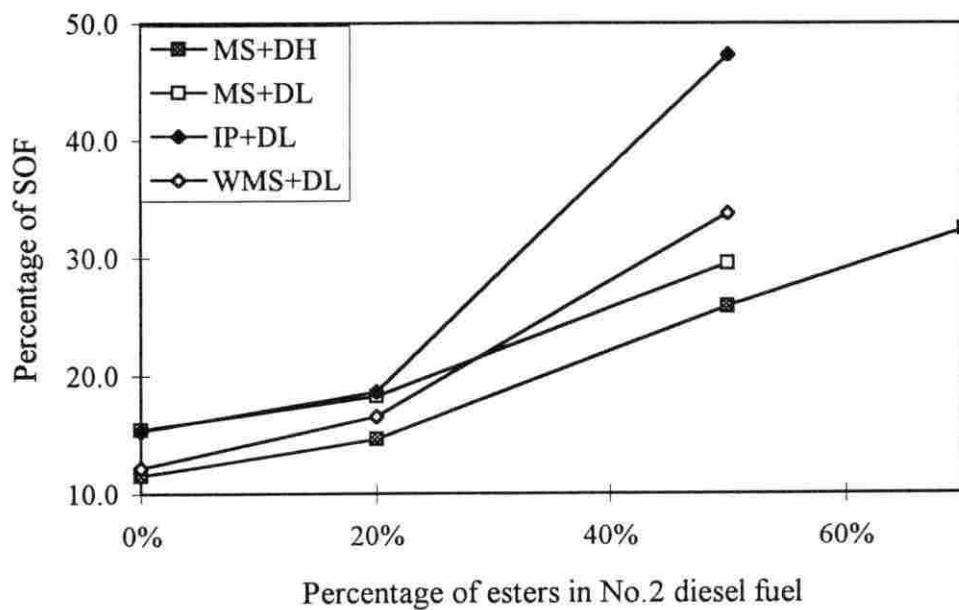
Figure 5.11   Percentage of SOF for different fuel blends at 100% load

Table 5.7   Emissions of methyl ester and diesel fuel under
1400 rpm and 20% of full load[1]

Fuel	Brake specific emissions g/kW hr						
	CO	HC	NO	NOx	PM[2]	SOL[3]	SOF[4]%
DH	8.7252[a]	6.0579[a]	7.9807[a]	14.4788[a]	1.2636[a]	0.1910[ac]	84.9670[a]
20%MS+DH	8.4614[a]	5.1837[b]	7.2481[a]	14.1586[a]	1.6764[b]	0.2476[a]	83.8631[a]
50%MS+DH	8.0372[a]	4.5056[c]	7.9039[a]	15.0428[a]	2.1206[c]	0.3775[b]	81.8776[a]
70%MS+DH	8.3209[a]	4.0463[d]	8.1913[a]	15.6327[a]	2.6869[d]	0.1258[c]	95.2868[b]

[1]After ANOVA, values within a column with different superscript letters are significantly different (probability<0.05).

[2]Total particulate emissions.

[3]Solid carbon emissions.

[4]Soluble organic fraction.

the diesel engine was fueled with 70% blend fuel. All reductions of CO emission were not statistically significant.

Figure 5.13 shows the data for brake specific unburned hydrocarbon emissions. All fuel blends revealed significant decreases of unburned hydrocarbon emissions compared with No.2 diesel fuel under light load conditions.   The more methyl ester in the blend, the more reduction of HC emissions. The largest reduction in HC emissions was 33.2% and the smallest was 14.4% compared with No.2 diesel fuel.
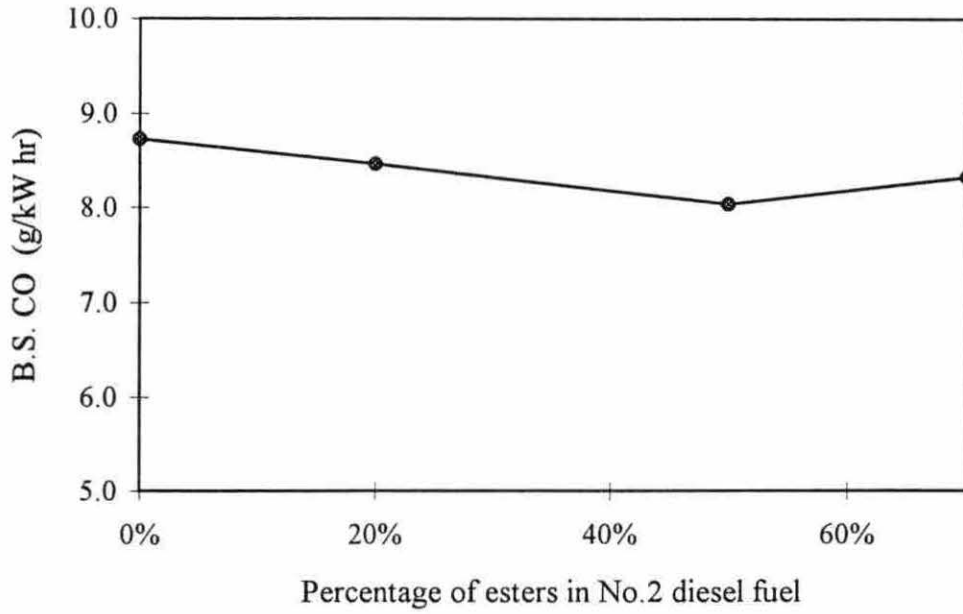
Figure 5.12   CO emissions for different fuel blends at 20% load
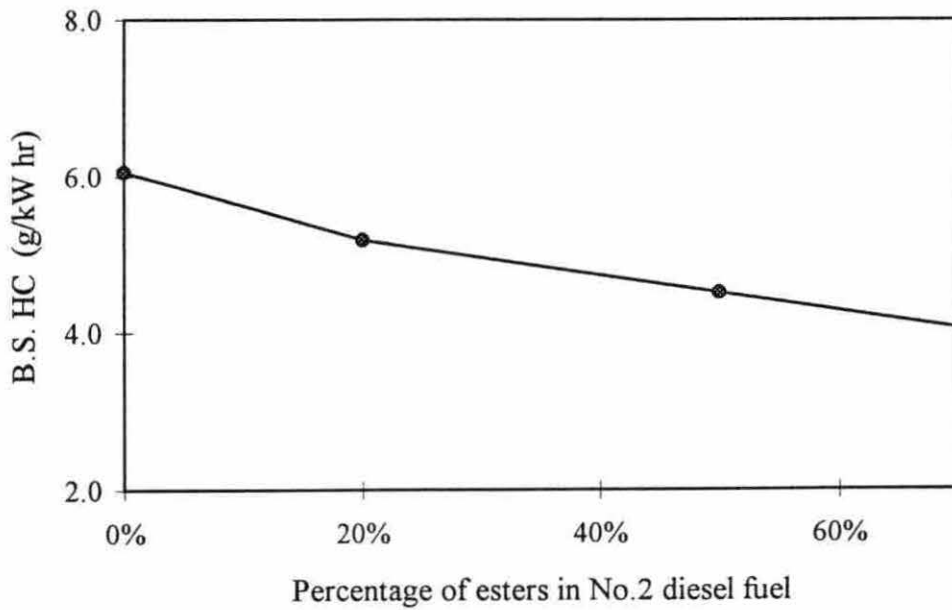
Figure 5.13   HC emissions for different fuel blends at 20% load

Figure 5.14 presents the brake specific NO_x emissions results. NO_x emissions between No.2 diesel fuel and all the fuel blends did not show any statistically significant change although 50%MS+DH and 70%MS+DH gave 3.9% and 8.0% increases, respectively. The NO_x emissions from 20%MS+DH was 2.2% lower than for No.2 diesel fuel.

The results of the particulate emissions from the fuel blends at 20% of full load were contrary to that observed at the full load condition. Figure 5.15 shows that the particulate emissions increased with increasing content of methyl ester. 20%, 50% and 70% blend fuels had 32.7%, 68.3% and 112.6% higher particulate emissions than No.2 diesel fuel. At light loads, hydrocarbon emissions are caused by fuel overmixing with air until it is beyond its lean flammability limit. Because the combustion temperature is lower under light load condition, most of this fuel will never burn. When the hydrocarbon in the exhaust gas is diluted with cold air in the dilution tunnel, more unburned hydrocarbon will condense and adsorb on the surface of the soot particles and cause an increase in particulate emissions.

The increase in particulate emissions was caused by a large increase in the soluble organic portion of the particulates. Figures 5.16 and 5.17 show the specific solid carbon emissions and the percentage of soluble organic fraction in the particulates, respectively. Over 80% of the particulate mass is soluble organic material. When the concentration of methyl ester reached 70%, the percentage of soluble organic was 95.29. 70%MS+DH had a significant increase of SOF percentage compared with the other three fuels, but a much higher overall amount emitted. However, the 20% and 50% methyl ester blends had about the same SOF percentage as the baseline diesel fuel, but a much higher overall amount emitted.

The trend in the brake specific solid carbon emissions was opposite to that for the SOF with increasing methyl ester in the fuel blends. The carbon emission of 70%MS+DH was lower than No.2 diesel fuel. 20%MS+DH and 50%MS+DH had 29.6% and 97.6% higher carbon emissions than No.2 diesel fuel, respectively. 70%MS+DH was 34.1% lower on carbon emissions.
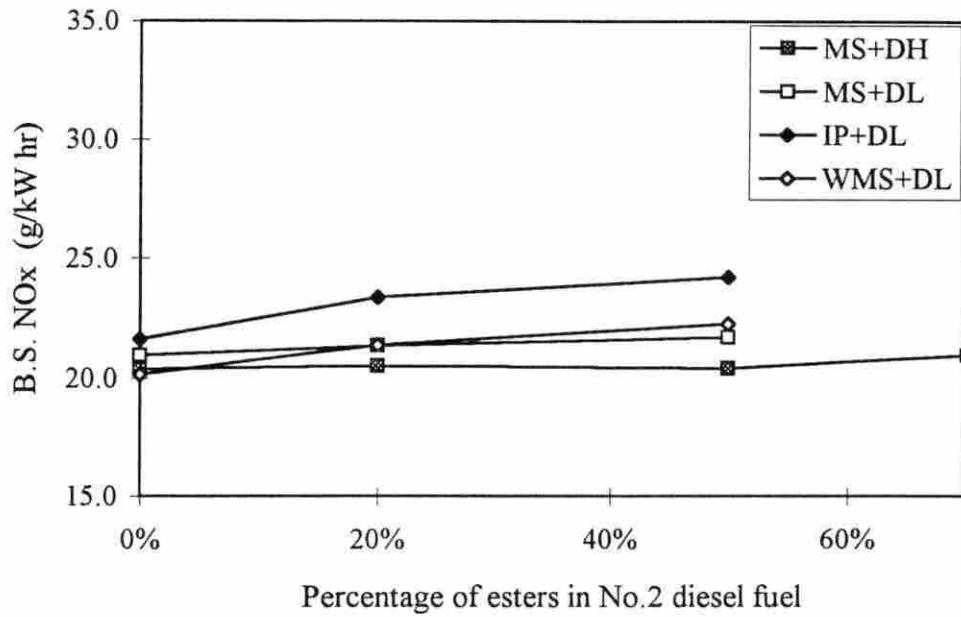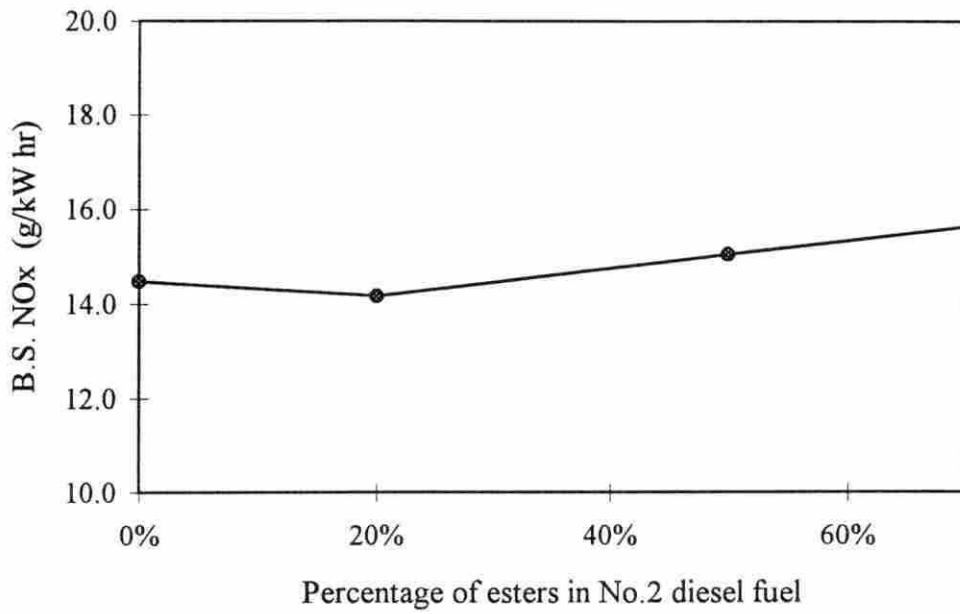
Figure 5.14   NOx emissions for different fuel blends at 20% load
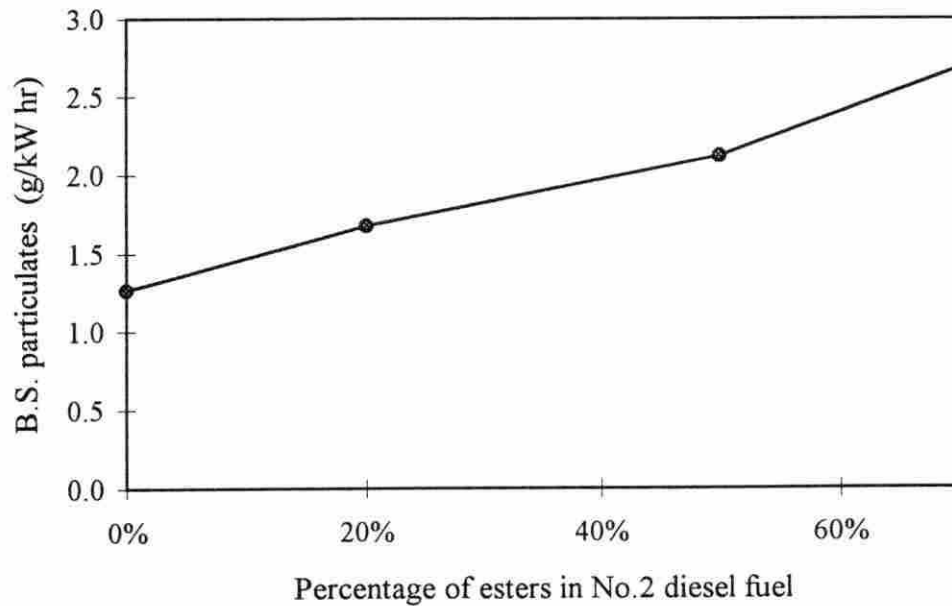
Figure 5.15   Particulate emissions for different fuel blends at 20% load
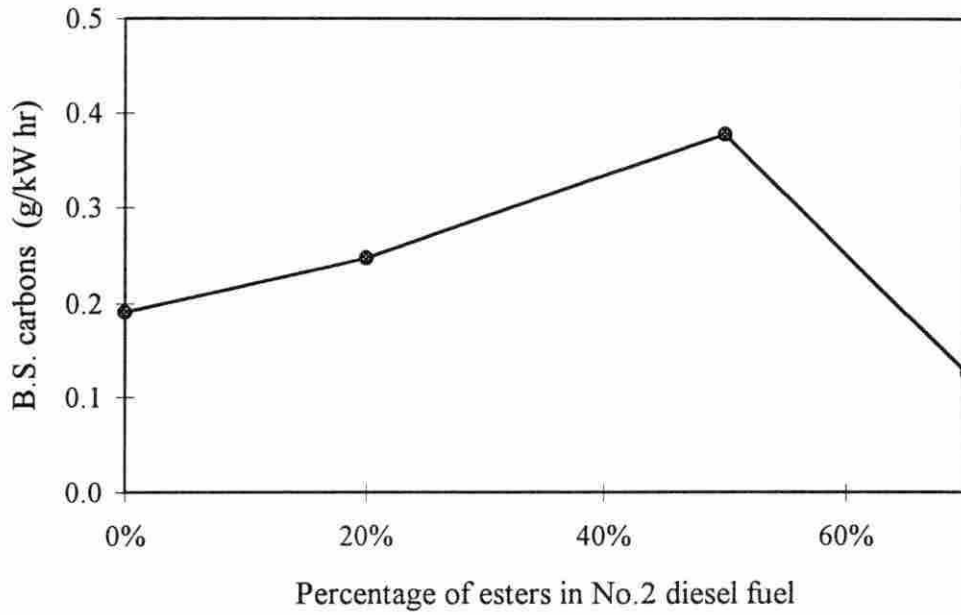
Figure 5.16   Carbon emissions for different fuel blends at 20% load
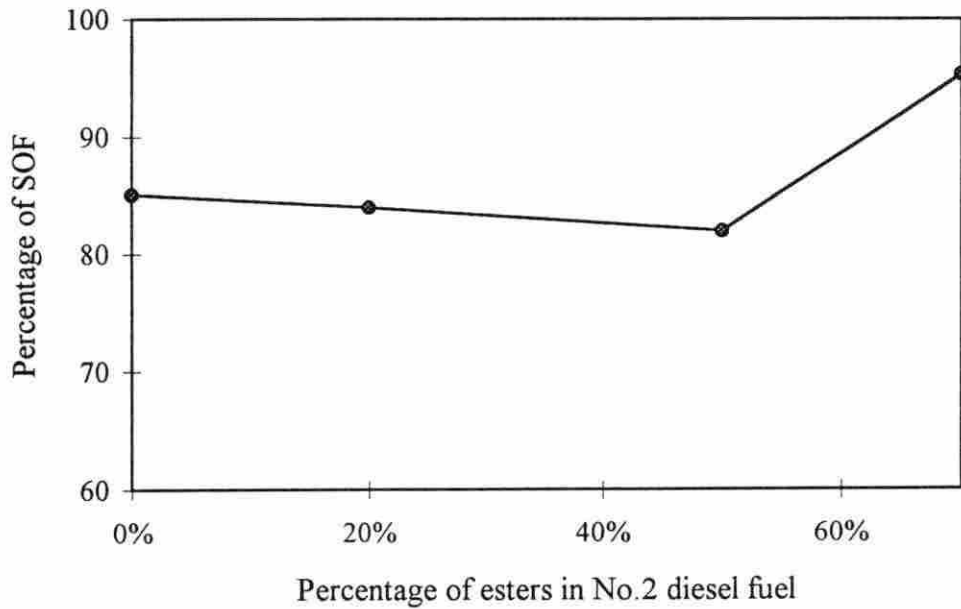
Figure 5.17   Percentage of SOF in particulates at 20% load

5.4   Heat Release Analysis

Heat release analysis and observation of the cylinder pressure trace allowed comparison of the combustion characteristics of the fuels. Heat release analysis was based on the combustion pressure data that were collected during the tests. The theoretical basis for these computations was discussed in Chapter 4. The burning rate shown in the plots for this section is the instantaneous normalized mass burning rate; that is, the burning rate of the fuel divided by the total mass of fuel burned during the combustion process. With this procedure, the integrated value of the normalized mass burning rate for the entire combustion process should be equal to unity for each fuel and the relative heights of the various portions of the curve reflect the importance of each phase of combustion, regardless of the total amount of fuel burned.

One of the most important parameters in diesel combustion is the ignition delay. The definition of the ignition delay is the time from the start of fuel injection to the start of combustion. The crankangle for the start of combustion was determined from the cylinder pressure data in this study. There are two ways to define the start of combustion: the start of visible combustion or the start of measurable heat release. Most researchers use the start of measurable heat release to determine the end of the ignition delay [78, 79]. Needham et al. [78] showed that ignition delay trends measured by each method were in agreement although small consistent differences in the absolute values were noted. The start of injection was determined from fuel injection line pressure data. A typical fuel injection pressure diagram is shown in Figure 5.18. The start of injection was $19.9°$ BTDC when the engine was operated at 1400 rpm and 100% of full load, and $15.9°$ BTDC for 1400 rpm and 20% of full load.

5.4.1   Comparison of fuel burning rates

Figures 5.19 to 5.22 show the normalized mass burning rate vs. crankangle for each fuel group. Normally, the combustion process in diesel engines takes place in two stages, pre-
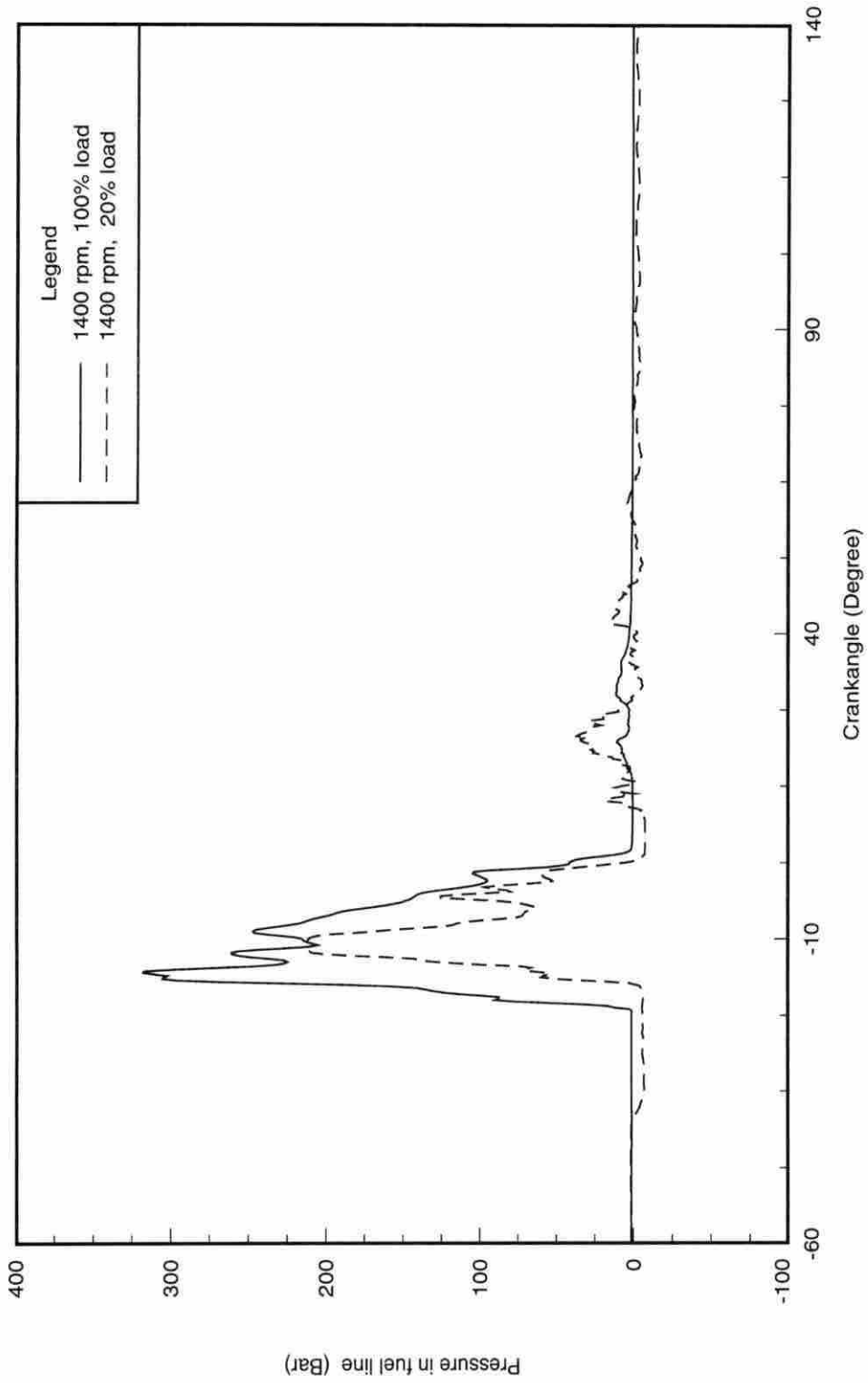
Figure 5.18   Pressure in fuel injector line
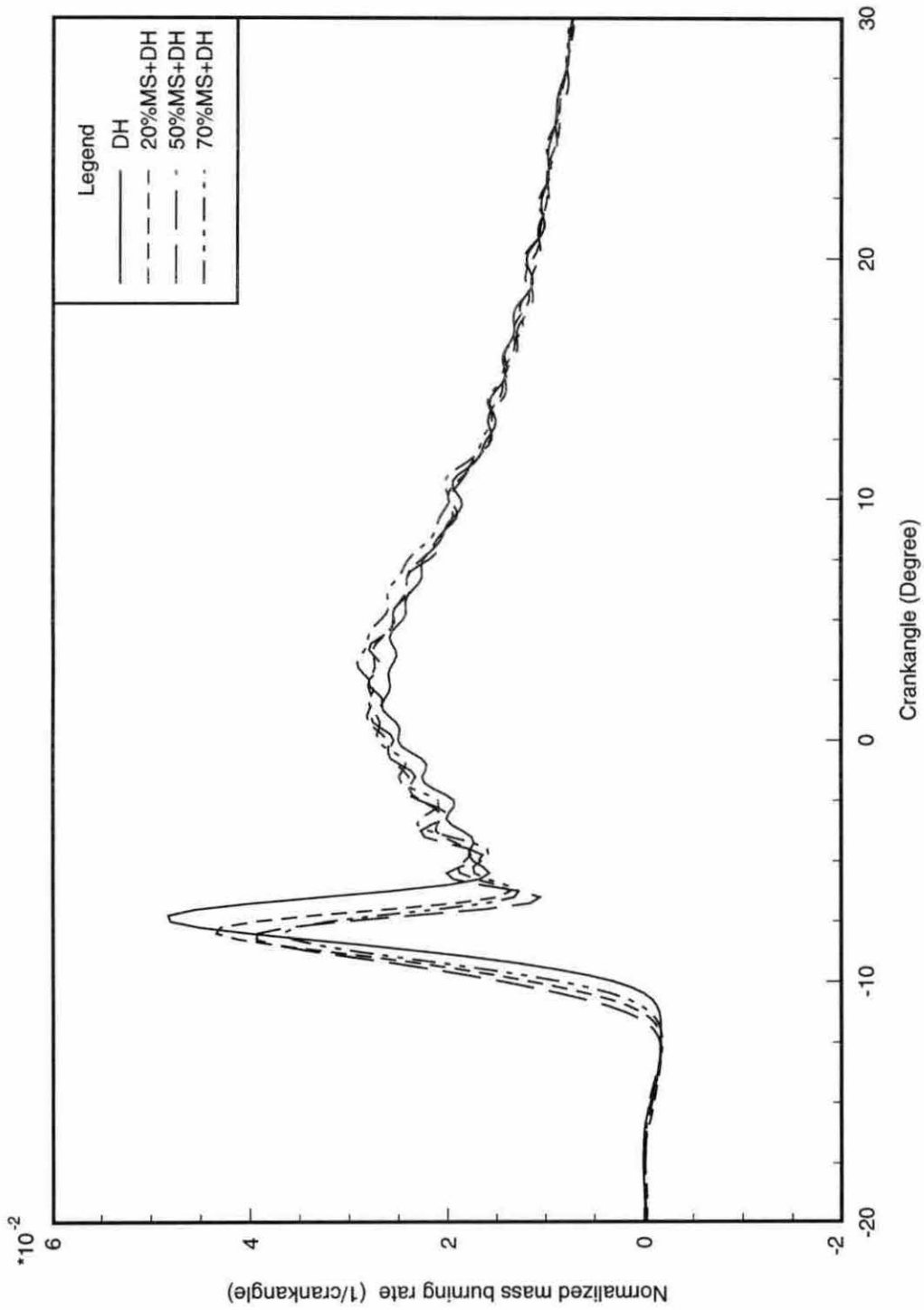
Figure 5.19 Normalized mass burning rate of first fuel group at 100% load

83
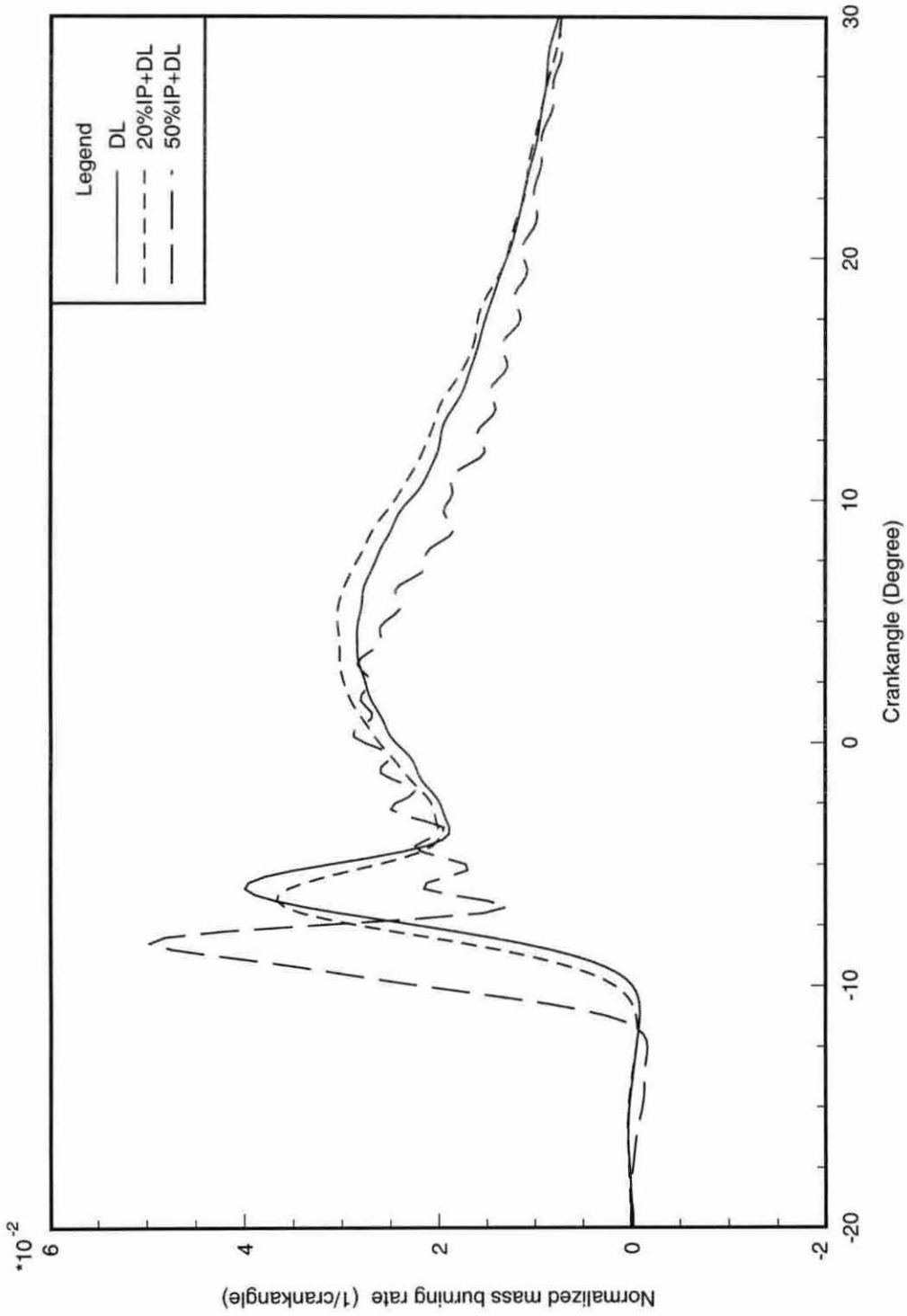
Figure 5.20   Normalized mass burning rate of second fuel group at 100% load
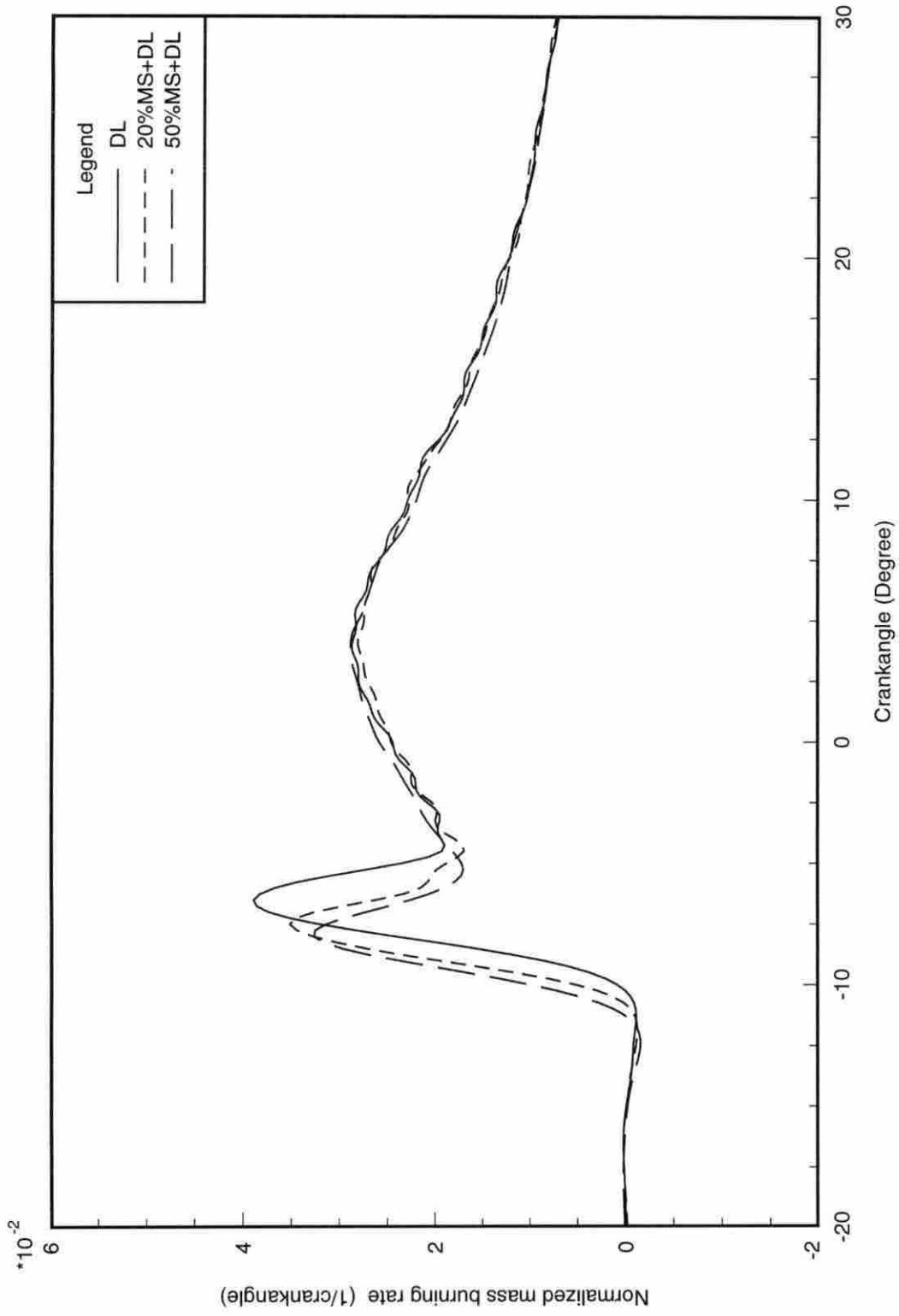
Figure 5.21   Normalized mass burning rate of third fuel group at 100% load

85
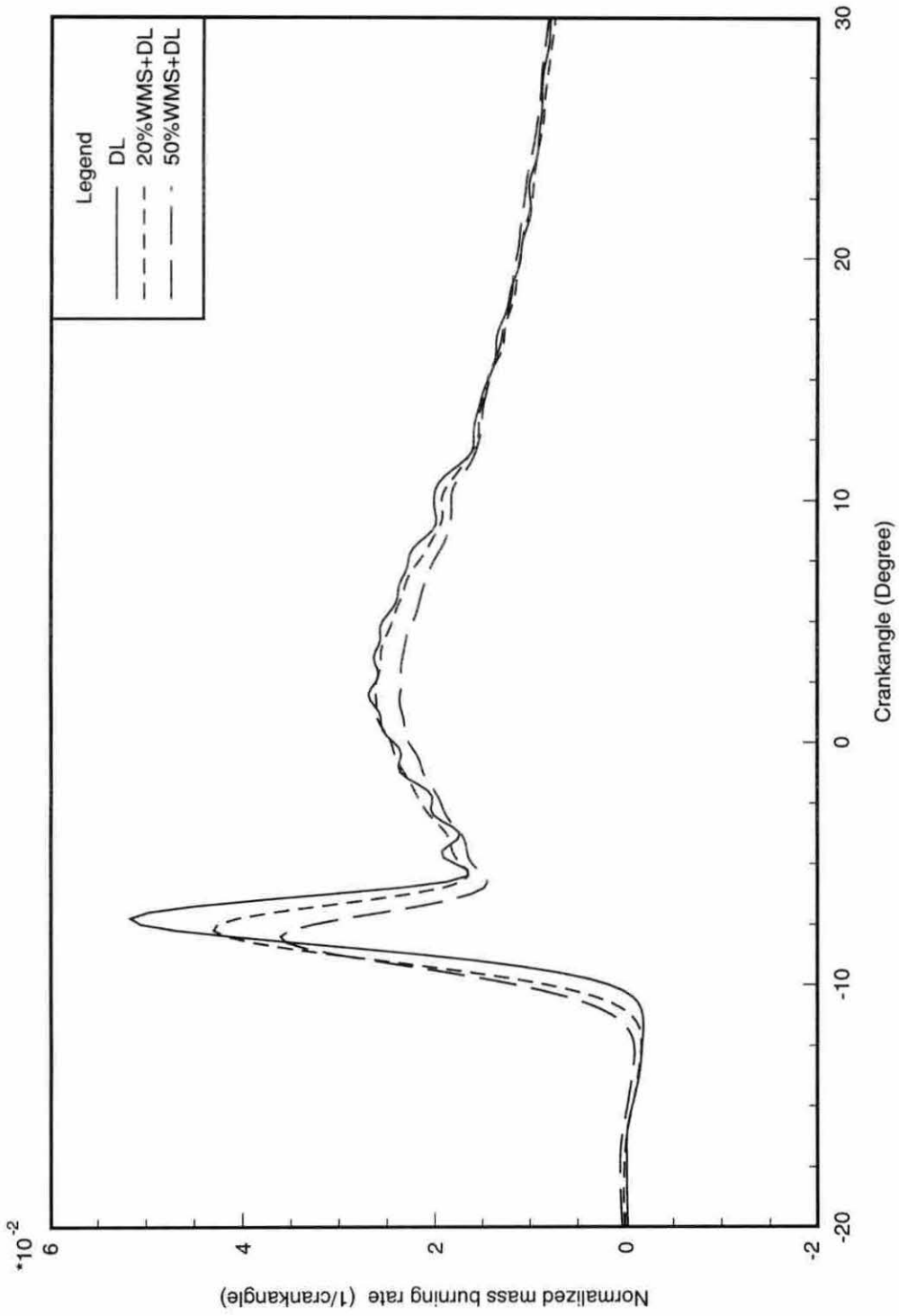
Figure 5.22   Normalized mass burning rate of fourth fuel group at 100% load

mixed and diffusion combustion. Injected liquid fuel has to undergo both physical and chemical processes before combustion can occur. Fine fuel droplets must vaporize and mix with air while the long carbon chain hydrocarbons break into shorter chain species or radicals. These processes are endothermic so the temperature in the cylinder drops slightly. The heat release curve also shows a slight drop. After the ignition delay period, the previously prepared fuel-air mixture begins to burn. This initial combustion phase, called premixed combustion, is very rapid so the pressure in the cylinder increases sharply, and the heat release also achieves its first peak. When the premixed combustion ends, the combustion will enter the diffusion stage where the burning rate is controlled by the availability of near-stoichiometric fuel-air mixture. The diffusion combustion is slower than the premixed combustion, and most of fuel will be burned in this period.

Fuel blends containing methyl ester revealed similar combustion behavior whether the ester was blended with high or low sulfur diesel or whether the ester was winterized. The iso-propyl ester showed some special behavior that will be discussed later in this section. It can be seen from Figures 5.19 to 5.22 that the fuel blends of esters burned in a similar manner to diesel fuel. All fuels experienced rapid premixed burning followed by a diffusion combustion period. All blends of esters had a shorter ignition delay than No.2 diesel fuel. Because No.2 diesel fuel experienced a longer ignition delay, after ignition it burned more rapidly than all the fuel blends, and had a higher peak premixed burning rate.

Figure 5.23 shows the ignition delay vs. the percentage of esters in No.2 diesel fuel. The ignition delay of the 20% and 50% blends decreased, but the 70% blend of methyl ester increased slightly although still shorter than No.2 diesel fuel. The ignition delays among the 20% blends and the 50% blends were very close. The largest change in ignition delay between the 20% blends and No.2 diesel fuel was 1.00° which corresponded to 20%MS+DH, and 1.75° for the 50% blends which came from 50%IP+DL. The phenomenon of shorter ignition delay confirmed the relationship between ignition quality and the cetane number of the fuel. As was shown in Table 5.3, a higher concentration of esters in the fuel blends means a higher cetane number due to the higher cetane number of the esters.

All the tested fuels had similar combustion behavior to No.2 diesel fuel under 1400 rpm

and 100% of full load condition. The amount of fuel burned during premixed combustion was determined by how much fuel was mixed with the air before the start of combustion. The longer the ignition delay, the more fuel and air mixture is prepared to burn, causing a higher initial burning rate, higher premixed burning fraction and higher rate of pressure rise. The process of premixed burning is an important factor in engine noise.

5.4.2   Premixed burning rate

Figure 5.24 shows that the mass burned fraction of diesel fuel during premixed combustion period was higher than for the fuel blends with only one exception. Diesel fuel had higher volatility and lower viscosity than the esters of soybean oil so more flammable fuel-air mixture was prepared during the ignition delay period. Furthermore, a longer ignition delay for diesel fuel gave a longer time to prepare the premixed fuel and air. Both of these factors could contribute to the observed results. Figure 5.25 shows the maximum combustion pressure with the different fuels. It shows very little effect of fuel change.
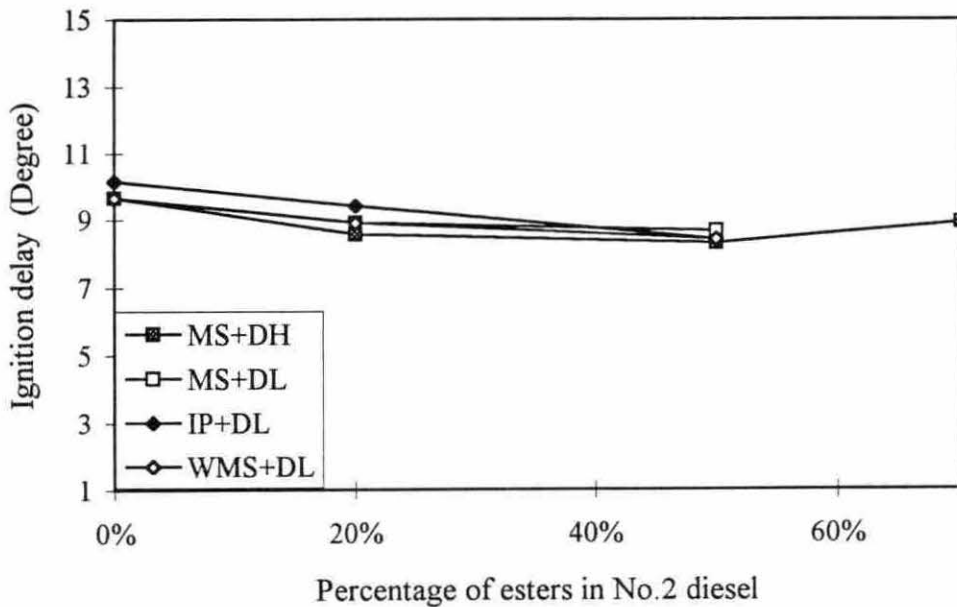
Figure 5.23   Ignition delay of different fuel blends at 100% load
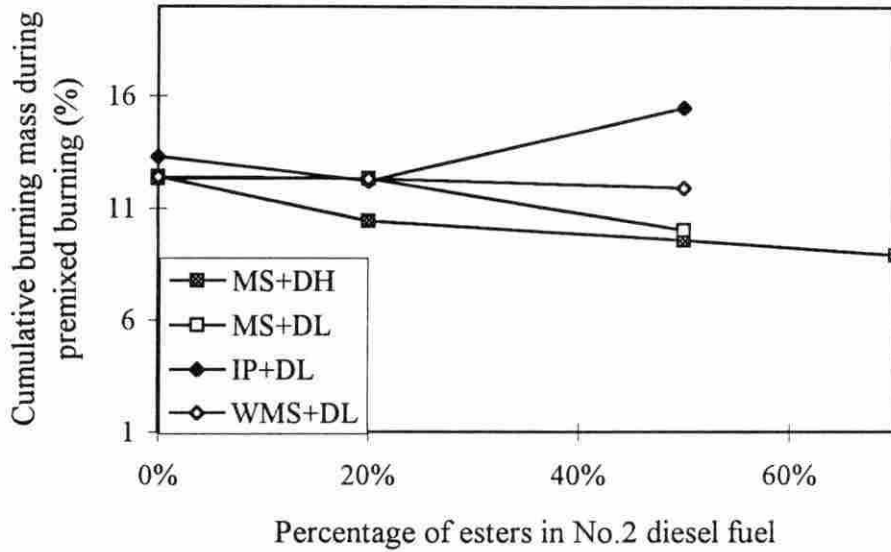
Figure 5.24   Cumulative mass of fuel burning within the premixed combustion period
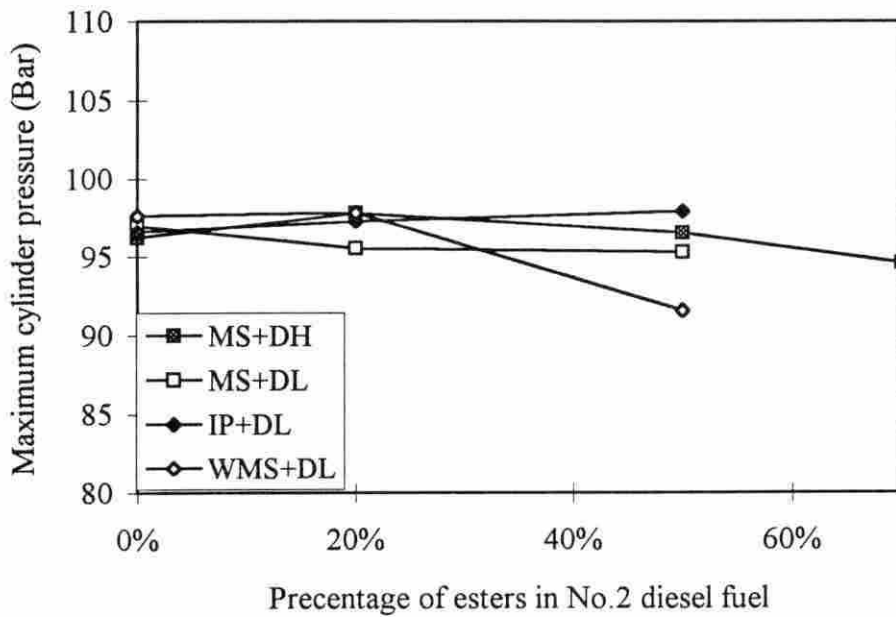
Figure 5.25   Maximum cylinder pressure at 100% load

5.4.3   Diffusion burning rate

After the premixed fuel-air mixture has been consumed, the combustion rate is con-
trolled by the rate at which mixture becomes available for burning. The injected fuel still
undergoes vaporization, mixing with air, and preflame chemical reactions. The heat release
curves shown in Figures 5.19 to 5.22 exhibit a second peak under the conditions of 1400
rpm and 100% of full load. Generally, the maximum burning rate of the diffusion burning
was lower than that during the premixed burning stage for all fuels.

The crankangle when the cumulative amount of fuel burned reaches 50%, 70% or 90%
can be used as an indicator of the overall duration of the combustion process. Figures 5.26
to 5.28 show the crankangle when cumulative burning mass fractions were 50%, 70% and
90%. All fuel blends, except 50%WMS+DL, required about the same time to reach the
50% burned point. Even the 70% and 90% burned times did not show a significant vari-
ation for increasing amounts of ester. The differences between tests conducted on different
days, as indicated by the diesel baselines for each fuel group, are more significant than the
changes in the ester percentage.
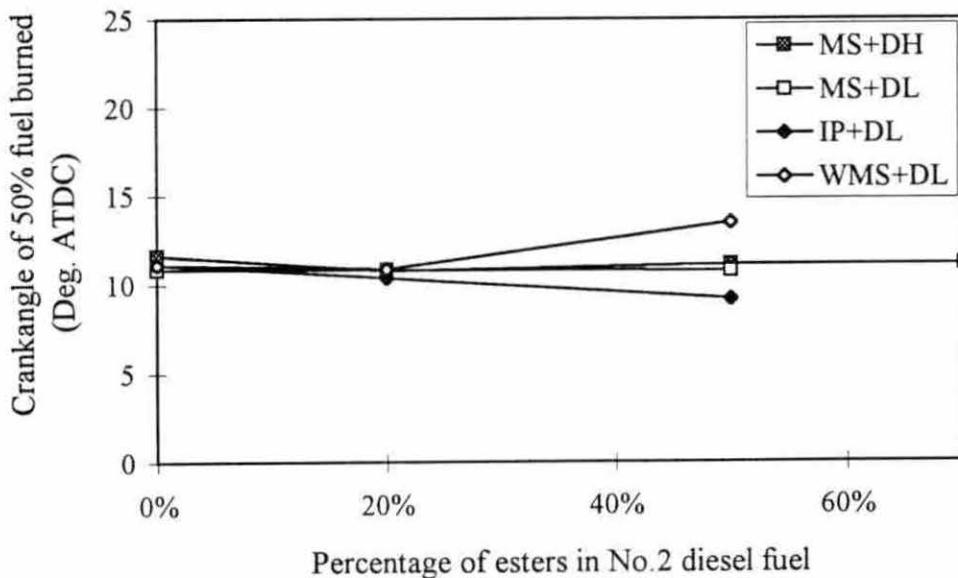
Figure 5.26   Timing of 50% of cumulative mass burned at 100% load
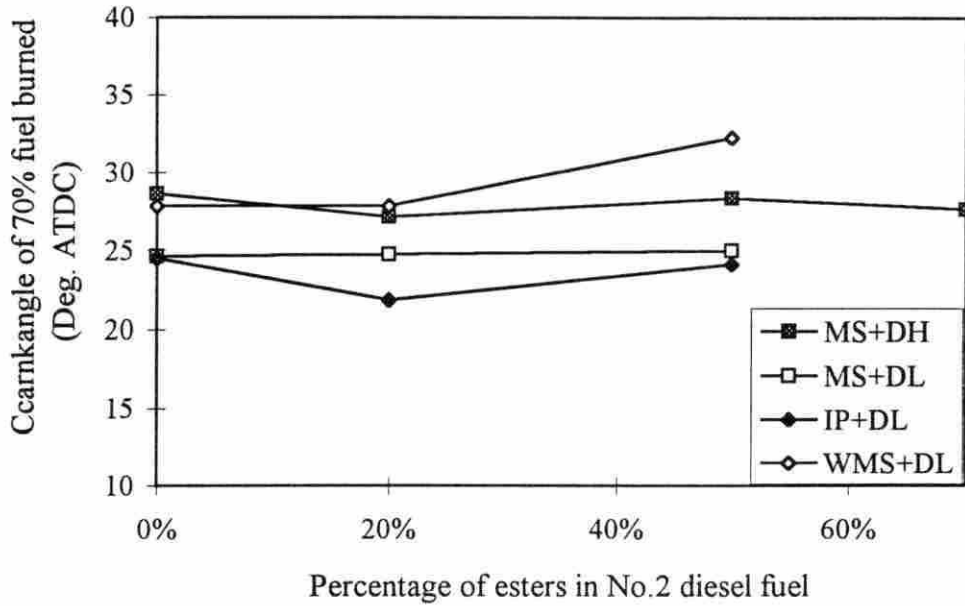
Figure 5.27   Timing of 70% of cumulative mass burned at 100% load
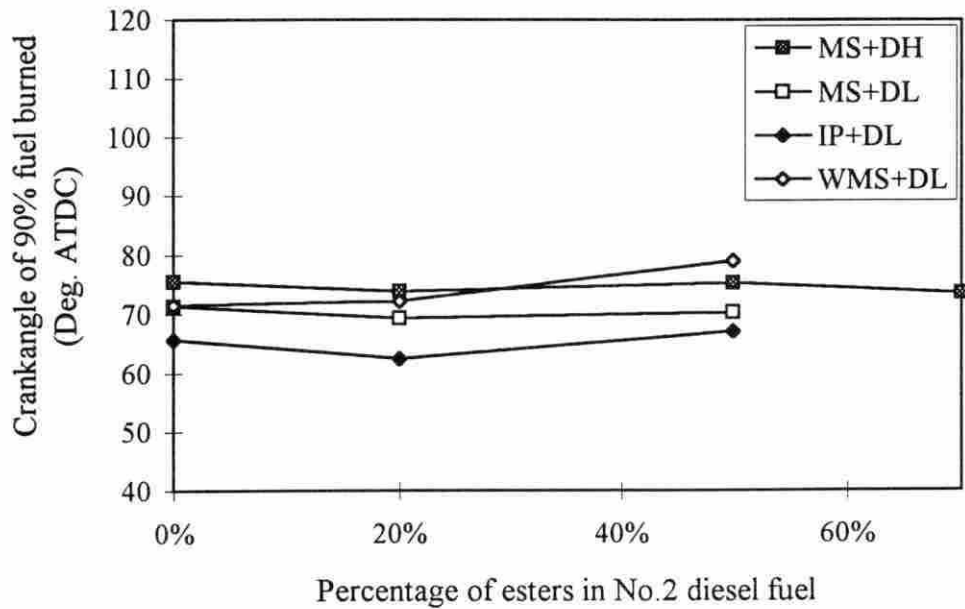
Figure 5.28   Timing of 90% of cumulative mass burned at 100% load

The physical and chemical properties of the fuels may have influenced their combustion characteristics. Zubik et al. [80] reported "During the distillation of the methyl ester, a significant change was noted at about 70% distillation where evidence of chemical decomposi-tion began and a white acrid smoke accompanied the vapors leaving the distillation flask". In their distillation of the methyl ester of sunflower oil, the temperature corresponding to 70% distillation was about 350 °C. They suggested that decomposition of vegetable oils would result in a series of short chain alkanes, alkenes and oxygenated compounds with chain lengths as short as five carbon atoms. The short chain alkenes would be especially susceptible to oxidation and could accelerate the combustion of the decomposed esters after the ignition delay.

It has been shown that alkenes are an essential intermediate in the oxidation of low molecular weight hydrocarbons at low temperatures [80]. Thus, if the methyl ester decomposed thermally to give a significant amount of alkenes during the ignition delay, the overall reaction path may be shortened compared to diesel fuel. This characteristic of the esters of vegetable oil could also be used to explain the higher cetane number of methyl esters compared with No.2 diesel fuel.

On the other hand, the esters of soybean oil and their mixtures with No.2 diesel fuel possess lower volatility and a slightly higher viscosity than No.2 diesel fuel. The quality of the spray and atomization when the fuels are injected into the cylinder, and the amount of fuel-air mixture formed, is lower so that all fuel blends give a lower premixed burning rate and less premixed burning mass fraction than No.2 diesel fuel.

The flame propagation speed of fuels is determined by many factors. Chemically, the flame speed peak occurs close to the stoichiometric fuel-air mixture. When the ratio of fuel to air decreases, the flame speed will decrease also. For fuels with double bonds, as the carbon number increases, the flame propagation speed decreases [81]. Physically, the flame speed is a strong function of flame temperature which is lower for esters [81]. For all of these reasons, the flame propagation speed of esters is expected to be lower than No.2 diesel fuel. This may be part of the reason why the premixed burning rate was lower for the esters than for diesel fuel. Niehaus et al. [79], Zubik et al. [80] and Faletti et al. [82] ob-

served a contrary result that vegetable oil and their esters had a higher premixed burning rate than No.2 diesel fuel.

5.4.4 Combustion irregularities

Since each set of data obtained as part of this project was repeated three times, there were three independent sets of cylinder pressure for each fuel blend. Comparison of the three burning rate curves of iso-propyl ester showed large differences between the different tests. These results are shown in Figures 5.29 to 5.31 corresponding to the three replications. The 50% fuel blends showed evidence of combustion before the normal start of premixed combustion. This is especially true for the last test, where two early small burning peaks occurred even before the start of injection.

The first test of the 50% fuel blend showed normal combustion behavior, except that the maximum premixed burning rate was higher than expected. 15.5% of the fuel was burned during the premixed burning period which was more than No.2 diesel fuel (13.3%). For the second test, about 18.0% was burned during premixed combustion, and 19.2% of the fuel was consumed during the premixed combustion period in the third test. The earliest burning occurred during the third test at about 39 degrees before top dead center. Its start of premixed combustion also occurred much earlier. The "ignition delay" was only 0.42 degree of crankangle. Because the two early combustion events resulted in the temperature and pressure in cylinder being higher than normal, when normal injection began, the new fuel ignited immediately. The diffusion burning portion of these curves was quit slow. All tests of the 20% iso-propyl ester followed the normal combustion behavior. The reasons which caused the abnormal combustion phenomenon of the 50% blends of iso-propyl ester and No.2 diesel fuel are still under investigation. The following are some possible reasons.

The iso-propyl esters used in this study contained 1.5% (by weight) of total glyceride which corresponded to 5.2% (by mole) monoglyceride. This high level was due to the difficulty of separating monoglyceride from ester. Monoglyceride was the product of incom-
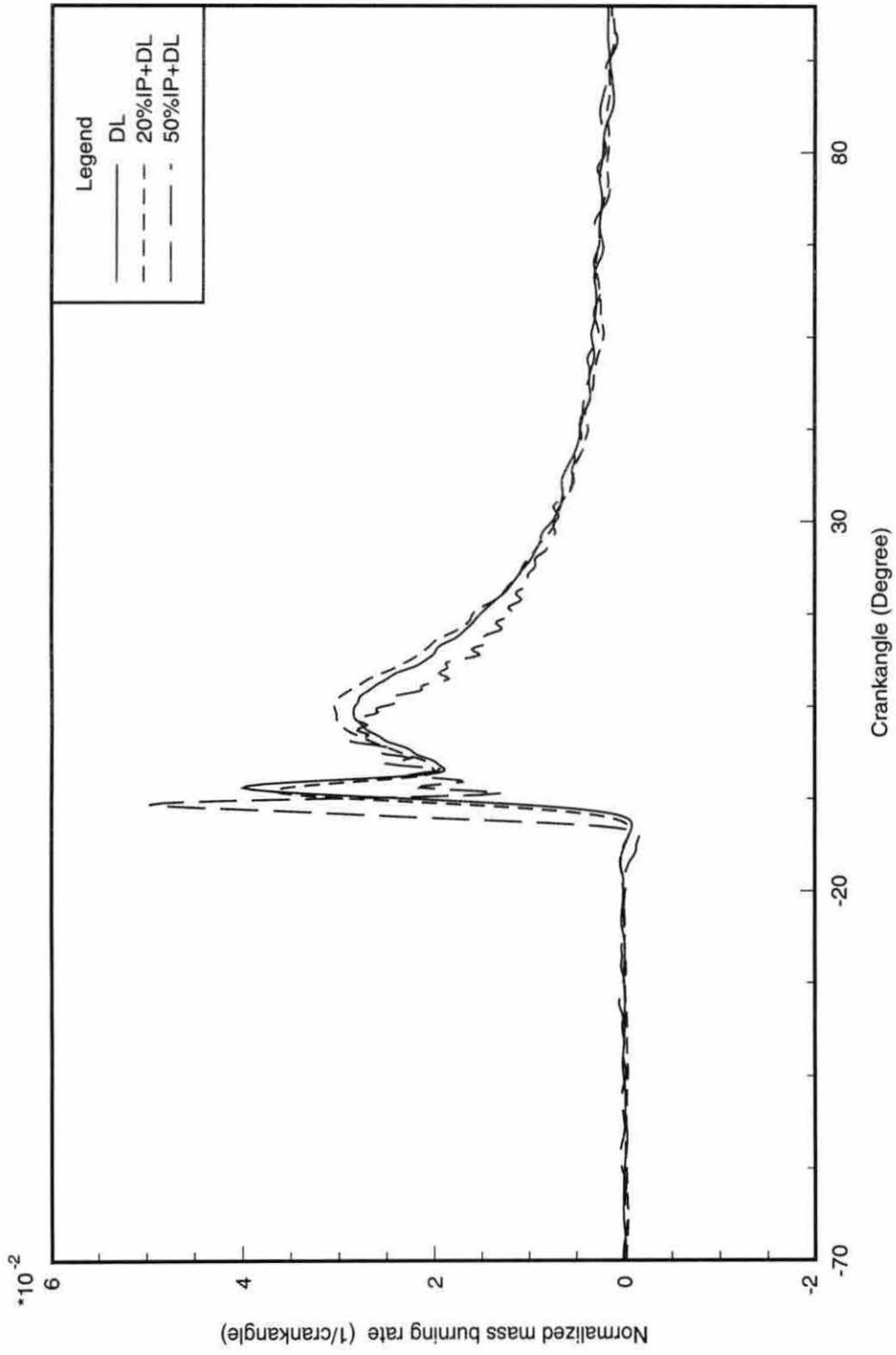
Figure 5.29   Burning rate calculated from first data set for iso-propyl blends

94
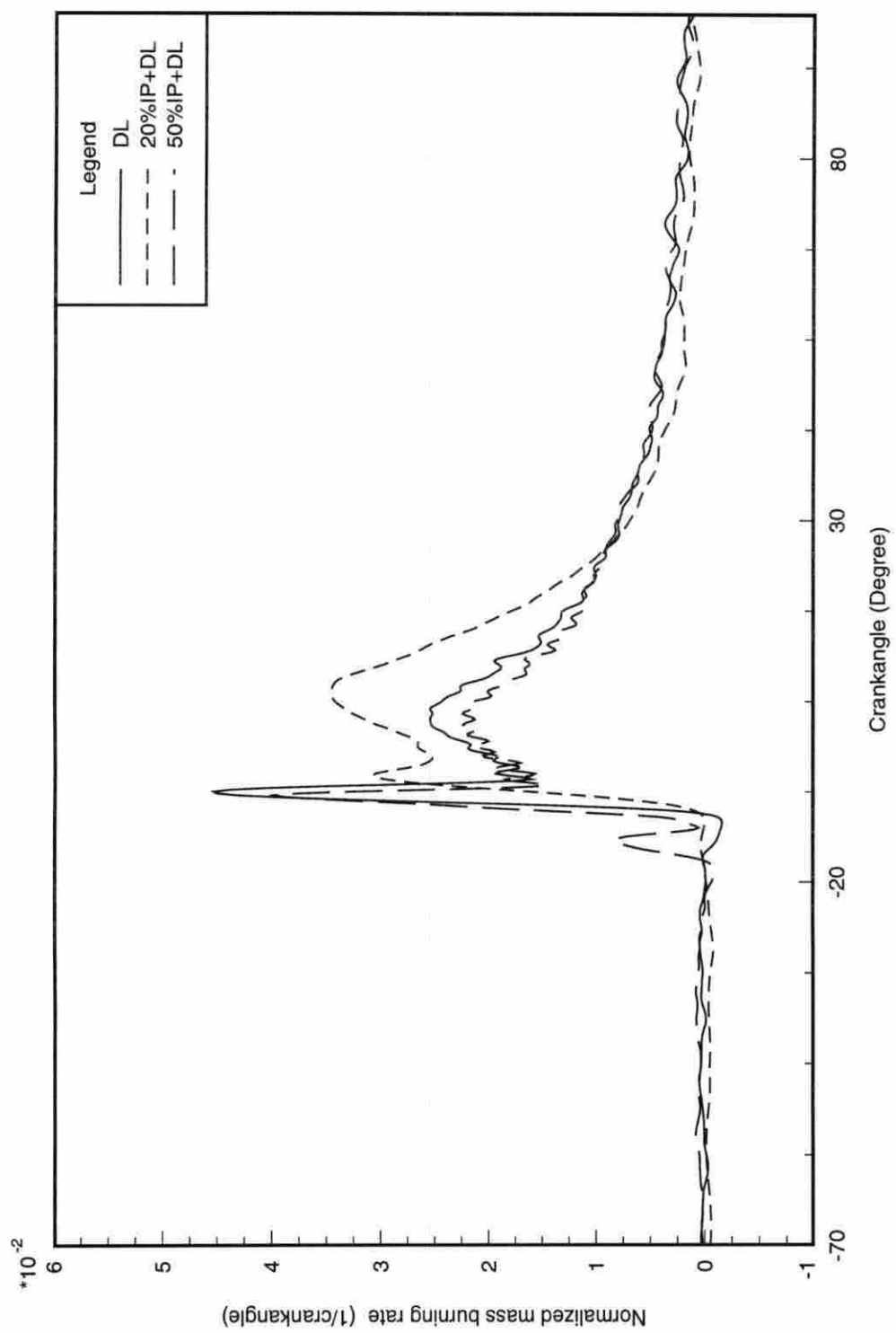
Figure 5.30   Burning rate calculated from second data set for iso-propyl blends
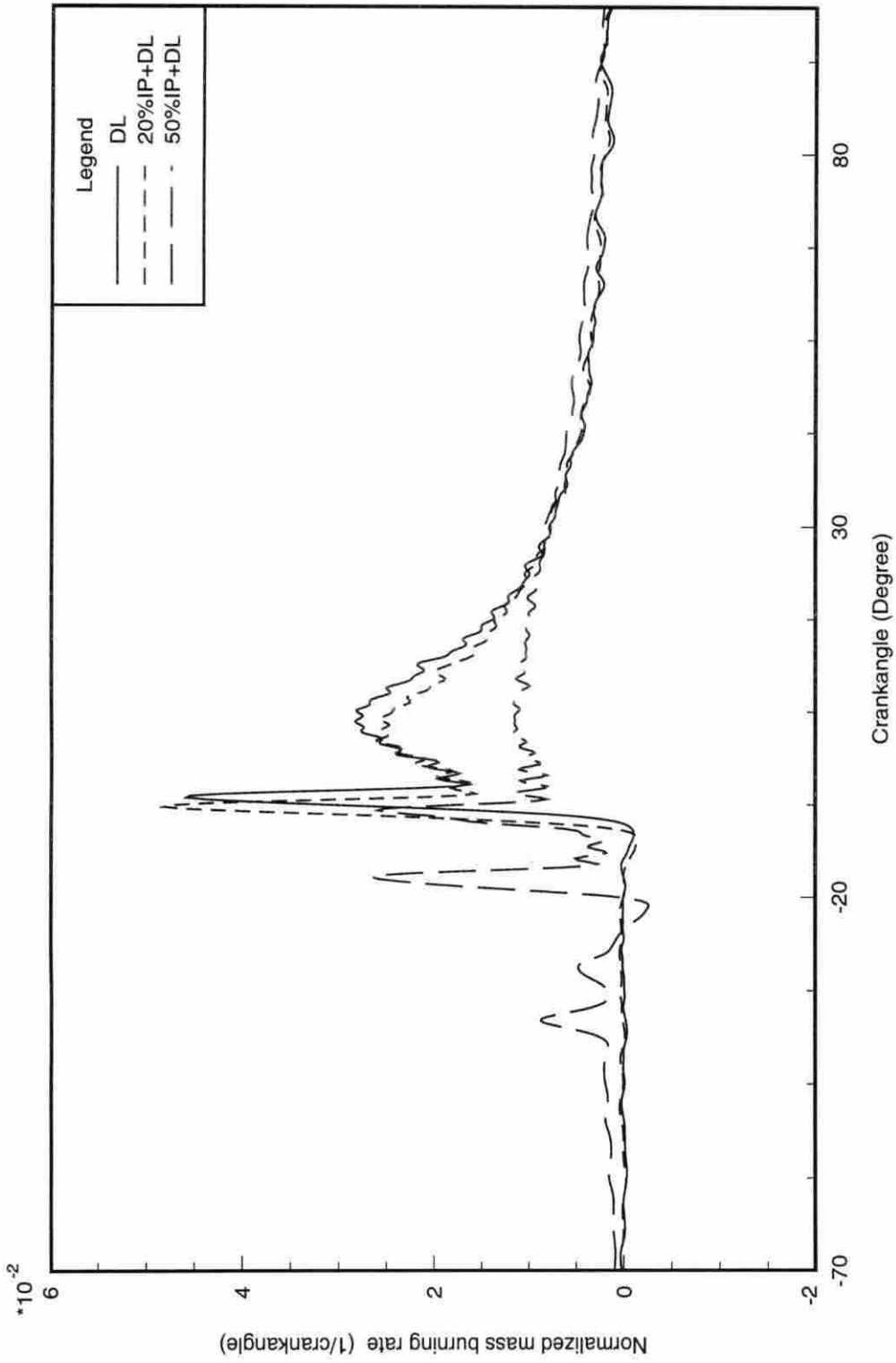
Figure 5.31   Burning rate calculated from third data set for iso-propyl blends

plete transesterification of soybean oil and had higher viscosity. When the iso-propyl ester, which contained monoglyceride, was blended with No.2 diesel fuel and supplied to the diesel engine, the higher viscosity monoglyceride may cause poor spray quality so that carbon deposits were produced at the nozzle holes of injectors. Excessive injector tip deposits were noted when the injectors were removed later in the study. The deposits may also have been present inside the injector tip and decreased the sealing ability of the needle valve surface. The normal test procedure was to run the engine for one hour to clear its fuel system when the fuel was changed, and an additional 15 minutes to take a particulate sample. After that, the combustion pressure data were collected. This amount of time may be long enough for carbon deposits to form on and in the injectors. When the fuel pressure increased in the injectors, some fuel could leak from the poorly sealed needle surface into the combustion chamber and lead to the early burning phenomenon.

After the 50% iso-propyl ester fuel was tested, the engine was fueled with No.2 diesel fuel again. With the engine running, the carbon deposits on the inside of the injectors may have gradually burned off. Because the diesel fuel was a commercial grade intended for on-highway use, it may also have contained a deposit inhibiting additive. Within a short time, the sealing ability of needle valve recovered and the combustion was back to normal. Heat release analysis of ester fuels is not widely available and that which is available does not show combustion irregularities like that observed here. Work is continuing to find the explanation for this phenomenon.

5.4.5   Light load combustion

When the diesel engine was tested at light load, the combustion of fuel blends revealed the same trends during premixed burning stage as at full load. Figure 5.32 shows the normalized burning rate. The fuel blends had shorter ignition delays than No.2 diesel fuel. At light load condition, all fuels showed a relatively flat diffusion combustion period. After initial, a large fraction of the fuel would be burned in the premixed mode. There was only one burning rate peak observed.
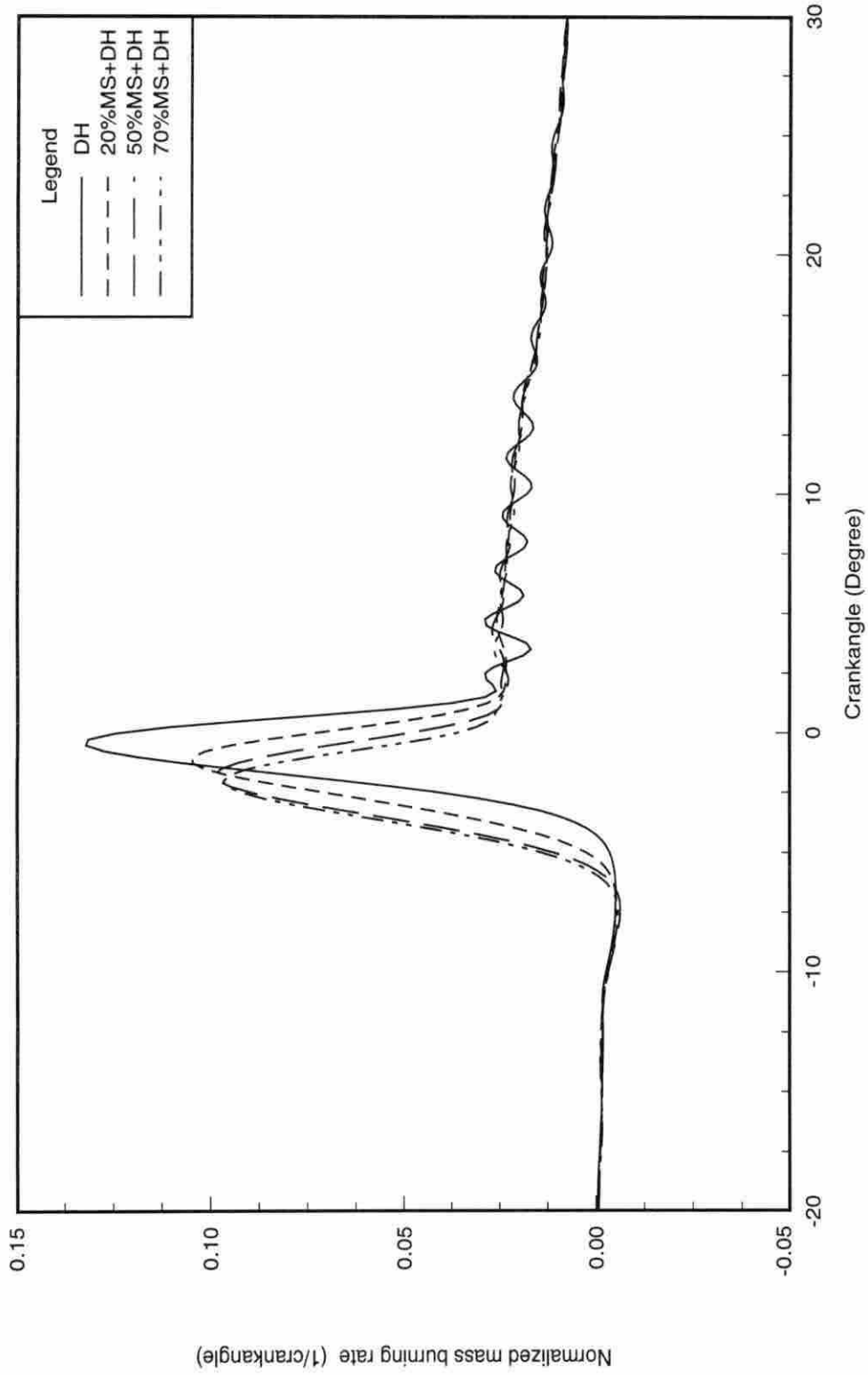
Figure 5.32   Normalized burning rate of methyl ester blends at 20% load

6. CONCLUSIONS AND RECOMMENDATIONS

6.1 Conclusions

A turbocharged diesel engine has been tested under steady state conditions to investigate the engine performance and emissions of methyl and iso-propyl esters of soybean oil with commercial No.2 diesel fuel. The results indicate that:

1. Methyl and iso-propyl esters of soybean oil have higher cetane numbers than No.2 diesel fuel. They can be used as cetane improvers to increase the cetane number of diesel fuel. The lower heating value of both of esters is about 12% lower than No.2 diesel fuel.

2. As a diesel engine fuel, the blends of methyl and iso-propyl esters with No.2 diesel fuel appear promising. The engine performance of these fuels is similar to operation with No.2 diesel fuel with slightly higher fuel consumption and lower brake power.

3. All fuel blends of methyl and iso-propyl esters of soybean oil produced lower emissions of carbon monoxide. 50% methyl ester blended with low sulfur No.2 diesel fuel had a CO emission reduction of 25.3%.

4. All fuel blends of methyl and iso-propyl esters of soybean oil produced lower emissions of unburned hydrocarbon with the maximum reduction of 29.0% from 50% iso-propyl ester blended with low sulfur No.2 diesel fuel.

5. Particulate and solid carbon emissions were significantly reduced when the diesel engine was fueled with fuel blends of methyl and iso-propyl esters. 50% iso-propyl ester blended with low sulfur No.2 diesel fuel gave the largest reductions in particulates and solid carbon emissions which were 28.0% and 55.3%, respectively. However, the soluble organic fraction for particulates of fuel blends increased with increasing percentage of esters in the fuel blends.

6. NOₓ emissions of all blend fuels were slightly higher than for No.2 diesel fuel.

7. At light load condition, ester/diesel fuel blends appeared to decrease CO and HC emissions and increase NOx, but none of the changes were statistically significant.

8. At light load condition, emissions of particulate and solid carbon for the blends were significantly increased due to large increases in the soluble organic portion of the particulate. The more ester in the fuel blends, the higher the particulate and SOF levels.

9. All fuel blends experienced the same combustion stages as No.2 diesel fuel.

10. All fuel blends experienced a shorter ignition delay under both 100% and 20% load conditions. At full load, they had a lower amount of premixed burning.

11. Blends of methyl or iso-propyl esters and No.2 diesel fuel showed similar diffusion burning rates to No.2 diesel fuel.

12. 50% blend fuel of iso-propyl ester showed evidence of some abnormal combustion and may cause carbon deposits on the injector nozzles.

6.2   Recommendations for Future Work

To further investigate the mechanisms that reduce emissions for esters of vegetable oils, some specific tests can be conducted.

1. Feed extra oxygen into the diesel engine with the intake air to inspect the effect of additional oxygen atoms on emission reductions.

2. Use cetane improver to simulate the effect of increasing cetane number of the ester fuels.

100

3. Individually test some long chain carbon compounds (saturated and un-saturated) which are contained in vegetable oils and their esters, such as:

Hexadecanoic acid $CH_3(CH_2)_{14}COOH$ (palmitate C 16:0)

Octadecanoic acid $CH_3(CH_2)_{16}COOH$ (stearate C18:0)

Trans-9-Octadecenoic acid $CH_3(CH_2)_7CH=CH(CH_2)_7COOH$ (oleic C18:1)

9, 12-Octadecadienoic acid $CH_3(CH_2)_4CH=CHCH_2CH=CH(CH_2)_7COOH$ (linoleic C18:2)

9, 12, 15-Octadecatrienoic acid

$CH_3CH_2CH=CHCH_2CH=CHCH_2CH=CH(CH_2)_7COOH$ (linolenic C18:3)

and their methyl and iso-propyl ester compounds.

4. Further purifying the iso-propyl ester of soybean oil, and performing engine tests to investigate the combustion irregularities.

REFERENCES

1. Baumgard, K.J. and Johnson, J.H.   The Effect of Low Sulfur Fuel and A Ceramic Particle Filter on Diesel Exhaust Particle Size Distributions.   SAE Transactions 101, 1992, 691-699.

2. Code of Federal Regulations (CFR 40).   Protection of the Environment.   Parts 100 to 149. Revised July 1, 1990.

3. Personal communication with Dr. Inmok Lee   Aug. to Nov., 1994.

4. Heywood, J.B. Internal Combustion Engine Fundamentals.   McGraw-Hill, New York, 1988.

5. Stone, R.   Introduction to Internal Combustion Engines. 2nd edition Macmillan Press Ltd., London, 1992.

6. Miyamoto, N., Ogawa, H., Shibuya, M. and Suda, T.   Description of Diesel Emissions by Individual Fuel Properties SAE paper 922221, 1992.

7. Uiiman, T.L., Mason, R.L. and Montalvo, D.A.   Study of Fuel Cetane Number and Aromatic Content-Effects on Regulated Emissions from A Heavy-duty Diesel Engine Southwest Research Institute SWRI 08-2940, Sept., 1990.

8. Wagner, L.E., Clark, S.J. and Schrock, M.D.   Effects of Soybean Oil Esters on the Performance, Lubricating Oil, and Wear of Diesel Engines SAE paper 841385, 1985.

9. Schumacher, L.G., Borgelt, S.C., Hires, W.G., Spurling, C., Humphrey, J.K. and Fink, J. Fueling Diesel Engines with Esterified Soybean Oil - Project Update.   ASAE paper MC93-101 1993.

10. Ferguson, C.R. Internal Combustion Engines Applied Thermosciences   John Wiley & Sons, New York, 1986.

11. Code of Federal Regulations. Title 40, Chapter 1, Subpart N Heavy-Duty Federal Test Procedure, 1988.

12. Mauderly, J.L., Griffith, E.C., Henderson, R.F., Jones, R.K. and McClellan, R.O. Evidence from Animal Studies for the Carcinogenicity of Inhaled Diesel Exhaust. Nitro-Arenes (PC Howard et al.). Plenum Press, New York. 1991, 1-13.

13. Mauderly, J.L. Diesel Exhaust. Environmental Toxicants: Human Exposures and Their health Effects. Van Nostrand Reinhold, New York, 1992, 119-162.

14. Heinrich, U. Carcinogenic Effects of Solid Particles. Toxic and Carcinogenic Effects of Solid Particles in the Respiratory Tract. Proceedings of the 4th International Inhalation Symposium, Hanover, Germany. ILSI Press, Washington, DC. 1993.

15. Nikula, K.J., Snipes, M.B., Barr, E.F., Griffith, W.C., Henderson, R.F. and Mauderly, J.L. Influence of Particle-associated Organic Compounds on the Carcinogenicity of Diesel Exic and Carcinogenic Effects of Solid Particles in the Respiratory Tract. Proceedings of the 4th International Inhalation Symposium, Hanover, Germany. ILSI Press, Washington, DC. 1993.

16. Johnson, J.H., Bagley, S.T., Gratz, L.D. and Leddy, D.G. A Review of Diesel Particulate Control Technology and Emissions SAE paper 940233, 1994.

17. Kamimoto, T. and Yagita, M. Particulate Formation and Flame Structure in Diesel Engines. SAE paper 890436, 1989.

18. Luo, L., Pipho, M.J., Ambs, J.L. and Kittelson, D.B. Particle Growth and Oxidation Direct-injection Diesel Engine. SAE paper 890580, 1989.

19. Smith, O.I. Fundamentals of Soot Formation in Flames with Application to Diesel Engine Particulate Emissions. Progress in Energy and Combustion Science 7 (1981): 275-291.

20. Cautreels, W. and Van Cauwenberghe, K. Extraction of Organic Compounds from Airborne Particulate Matter Water, Air, and Soil Pollution, Vol. 6, 1976, 103-110.

21. Hill, H.H., Jr, Chan, K.W. and Karasek, F.W. Extraction of Organic Compounds from Airborne Particulate Matter for Gas Chromatographic Analysis. Journal of Chromatography, Vol. 131, 1977, 245-252.

22. Grosjean, W. Solvent Extraction and Organic Carbon Determination in Atmospheric Particulate Matter: The Organic Extraction-Organic Carbon Analyzer Technique. Analytical Chemistry, Vol. 47, 797-805.

23. Cautreels, W. and Van Cauwenberghe, K. Experiments on the Distribution of Organic Pollutants Between Airborne Particulate Matter and the Corresponding Gas Phase. Atmospheric Environment, Vol. 12, 1976, 1133-1141.

24. Karasek, F.W., Denney, D.W., Chan, K.W. and Clement, R.E. Analysis of Complex Organic Mixtures on Airborne Particulate Matter. Analytical Chemistry, Vol. 50, 82-87.

25. Schreck, R.M., McGrath, J.J., Swarin, S.J., Hering, W.E., Groblicki, P.J. and MacDonald, J.S. Characterization of Diesel Exhaust Particulate Under Different Engine Load Conditions. The 71st Annual Meeting of the Air Pollution Control Association, Houston, June, 1978.

26. Huisingh, J., Bradow, R., Jungers, R., Claxton, L., Zweidinger, R., Teieda, S., Bumgarner, J., Duffield, R., Waters, M., Simmon, V., Hare, C., Rodriguez, C. and Snow, L. Application of Bioassay to the Characterization of Diesel Particulate Emissions: Part I. Characterization of Heavy Duty Diesel Particle Emissions. Symposium on Application of Short Term Bioassay in the Fractionation and Analysis of Complex Environmental Mixtures, Williamsburg, Feb., 1978.

27. Huisingh, J., Bradow, R., Jungers, R., Claxton, L., Zweidinger, R., Teieda, S., Bumgarner, J., Duffield, R., Waters, M., Simmon, V., Hare, C., Rodriguez, C. and Snow, L Application of Bioassay to the Characterization of Diesel Particulate Emissions: Part II. Application of a Mutagenicity Bioassay to Monitoring Light Duty Diesel Particle Emissions. Symposium on Application of Short Term Bioassay in the Fractionation and Analysis of Complex Environmental Mixtures, Williamsburg, Feb., 1978.

28. Information Report: 1979 Progress of the Chemical Characterization Panel of the Composition of Diesel Exhaust Project and Results of Particulate Extraction Round-robin. CRC Report No. 516. Coordinating Research Council, Inc. 219 Perimeter Center Parkway, Atlanta, Georgia, March, 1980.

29. Funkenbusch, E.F., Leddy, D.G. and Johnson, J.H. The Characterization of the Soluble Organic Fraction of Diesel Particulate Matter. The Measurement and Control of Diesel Particulate Emissions PT-17, 1979, 123-143.

30. Lipkea, W.H., Johnson, J.H. and Vuk, C.T. The Physical and Chemical Character of Diesel Particulate Emissions-Measurement Techniques and fundamental Considerations. The Measurement and Control of Diesel Particulate Emissions PT-17, 1979, 1-57.

31. Goering, C.E., Schwab, A.W., Daugherty, M.J., Pryde, E.H. and Heakin, A.J. Fuel Properties of Eleven Vegetable Oils. Transactions of the ASAE Vol. 25(6): Nov., 1982, 1472-1483.

32. Ziejewski, M., Goettler, H.J., Cook, L.W. and Flicker, J. Polycyclic Aromatic Hydrocarbons Emissions from Plant Oil Based Alternative Fuels. SAE paper 911765, 1991.

33. Freedman, B., Bagby, M.O., Callahan, T.J. and Ryan, T.W. Cetane Numbers of Fatty Esters, Fatty Alcohols and Triglycerides Determined in a Constant Volume Combustion Bomb. SAE paper 900343, 1990.

34. Bagby, M.O. and Freedman, B. Seed Oils for Diesel Fuels: Sources and Properties. ASAE paper 871583, 1987.

35. Braun, D.E. and Stephenson, K.Q. Alternative Fuel Blend and Diesel Engine Tests. Vegetable Oil Fuels Proceeding of the International Conference on Plant and Vegetable Oils as Fuels Aug., 1982, 294-302.

36. Mazed, M.A., Summers, J.D. and Batchelder, D.G. Peanut, Soybean and Cottonseed Oil as Diesel Fuels Transactions of the ASAE Vol. 28(5): 1985, 1375.

37. Mazed, M.A., Summers, J.D. and Batchelder, D.G. Diesel Engine-Diesel/Vegetable Oil Short Term Performance Tests ASAE paper 851058, 1985.

38. Ishii, Y. and Takeuchi, R. Vegetable Oils and Their Effect on Farm Engine Performance. Transactions of the ASAE Vol. 30(1): Jan.-Feb., 1987, 2-6.

39. Hemmerlein, N., Korte, V., Richter, H. and Schroder, G. Performance, Exhaust Emissions and Durability of Modern Diesel Engines Running on Rapeseed Oil. SAE paper 910848, 1991.

40. Ryan, T.W., Callahan, T.J. and Dodge, L.G. Characterization of Vegetable Oils for Use as Fuels in Diesel Engines. Vegetable Oil Fuels-Proceedings of the International Conference on Plant and Vegetable Oils as Fuels, Aug., 1982, 70-81.

41. Tahir, A.R., Lapp, H.M. and Buchanan, L.C. Sunflower Oil as a Fuel for Compression Ignition Engines. Vegetable Oil Fuels-Proceedings of the International Conference on Plant and Vegetable Oils as Fuels Aug., 1982, 82-91.

42. Fort, E.F. and Blumberg, P.N. Performance and Durability of a Tubocharged Diesel Fueled with Cottonseed Oil Blends. Vegetable Oil Fuels-Proceedings of the International Conference on Plant and Vegetable Oils as Fuels Aug., 1982, 374-382.

43. Van der Walt, A.N. and Hugo, F.J.C. Attempts to Prevent Injector Coking with Sunflower Oil by Engine Modifications and Fuel Additives. Vegetable Oil Fuels-Proceedings of the International Conference on Plant and Vegetable Oils as Fuels Aug., 1982, 230-238.

44. Schlick, M.L., Hanna, M.A. and Schinstock, J.L. Soybean and Sunflower Oil Performances in a Diesel Engine. Transactions of the ASAE Vol. 31(5): Sept.-Oct., 1988.

45. Hassett, D.J. and Hasan, R.A. Sunflower Oil Methyl Ester as a Diesel Fuel Vegetable Oil Fuels Proceedings of the International Conference on Plant and Vegetable Oils as Fuels Aug., 1982, 123-126.

46. Kusy, P.F. Transesterification of Vegetable Oils for Fuels. Vegetable Oil Fuels Proceedings of the International Conference on Plant and Vegetable Oils as Fuels Aug., 1982, 127-137.

47. Vander Griend, L. Characterization of Vegetable Oil Combustion. Process to Manufacture Ethyl Ester of Rape Oil. First Biomass Conference of the Americas: Energy, Environment, Agriculture, and Industry Proceedings Vol. II Aug.-Sept., 1993, 815-826.

48. Peterson, C.L., Feldman, M., Korus, R. and Auld, D.L. Batch Type Transesterification Process for Winter Rape Oil. Applied Engineering in Agriculture Vol. 7(6): Nov., 1991, 711-716.

49. Romano, S. Vegetable Oils - A New Alternative. Vegetable Oil Fuels-Proceedings of the International Conference on Plant and Vegetable Oils as Fuels Aug., 1982, 106-116.

50. Engler, C.R., Lepori, W.A., Johnson, L.A. and Yarbrough, C.M. Processing Requirements for Plant Oils as Alternative Diesel Fuels. Liquid Fuels from Renewable Resources, Proceedings of an Alternative Energy Conference Dec., 1992, 79-88.

51. Freedman, B. and Pryde, E.H. Fatty Esters from Vegetable Oils for Use as a Diesel Fuel. Vegetable Oil Fuels-Proceedings of the International Conference on Plant and Vegetable Oils as Fuels Aug., 1982, 117-122.

52. Geyer, S., Jacobus, M. and Lestz, S. Comparison of Diesel Engine Performance and Emissions from Neat and Transesterified Vegetable Oils. Transactions of the ASAE Vol. 27(2): March - April, 1984, 375-384.

53. Kaufman, K.R. and Ziejewski, M. Sunflower Methyl Esters for Direct Injected Diesel Engines. Transactions of the ASAE 2706, 1984, 1626-1633.

54. Zhang, Q., Feldman, M.E. and Peterson, C.L. Diesel Engine Durability when Fueled with Methyl Ester of Winter Rapeseed Oil. ASAE paper No. 88-1562, 1988.

55. Barsic, N.J. and Humke, A.L. Performance and Emissions Characteristics of a Naturally Aspirated Diesel Engine with Vegetable Oil Fuels SAE paper 810262, 1981.

56. Hemmerlein, N. Korte, V. and Richter, H.   Performance, Exhaust Emissions and Durability of Modern Diesel Engines Running on Rapeseed Oil   SAE paper 910848, 1991.

57. Schumacher, L.G., Hires, W.G. and Borgelt, S.C.   Fueling a Diesel Engine with Methyl-Ester Soybean Oil.   Liquid Fuels from Renewable Resources Proceedings of an Alternative Energy Conference Dec., 1992, 124-131.

58. Pischinger, G.H. and Falcon, A.M.   Methylesters of Plant Oils as Diesel Fuels, Either Straight or in Blends.   Vegetable Oil Fuels-Proceedings of the International Conference on Plant and Vegetable Oils as Fuels.   Aug., 1982, 198-208.

59. Alfuso, S., Auriemma, M., Police, G. and Prati, M.V.   The Effect of Methyl-Ester of Rapeseed Oil on Combustion and Emissions of DI Diesel Engines.   SAE paper 932801, 1993.

60. Mittelbach, M., Tritthart, P. and Junek, H.   Diesel Fuel Derived from Vegetable Oils, II: Emission Tests Using Rape Oil Methyl Ester.   Energy in Agriculture   Vol. 4, 1985, 207-215.

61. Harrington, J.A. and Yetter, R.A.   Application of a Mini-Dilution Tube in the Study of Fuel Effects on Stratified Charge Engine Emissions and Combustion.   SAE paper 811198, 1981.

62. Suzuki, J.   Development of Dilution Mini-Tunnel and Its Availability for Measuring Diesel Exhaust Particulate Matter.   SAE paper 851547, 1985.

63. Hirakouchi, N., Fukano, I. and Shoji, T.   Measurement of Diesel Exhaust Emissions with Mini-Dilution Tunnel.   SAE paper 890181, 1989.

64. Heden, P., Eriksson, C. and Gustavsson, L.   A Simplified Dilution Tunnel System Intended for Heavy-Duty Diesel Development.   SAE paper 861279, 1986.

65. Murray, B.C.   Development of a Transient Diesel Exhaust Emissions Measurement System.   M.S. Thesis, Iowa State University, 1989.

66. Effect of Intake-Air Humidity and Temperature on Diesel Emission with Correlation Studies SAE paper 730213, 1973

67. 1993 SAE Handbook Society of Automotive Engineers, Inc. Warrendale, 1993, 25.04-25.05.

68. Standard Method for Determining Relative Humidity by Wet and Dry-Bulb Psychrometer American Society for Testing Materials ASTM E337-72.

69. Keenan, J.H., Keyes, F.G., Hill, P.G. and Moore, J.G. Steam Tables: Thermodynamic Properties of Water Including Vapor, Liquuid, and Solid Phases John Wiley & Sons, Inc., New York, 1978.

70. Krieger, R.B. and Borman, G.L. The Computation of Apparent Heat Release for Internal Combustion Engines ASME paper 66-WA/DGP-4, 1966.

71. Olikara, C. and Borman, G.L. A Computer Program for Calculating Properties of Equilibrium Combustion Products with Some Applications to I.C. Engines SAE paper 750468, 1975.

72. Ryan III, T.W., Erwin, J., Mason, R.L. and Moulton, D.S. Relationships between Fuel Properties and Composition and Diesel Engine Combustion Performance and Emissions SAE paper 941018, 1994.

73. Ullman, T.L. Investigation of the Effects of Fuel Composition, and Injection and Combustion System Type on Heavy-Duty Diesel Exhaust Emissions SAE paper 892072, 1989.

74. McCarthy, C.I., Slodowske, W.J., Sienicki, E.J. and Jass, R.E. Diesel Fuel Property Effects on Exhaust Emissions from a Heavy Duty Diesel Engine that Meets 1994 Emissions Requirements SAE paper 922267, 1992.

75. Tosaka, S., Fujiwara, Y. and Murayama, T. The Effect of Fuel Properties on Diesel Engine Exhaust Particulate Formation SAE paper 890421, 1989.

76. Ullman, T.L., Hare, C.T. and Baines, T.M. Heavy-Duty Diesel Emissions as a Function of Alternate Fuels SAE paper 830377, 1983.

77. Ziejewski, M. and Kaufman, K.R.   Vegetable Oils as a Potential Alternate Fuel in Direct Injection Diesel Engines   SAE paper 831359, 1983.

78. Needham, J.R. and Doyle, D.M.   The Combustion and Ignition Quality of Alternative Fuels in Light Duty Diesel   SAE paper 852101, 1985.

79. Niehaus, R.A., Goering, C.E., Savage, L.D. and Sorennson, Jr., S.C.   Cracked Soybean Oil as a Fuel for a Diesel Engine   Transactions of the ASAE Vol. 29(3): May-June, 1986.   683-689.

80. Zubik, L Sorenson, C. and Goering, C.E.   Diesel Engine Combustion of Sunflower Oil Fuels.   Transactions of the ASAE Vol. 27(3), 1984,   1252-1256.

81. Kuo, K.K.   Principles of Combustion   John Wiley & Sons, New York, 1986.

82. Faletti, J.J., Sorenson, S.C. and Goering, C.E.   Energy Release Rates from Hybrid Fuels   Transactions of the ASAE Vol. 27(2), 1984,   322-325.

83. Jiang, Q   Prediction of Diesel Engine Particulate Emission During Transient Cycles   Dissertation of PH.D., Iowa State University, 1991.

ACKNOWLEDGMENTS

APPENDIX A CALIBRATIONS OF PRESSURE TRANSDUCERS

Four pressure transducers were used during the experiment. Two of them were Viatran model 141 pressure transducers, and one was a Kistler model 6061A pressure transducer. They were calibrated with an Amthor type 452 dead-weight tester. The fourth was a Baratron differential pressure transducer which was calibrated with regulated compressed air and a water manometer. The specifications of these pressure transducers are shown in Table A.1.

Table A.1   Specifications of pressure transducers

Type	Range	Output	Application
Viatran 141	0.0-21.0 bar	1-8 mV	Primary dilution
Viatran 141	0.0-6.9 bar	1-8 mV	2nd dilution
Kistler 6061A	0.0-250.0 bar		Cylinder pressure
Baratron (Diff)	0.0-2.49 kPa	0-10 V	Intake air pressure drop

One of the two Viatran pressure transducers was installed upsteam of the orifice in the primary dilution air line, and the other was located just before an orifice in the secondary dilution air line. The two Viatran pressure transducers were calibrated by another student working on an earlier project. The calibration data that are shown in Table A.2 are extracted from Qiqing Jiang's PH.D. dissertation [83].

Before installation, the Kistler pressure transducer was calibrated on a dead-weight tester. The calibration procedure was to load and unload the known weights on the tester plate. The output signal from the pressure transducer, which was recorded as a voltage for each pressure setting, was amplified by a PCB charge amplifier, and received by a Zenith

Z-386 computer and an Analog Devices RTI-860 data acquisition board. A linear regression analysis was performed to fit a straight line to the test data.

The differential pressure transducer was used to measure the pressure drop across a Meriam Laminar Flow Element to determine the engine's intake air flow rate. During calibration, a regulated compressed air supply was applied to a valve and the pressure drop was measured with the differential pressure transducer and a Dwyer water manometer simultaneously. After calibration, a linear regression analysis was carried out to check the validity of the linear equation. The general equation to calculate the pressure or pressure difference is as follows:

$$P = a_0 + a_1 V$$

where P = pressure or pressure difference applied to the pressure transducer;

              V = voltage output from the pressure transducer;

              a_0 and a_1 = linear regression coefficients.

The linear regression coefficients and the correlation coefficients are shown in Table A.2. The data and the linear regression lines for the Kistler pressure transducer and the differential pressure transducer are shown in Figure A.1 and A.2, respectively.

Table A.2   Linear regression coefficients

Type	a_0	a_1	r^2
Viatran 141	0.5486 bar	0.7469 bar/mV	1.0000
Viatran 141	-0.0339 bar	0.1488 bar/mV	0.9992
Kistler 6061A	-0.3728 bar	25.3716 bar/V	1.0000
Baratron (Diff.)	-0.00027 kPa	0.2512 kPa/V	1.0000
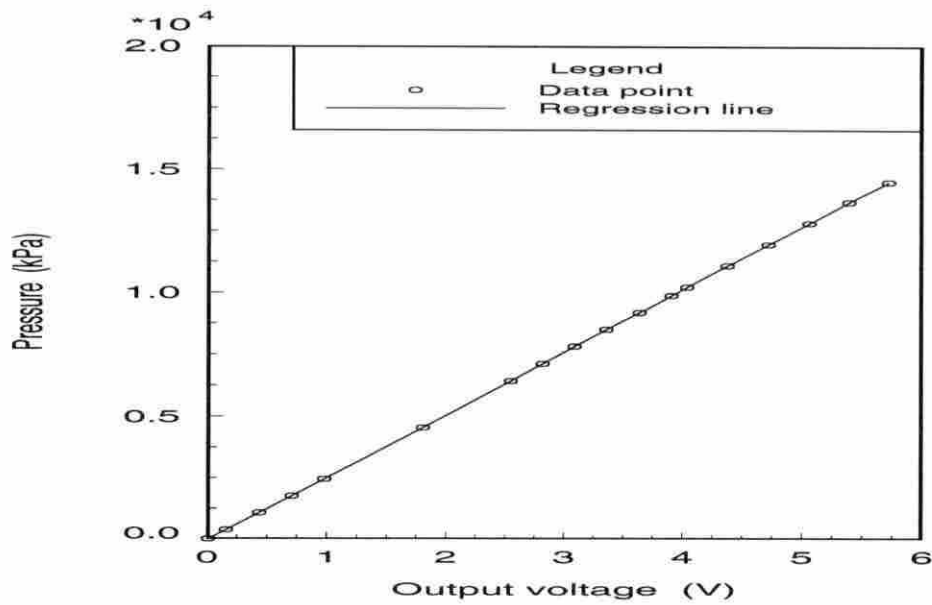
Figure A.1   Calibration of Kistler 6061A pressure transducer
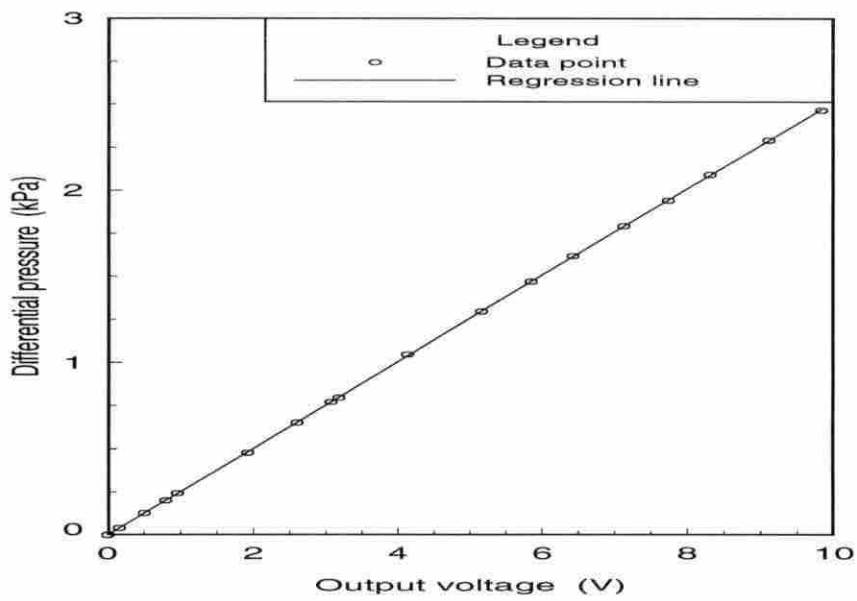
Figure A.2   Calibration of differential pressure transducer

APPENDIX B CALIBRATION OF THE DILUTION AIR SYSTEM

The mass flow rate of dilution air can be determined by measuring the pressure and temperature of the dilution air on the upstream side of an orifice. The primary dilution air system was calibrated during an earlier study. The following equations, which were used to calculate the mass flow rate of dilution air, were extracted from B.C. Murray's M.S. thesis [65].

$$\dot{m}_{pda} = -0.195 + 0.0705 \left(P_{por} / \sqrt{T_{por}} \right) - 8.806 \times 10^{-4} \left(P_{por} / \sqrt{T_{por}} \right)^2 \qquad \text{(B-1)}$$

where $\dot{m}_{pda}$ = the mass flow rate of primary dilution air in kg/s.

P_{por} = the absolute static pressure upstream of the orifice in kPa.

T_{por} = the temperature upstream of the orifice in K.

APPENDIX C   PRIMARY DILUTION AIR QUALITY TEST

To accurately measure the particulate emissions, the dilution air must not contain foreign particles. The procedure used to determine the influence of particles originating from sources other than the engine is described in this appendix.

The dilution air is provided by an Ingersoll-Rand Centac II two-stage air compressor. This test was divided into two steps. First, the air filter in the primary air supply line located near ball valve 2 (see Figure 3.2) was removed. Three particulate samples were taken with Pallflex glass fiber filters, using the particulate sampling system, on three separate days. The mass flow rates of the dilution air and the sample gas were set to the values used for engine testing. Then, a new air filter was installed in the air filter holder, and the same test was repeated for another three days. After each filter was allowed to equilibrate in the enviromentially controlled weighing chamber for 48 hours, it was weighed with an analytical balance. The summarized data for those filters is shown in Table C.1.

These results show:

1. Filter weight increase due to particulates in the air line is only a small fraction of the weight increase when the engine is tested.

2. When the air filter is used, some increase in filter weight is still observed, probably due to blow-off from the tunnel walls. However, the amount of material is much less than observed without filter.

Table C.1   Summarized data of tested filters

	without air filter	with air filter	dirt reduction rate %
Dilution air flow rate=0.5942 (kg/s)			
Mean weight of sample on first filter (mg)	0.13	0.09	34.96
Mean weight of sample on second filter (mg)	0.03	0.01	60.06
Dilution air flow rate=0.6958 (kg/s)			
Mean weight of sample on first filter (mg)	0.15	0.05	65.92
Mean weight of sample on second filter (mg)	0.02	0.00	100.00
Dilution air flow rate=0.8329 (kg/s)			
Mean weight of sample on first filter (mg)	0.38	0.27	28.00
Mean weight of sample on second filter (mg)	0.04	0.02	42.86

117

APPENDIX D   DILUTION TUNNEL MIXING TEST

The objective of the mixing test was to determine the effectiveness of the mixing of dilution air with exhaust gas in the dilution tunnel. A similar mixing test was performed by B.C. Murray [65] who supplied a constant flow rate of CO_2 into the dilution tunnel and measured the CO_2 concentration in the diluted gas. However, to check the actual mixture of engine exhaust gas with the dilution air, the test described here was conducted with engine exhaust gas.

Four probes located near the particulate sampling cross section were mounted around the dilution tunnel (shown in Figure D.1) to sample the diluted exhaust gas. Each of them was inserted into the dilution tunnel 7.5 cm. Nitric oxide was chosen as the gas to measure as an indicator of the effectiveness of the mixing. Since diesel particulates are small enough (0.0075-1.00 μm) [1] to behave essentially as gaseous emissions, the results should be valid for particulates, also. Between the NO analyzer and the probes there was a switching valve which made it easy to take samples from different probes.

The mixing test was conducted for several dilution air flow rates and engine operating conditions. Figure D.2 shows results that prove the NO concentration was even cross the diameter of the tunnel. It was concluded that the mixing is adequate.
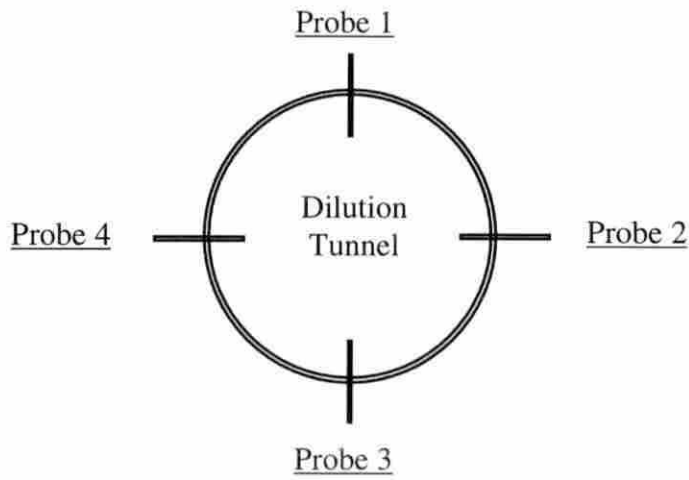
Figure D.1   Schematic diagram of sampling probes distribution
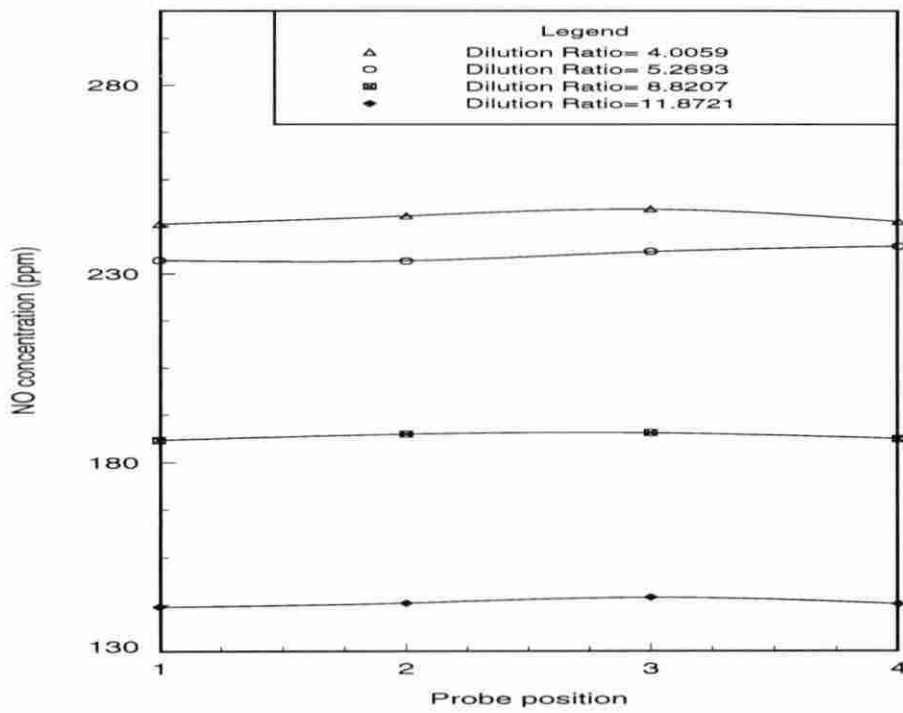
Figure D.2   Mixing test results

APPENDIX E PARTICULATE SAMPLING SYSTEM LEAK TEST

To measure particulate emission with the dilution tunnel, the sampling system must be sealed so that no air leaks into the sampling system. This air would reduce the amount of diluted exhaust gas which passed through the particulate filters. While the measured particulate emission would have a systematic error if the amount of the leakage remains constant, it will possess a random error if the leakage rate is intermittent in nature. However, both errors will shift the data in one direction. The procedure used for the leak test is discussed in this appendix.

To conduct a leak test, the ball valves in the particulate sample transfer tube, in the secondary dilution air line, and the valve between the sample pump and gas meter, as shown in Figure 3.3, were closed. The inlet to the filter holder was also capped. The vacuum valve was opened and the vacuum pump was used to draw the system down to a vacuum of 85 kPa (25 inHg). Then, the vacuum pump was shut off and the time required for air to leak back into the system was measured. The vacuum valve was closed during the leak-down so that the vacuum pump and connecting hoses would not be a part of the leak test. A stopwatch was used with the system's vacuum gage to monitor the leak-down of the system.

The leak test data are plotted in Figure E.1. This leak-down rate is acceptable. The vacuum of the sampling system is usually in the vacuum range of 19 to 51 kPa, depending on the particulate loading of the filter. The leak down rate can be used to estimate a mass flow rate. This rate of leakage is less than 0.16% of the mass flow rate of the particulate sample as long as the vacuum in the system is less than 51 kPa. The sampling system was periodically tested for leakage following this same procedure throughout the experiment.
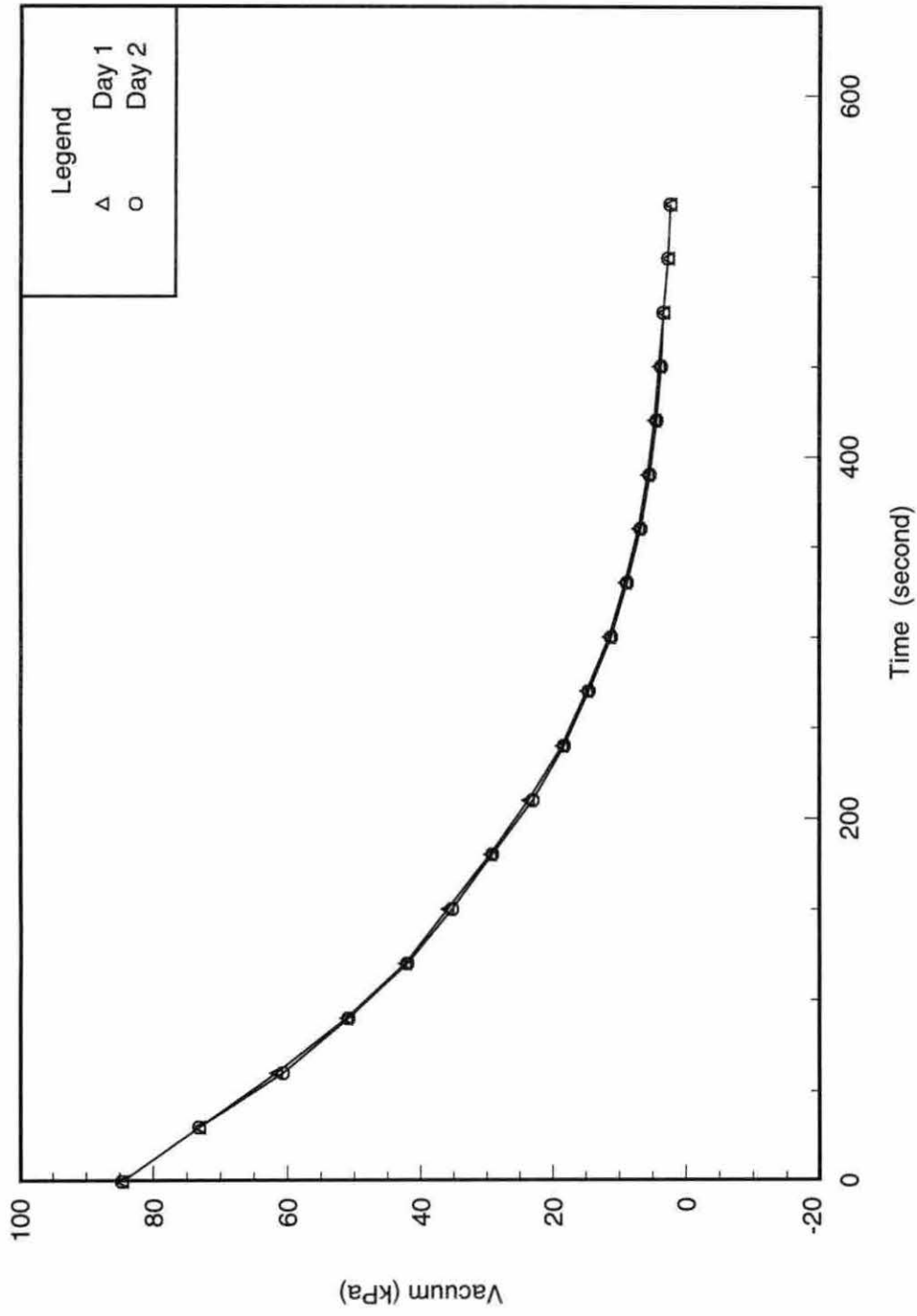
Figure E.1   Particulate sampling system leak test

APPENDIX F   FILTER WEIGHING PROCEDURE

This appendix will discuss the procedure used for weighing particulate filters.

The balance used was a Mettler AE240 dual range balance located in an enviromentally controlled weighing chamber. The humidity and temperature in the weighing chamber were kept constant with oil-free compressed air continuously diffused into the chamber. The temperature and relative humidity in the chamber were recorded over the duration of the project. The recorded data of temperature and relative humidity are plotted in Figures F.1 and F.2, respectively, for 40 days. To satisfy the EPA requirements of temperature and relative humidity in the weighing chamber, which should be in the range of 293.15 to 303.15 K for temperature, and 30% to 70% for relative humidity [11], both of them were controlled at 298 K and 30%. From the recorded data, the average temperature was about 298 K and the variations of temperature were within $\pm$ 2K. The average relative humidity was about 30% and the variations of the relative humidity were within $\pm$ 3%. Therefore, the environmental conditions in the weighing chamber met the weighing chamber specification of EPA.

The weighing range of the balance was set to 40 grams. After the selection of the range was set and after the power supply had been left on for more than 60 minutes, the balance was calibrated. The stability detector and the integration time (measuring cycle) were selected at normal settings. These settings gave the best performance in terms of measuring accuracy and precision. The power supply for the balance was left on during the whole experiment period. .

During the early part of the project it was noticed that after several weighings, a filter could show different weights on each weighing. Also, when the filter was on the balance, the weight display was unstable.

To find the reason, four clear filters were randomly sampled and weighed. The weighing procedure was that the filter was put on the balance pan and the glass door was closed. After the stability detector light of the balance went off, a stopwatch was started, and the
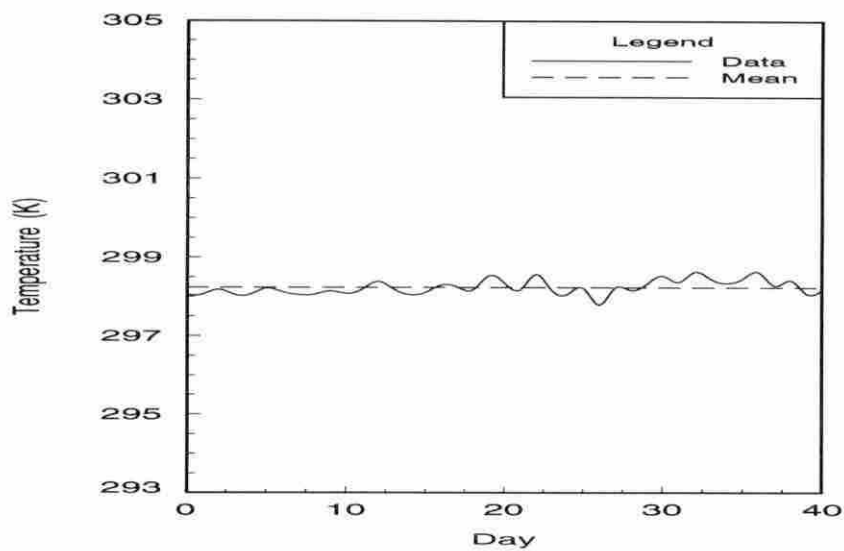
Figure F.1   Temperature variations in weighing chamber during test
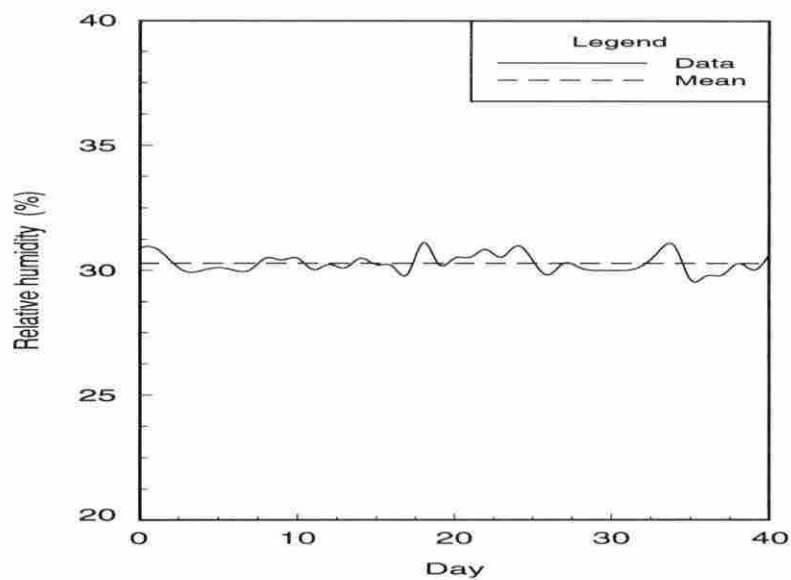
Figure F.2   Relative humidity variations in weighing chamber during test

displayed weight of the filter was written down. The weight of the filter was recorded continuously every 30 seconds for 10 minutes. These filter weights are plotted in Figure F.3. As seen in Figure F.3, all of the filter weights tended to decrease, and the change tended to slow down after about seven minutes. The largest change of filter weight was 19.88 mg which was of the same order as the weight of particulate to be measured.

Because the filters were kept in plastic petri dishes, some electrostatic charge was easily produced on the surface of the petri dishes through friction during the handling and transport of petri dishes into and out the weighing chamber. Moreover, these electrostatic charges could not be discharged or at least only very slowly over a long period due to the high degree of electrical insulation of the plastic petri dishes, and the low relative humidity in the weighing chamber. The filters in the petri dishes collected some of the electrostatic charge from the petri dishes. This electrostatic charge, as it was attracted and repelled by surfaces in the balance, caused the filter weight to change. Since the balance pan was electrically grounded via the three-pin power plug, the electrostatic charge was discharged quickly after the filter was placed on the balance pan. The weights of the filters decreased during the weighing period.

To check this validity of the conclusion, four other clear filters were randomly selected. Before weighing, all of them were placed directly on a grounded shelf for 10 minutes. The weighing procedure was the same as before. The data are plotted in Figure F.4 which shows that the filter weights changed very little with time. The maximum change of filter weight was 0.39 mg, corresponding to only 2.98 % of the minimum particulate sample weight 13.08 mg. During the period of the experiment, each filter was grounded first by placing it on the grounded shelf for 10 minutes before weighing.

Some possible methods that may be used to avoid the interference of electrostatics in future tests are:

1. Increase the relative humidity in the weighing chamber to 45 to 60%;

2. Screen electrostatic forces by placing the filters in a metal container.
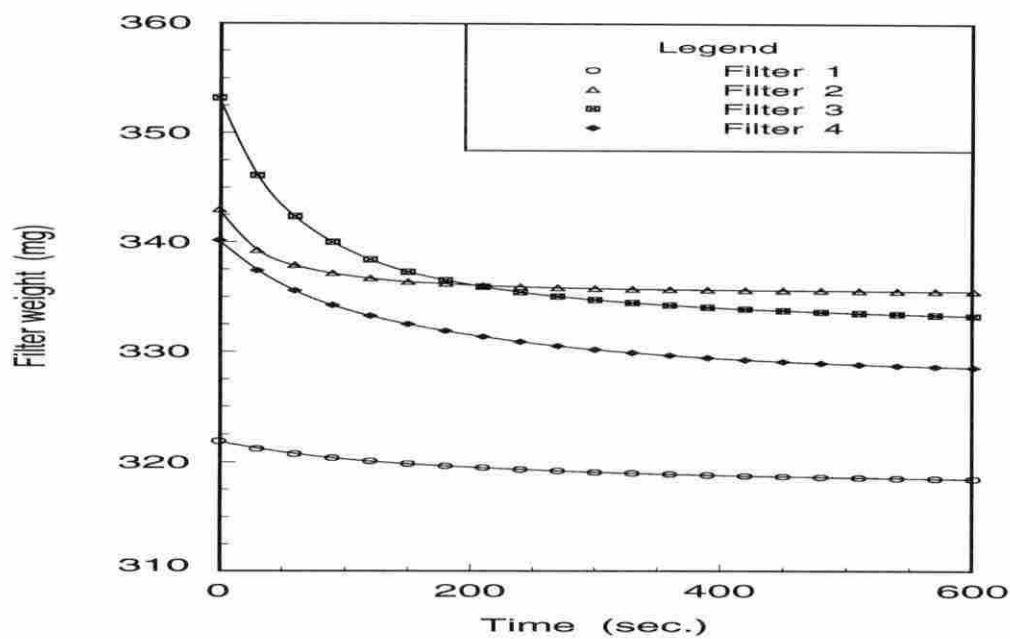
Figure F.3   Filter weight drift before grounding
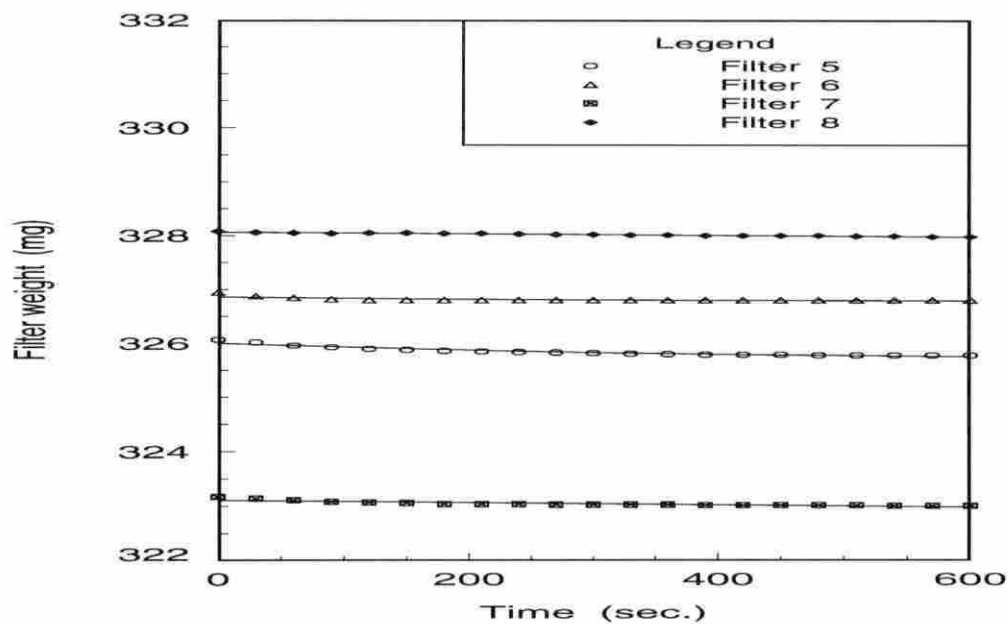
Figure F.4   Filter weight drift after grounding

During this experiment, four filters were used as reference filters. Before weighing any sample filters, two reference filters were weighed first to make sure the balance and the weighing chamber were working properly. EPA regulations require the reference filters be changed at least once per month, so two of four filters were kept in the weighing chamber at any given time. Table F.1 shows the statistical data of the reference filter weights. The variations could be neglected due to the small coefficients of variation of those reference filters.

After having been stabilized for at least 48 hours in the weighing chamber, the sample filters were ready to be weighed. The display of the balance was set to zero by pressing the control bar briefly before each weighing. The filter was removed from the petri dish by using a steel forceps and gently placed on the center of the balance pan. The glass door was slowly closed. When the stability detector light went off, the filter weight was read immediately. Then, the filter was replaced in the petri dish. After the balance stability detector went off again, it was ready to weigh another filter. To check the reproducibility of the balance, each filter was usually weighed two times. The final weight of the filter was the average of the two readings.

Table F.1   Statistical data for the reference filters

	Filter 1	Filter 2	Filter 3	Filter 4
Min. weight (mg)	318.00	335.53	332.56	328.09
Max. weight (mg)	318.21	335.67	332.68	328.18
No. of weighings	12	12	12	12
Mean (mg)	318.10	335.61	332.60	328.13
S. D[a]. (mg)	0.05	0.06	0.04	0.03
C.V. %	0.02	0.02	0.01	0.01

[a] standard deviation

APPENDIX G   EFFECT OF METHYLENE CHLORIDE SOLVENT TESTS

Tests were conducted to determine the effectiveness of methylene chloride (CH_2Cl_2) solvent in dissolving the soluble organic fraction (SOF) of diesel particulate during the extraction. This appendix contains a description of the tests.

Pallflex T60A20 filters were used to take the particulate sample during the experiment. To determine whether or not the empty filters were stable enough, six empty filters were random sampled and extracted with methylene chloride solvent in a Soxhlet extractor for an average of 60 cycles. The data are shown in Table G.1. The average mass of soluble substance on the empty filters is 0.03 mg which corresponds to only 0.16% of the minimum mass of particulate under 100% of full load, and 0.19% of the minimum mass of particulate under 20% of full load. So, the empty filters are considered clear enough.

A second test was conducted to determine whether the solvent used for the extraction tests would remove all the materials in the soluble organic fraction (SOF). Because of its strong solvent properties, methylene chloride is used widely as the solvent during extraction

Table G.1   Statistical data for extracted empty filters

	Weight change
Filter 1 (mg)	0.02
Filter 2 (mg)	0.06
Filter 3 (mg)	0.07
Filter 4 (mg)	0.01
Filter 5 (mg)	0.01
Filter 6 (mg)	0.01
Mean weight change (mg)	0.03
Standard deviation (mg)	0.03

of diesel particulate SOF [22], [29]. The primary compounds in SOF are unburned fuel, lube oil, and some aromatic or aliphatic species such as pyridine and aniline [29]. However, since the volatility of pyridine and aniline is high, making it very hard to weigh a consistent amount of these organic substances, they were not tested. Only No.2 diesel fuel, methyl soyate and low detergent oil (30W) were selected as test samples.

A small amount of each substance, with mass ranging from 2.13 to 40.00 mg, was put on six different empty filters. Each loaded filter was extracted with methylene chloride in a Soxhlet extractor for an average of 60 cycles. After extraction, these filters were set in the weighing chamber for 48 hours, and weighed. The average extraction rates based on six loaded filters are shown in Table G.2.

Inspection of those results shows that the average extraction rate of CH_2Cl_2 is greater than 99.2%. Therefore, the solvent CH_2Cl_2 is a good choice as an extraction solvent.

Table G.2   Methylene chloride extractable rate for components of SOF

Removed rate (%)			
Sample	No.2 diesel	MS[a]	Oil[b]
Filter 1	98.29	100.00	99.88
Filter 2	98.85	99.60	100.00
Filter 3	99.72	100.00	99.85
Filter 4	98.87	98.47	99.89
Filter 5	99.82	99.96	98.89
Filter 6	99.77	99.34	99.92
Mean (%)	99.22	99.56	99.74
Standard deviation	0.64	0.60	0.42

[a]methyl ester of soybean oil

[b]low detergent oil (30W)

APPENDIX H   TEST DATA

This appendix contains the measured data from the study.

	8/15/94 Diesel	8/15/94 20%MS+DH	8/15/94 20%MS+DH	8/15/94 50%MS+DH	8/15/94 70%MS+DH	8/15/94 50%MS+DH	8/15/94 70%MS+DH	8/16/94 Diesel	8/16/94 Diesel	8/16/94 20%MS+DH	8/16/94 20%MS+DH
Date	8/15/94	8/15/94	8/15/94	8/15/94	8/15/94	8/15/94	8/15/94	8/16/94	8/16/94	8/16/94	8/16/94
Fuel	Diesel	20%MS+DH	20%MS+DH	50%MS+DH	70%MS+DH	50%MS+DH	70%MS+DH	Diesel	Diesel	20%MS+DH	20%MS+DH
Engine speed (rpm)	1400	1400	1400	1400	1400	1400	1400	1400	1400	1400	1400
% of rated load	100	100	20	100	20	100	20	100	100	100	20
Brake torque (ft.lbf)	214.50	213.00	43.00	207.25	41.00	203.50	41.75	214.00	214.00	211.0000	42.0000
Time (sec.)	900.46	912.14	899.88	901.45	901.01	900.52	900.38	900.64	900.13	900.3500	901.2200
Fuel weight (kg)	2.42	2.43	0.77	2.50	0.78	2.51	0.81	2.43	0.75	2.4600	0.7600
Coolant counts	95974	101230	34325	90840	32911	91678	33829	104070	32977	94067	34118
Ambient air T. (F)	76	76	76	76	76	76	76	75	75	75	75
Patm (mmHg)	738.0	738.0	738.0	738.0	738.0	738.0	738.0	733.0	733.0	733.0	733.0
1. Inlet air T. (F)	76	80	81	82	81	84	83	92	90	88	87
2. Inlet air wet bulb T. (F)	62	63	68	65	70	67	68	73	73	71	73
3. Inlet manifold T. (F)	140	141	101	140	102	141	103	152	109	151	108
4. Fuel T. (F)	115	106	104	103	103	103	104	104	104	103	104
5. Oil T. (F)	167	153	180	196	172	204	191	216	192	210	193
6. Cooling water inlet T. (F)	158	145	159	157	145	157	147	160	144	158	144
7. Cooling water outlet T. (F)	182	172	182	182	172	181	174	182	172	182	172
8. Exhaust manifold T. (F)	885	369	874	852	371	841	375	908	372	889	373
9. Exhaust T. shielded (F)	938	404	931	911	401	900	402	958	407	946	408
10.Thermocouple shield T. (F)	910	404	923	903	400	893	401	950	407	938	407
11.Exhaust T. unshielded (F)	947	410	939	919	408	908	409	967	413	956	414
13.Building cooling water inlet T. (F)	63	62	62	62	62	62	62	62	63	62	62
14.Building cooling water outlet T. (F)	84	101	84	84	104	84	108	82	100	83	100
Pressure difference of LFE (in H2O)	2.14	1.92	2.14	2.14	1.94	2.15	1.94	2.20	1.97	2.20	1.96
Boost pressure (Psi)	3.2	0.0	3.2	3.1	3.0	3.0	0.0	3.2	0.0	3.2	0.0
Oil pressure (Psi)	48.0	50.0	47.5	48.0	50.0	48.0	50.0	47.5	50.0	47.0	50.0
Exhaust gas pressure (Psi)	3.2	1.8	3.2	3.0	1.8	3.0	1.8	3.2	1.8	3.2	1.6
Static pressure of 1st dilution tunnel (Psi)	32.5	28.5	32.0	32.5	28.5	32.5	29.5	32.0	28.5	32.0	28.5
1st Dilution pressure transducer volt.(mV)	2.70	2.29	2.57	2.66	2.29	2.67	2.42	2.69	2.29	2.6950	2.3200
Static T. of 1st dilution tunnel(F)	69	68	69	69	69	69	69	69	69	69	69
15. Static T. of 1st dilution tunnel(F)	108	91	112	110	91	111	90	114	90	112	89
17. Filter chamber T. (F)	98	96	97	101	97	100	98	113	99	106	98
18. Sample T. at Roots (F)	131	93	132	129	93	128	92	134	95	132	95
19. Diluted exhaust gas T. at point 1 (F)	148	100	146	146	99	146	100	146	103	146	102
20. Diluted exhaust gas T. at point 2 (F)											
Total sample volume (Ft^3)	105.79	105.76	105.60	105.48	105.66	105.64	105.77	105.64	105.77	105.38	105.66
CO (ppm)	552.28	440.48	490.76	453.94	431.09	375.43	552.28	413.64	572.26	476.02	552.82
NO (ppm)	1903.92	300.73	1990.02	1871.17	291.84	1831.43	1903.92	296.78	1889.55	310.40	1853.50
NOx (ppm)	2299.50	387.83	2408.69	2338.82	379.00	2295.91	2299.50	393.54	2231.80	379.97	2161.60
HC (ppm)	61.05	74.84	58.31	51.74	57.14	45.84	61.05	50.29	65.28	86.30	62.34
CO2 %	15.02	3.05	14.64	15.19	3.08	13.89	15.02	3.05	15.12	3.05	15.47
O2 %	8.28	15.41	7.85	8.05	14.56	7.99	8.28	13.98	7.04	13.71	7.10
Filter A serial No.	A/D1400/100	A/M20/1400/020	A/M20/1400/100	A/M50/1400/100	A/M70/1400/100	A/M50/1400/100	A/M70/1400/020	A/D1400/100	A/D1400/100	A/M20/1400/100	A/M20/1400/020
Filter B serial No.	B/D1400/100	B/M20/1400/020	B/M20/1400/100	B/M50/1400/100	B/M70/1400/100	B/M50/1400/100	B/M70/1400/020	B/D1400/100	B/D1400/100	B/M20/1400/100	B/M20/1400/020
Filter A weight before sampling (mg)	323.75	320.22	326.33	331.32	323.17	325.06	316.94	324.98	325.38	325.63	325.53
Filter B weight before sampling (mg)	325.90	324.86	321.77	320.94	325.48	319.31	322.65	321.33	319.93	320.82	323.63
Filter A weight after sampling(mg)(24hr)	352.26	334.29	350.33	352.62	348.18	347.40	348.25	352.53	341.83	352.30	346.76
Filter B weight after sampling(mg)(24hr)	326.22	326.36	322.36	321.66	329.12	320.17	328.48	321.62	321.99	321.19	327.99
Filter A weight after sampling(mg)(48hr)	352.45	333.29	350.36	352.12	344.14	346.30	343.97	352.55	341.45	352.29	245.30
Filter B weight after sampling(mg)(48hr)	326.23	326.15	322.29	327.65	328.21	320.06	326.72	321.62	321.36	321.15	325.70
Wt. of filter A w/ thimble B. extraction (g)	22.412185	22.392350	23.002015	22.881845	23.221760	22.528620	22.392350	22.412185	22.869745	23.950220	22.536360
Wt. of filter A w/ thimble A. extraction (g)	22.408730	22.381010	22.998310	22.875980	23.205330	22.521525	22.381010	22.856740	22.408730	23.246500	22.519405
Extraction time	4hr 20'	4hr 5'	4hr 9'	4hr 3'	4hr 3'	4hr 3'	4hr 24'	4hr 5'	4hr 5'	4hr 2'	4hr 2'
Emission and pressure data file names	1R.100	1RM2.100	1RM2.100	1RM5.100	1RM5.20	1RM5.20	1RM7.100	1RM7.100	2R.20	2R.100	2RM2.20
	1E1.100	1E1M2.100	1E1M2.100	1E1M5.100	1E1M5.20	1E1M5.20	1E1M7.20	1E1M7.100	2E1.100	2E1.20	2E1M2.20
	1E2.100	1E2M2.100	1E2M2.100	1E2M5.100	1E2M5.20	1E2M5.20	1E2M7.20	1E2M7.100	2E2.100	2E2.20	2E2M2.20
	1P.100	1PM2.100	1PM2.100	1PM5.100	1PM5.20	1PM5.20	1PM7.20	1PM7.100	2P.100	2P.20	2PM2.20
	1PG.100	1PGM2.100	1PGM2.100	1PGM5.100	1PGM5.20	1PGM5.20	1PGM7.20	1PGM7.100	2PG.100	2PG.20	2PGM2.20

Date	8/17/94	8/17/94	8/17/94	8/17/94	8/17/94	8/17/94	8/17/94	8/17/94	8/16/94	8/16/94	8/16/94	8/16/94
Fuel	70%MS+DH	70%MS+DH	50%MS+DH	50%MS+DH	20%MS+DH	20%MS+DH	Diesel	Diesel	70%MS+DH	70%MS+DH	50%MS+DH	50%MS+DH
Engine speed (rpm)	1400	1400	1400	1400	1400	1400	1400	1400	1400	1400	1400	1400
% of rated load	20	100	20	100	20	100	20	100	20	100	20	100
Brake torque (ft.lbf)	40.00	203.00	40.25	207.25	41.50	211.75	41.75	215.75	40.25	203.50	40.00	206.00
Time (sec.)	900.42	900.32	900.43	900.20	900.21	900.41	900.36	900.13	900.29	900.37	900.46	900.43
Fuel weight (kg)	0.80	2.52	0.78	2.49	0.75	2.46	0.73	2.45	0.80	2.52	0.78	2.50
Coolant counts	324.83	94202	33166	98924	33020	103349	32271	101840	32699	88628	33378	91626
Ambient air T. (F)	76	76	76	76	76	76	76	76	75	75	75	75
Patm (mmHg)	733.0	733.0	733.0	733.0	733.0	733.0	733.0	733.0	733.0	733.0	733.0	733.0
1. Inlet air T. (F)	91	89	88	90	86	86	83	82	79	80	87	88
2. Inlet air wet bulb T. (F)	76	77	76	75	73	73	72	71	69	68	70	78
3. Inlet manifold T. (F)	111	148	109	148	107	147	105	146	100	140	106	150
4. Fuel T. (F)	104	104	104	102	102	98	103	104	103	103	102	104
5. Oil T. (F)	187	210	188	212	183	203	168	212	191	216	192	217
6. Cooling water inlet T. (F)	143	158	144	159	144	160	144	159	144	157	145	158
7. Cooling water outlet T. (F)	172	182	172	182	172	182	172	182	172	182	172	182
8. Exhaust manifold T. (F)	372	853	373	869	371	892	365	902	365	842	375	863
9. Exhaust T. shielded (F)	403	912	403	922	405	938	399	950	396	900	402	925
10.Thermocouple shield T. (F)	402	904	402	915	404	930	398	942	395	893	401	918
11.Exhaust T. unshielded (F)	409	918	409	930	412	947	406	961	402	907	407	934
13.Building cooling water inlet T. (F)	62	62	62	62	62	62	63	62	62	62	62	62
14.Building cooling water outlet T. (F)	97	82	99	82	98	83	100	82	103	84	102	83
Pressure difference of LFE (in H2O)	1.98	2.17	1.97	2.17	1.96	2.17	1.95	2.17	1.93	2.14	1.96	2.19
Boost pressure (Psi)	0.0	3.0	0.0	3.0	0.0	3.2	0.0	3.2	0.0	3.0	0.0	3.0
Oil pressure (Psi)	50.0	47.5	51.0	47.5	50.0	47.0	50.0	47.0	50.0	47.0	51.0	47.5
Exhaust gas pressure (Psi)	1.6	3.0	1.6	3.0	1.7	3.1	1.8	3.2	1.8	3.0	1.6	3.1
Static pressure of 1st dilution tunnel (Psi)	27.5	31.5	27.6	31.0	28.5	31.0	28.5	31.0	28.5	32.0	27.5	32.0
1st Dilution pressure transducer volt.(mV)	2.29	2.64	2.29	2.61	2.36	2.61	2.41	2.64	2.27	2.66	2.30	2.66
15. Static T. of 1st dilution tunnel(F)	70	70	69	70	70	70	69	69	68	69	69	69
17. Filter chamber T. (F)	92	112	92	114	92	113	91	111	86	111	88	109
18. Sample T. at Roots (F)	102	105	103	107	103	107	98	103	86	101	96	101
19. Diluted exhaust gas T. at point 1 (F)	96	131	95	133	95	134	95	135	92	129	94	130
20. Diluted exhaust gas T. at point 2 (F)	104	146	103	146	105	146	105	146	100	146	100	146
Total sample volume (Ft^3)	105.50	105.53	105.52	105.55	105.55	105.34	105.69	105.27	105.16	105.41	105.16	105.73
CO (ppm)	363.09	382.85	360.42	355.05	382.66	393.65	423.50	421.81	442.28	450.15	354.19	464.64
NO (ppm)	328.82	2046.38	323.25	1991.87	311.02	2031.40	302.16	2075.79	286.86	1990.94	262.66	1914.62
NOx (ppm)	387.69	2366.89	389.45	2349.39	382.69	2398.35	371.36	2358.72	354.55	2215.71	326.28	2169.15
HC (ppm)	52.51	45.41	59.67	50.82	73.49	53.08	87.15	56.64	56.45	56.73	60.43	58.78
CO2 %	2.95	14.45	3.17	14.70	3.02	15.49	3.06	16.47	3.16	14.07	2.96	14.70
O2 %	13.67	7.42	14.20	7.35	13.67	7.10	14.17	7.41	15.67	8.12	14.49	7.46
Filter A serial No.	A/M70/1400/20	A/M70/1400/100	A/M50/1400/20	A/M50/1400/100	A/M20/1400/20	A/M20/1400/100	A/D/1400/20	A/D/1400/100	A/M70/1400/20	A/M70/1400/100	A/M50/1400/20	A/M50/1400/100
Filter B serial No.	B/M70/1400/20	B/M70/1400/100	B/M50/1400/20	B/M50/1400/100	B/M20/1400/20	B/M20/1400/100	B/D/1400/20	B/D/1400/100	B/M70/1400/20	B/M70/1400/100	B/M50/1400/20	B/M50/1400/100
Filter A weight before sampling (mg)	318.68	326.41	321.28	331.78	314.60	333.92	326.38	319.41	322.08	323.23	321.14	325.05
Filter B weight before sampling (mg)	318.54	324.28	323.05	324.77	318.25	324.84	322.35	324.90	320.53	318.99	321.93	323.69
Filter A weight after sampling(mg)(24hr)	354.45	347.14	349.67	351.53	335.22	359.68	343.13	348.63	359.86	344.47	350.91	347.78
Filter B weight after sampling(mg)(24hr)	325.79	325.22	327.54	325.52	320.81	325.19	324.10	325.18	326.43	319.73	326.20	324.38
Filter A weight after sampling(mg)(48hr)	350.22	346.35	345.65	351.57	333.61	359.46	342.32	348.77	356.05	343.13	348.51	347.30
Filter B weight after sampling(mg)(48hr)	322.60	325.06	326.16	325.35	320.50	325.11	324.00	325.14	324.39	319.66	325.16	324.34
Wt. of filter A w/ thimble B. extraction (g)	23.292665	23.226845	23.240835	23.002995	22.516145	22.419055	22.993425	22.999770	23.233615	23.284110	22.538295	23.289470
Wt. of filter A w/ thimble A. extraction (g)	23.262420	23.220900	23.220765	22.998515	22.499695	22.415655	22.979510	22.996600	23.204785	23.277380	22.515055	23.283515
Extraction time	5hr44'	5hr44'	4hr5'	4hr5'	4hr5'	4hr5'	4hr3'	4hr3'	5hr2'	5hr2'	4hr 2'	4hr 2'
Emission and pressure data file names	3RM7.20	3RM7.100	3RM5.20	3RM5.100	3RM2.20	3RM2.100	3R.20	3R.100	2RM7.20	2RM7.100	2RM5.20	2RM5.100
	3E1M7.20	3E1M7.100	3E1M5.20	3E1M5.100	3E1M2.20	3E1M2.100	3E1.20	3E1.100	2E1M7.20	2E1M7.100	2E1M5.20	2E1M5.100
	3E2M7.20	3E2M7.100	3E2M5.20	3E2M5.100	3E2M2.20	3E2M2.100	3E2.20	3E2.100	2E2M7.20	2E2M7.100	2E2M5.20	2E2M5.100
	3PM7.20	3PM7.100	3PM5.20	3PM5.100	3PM2.20	3PM2.100	3P.20	3P.100	2PM7.20	2PM7.100	2PM5.20	2PM5.100
	3PGM7.20	3PGM7.100	3PGM5.20	3PGM5.100	3PGM2.20	3PGM2.100	3PG.20	3PG.100	2PGM7.20	2PGM7.100	2PGM5.20	2PGM5.100

Date	8/31/94	8/31/94	8/31/94	8/31/94	8/31/94	8/31/94	9/1/94	9/1/94	9/1/94	9/5/94	9/5/94	9/5/94
Fuel	Diesel	20%iP+DL	50%iP+DL	Diesel	20%iP+DL	50%iP+DL	Diesel	20%iP+DL	50%iP+DL	Diesel	20%MS+DL	50%MS+DL
Engine speed (rpm)	1400	1400	1400	1400	1400	1400	1400	1400	1400	1400	1400	1400
% of rated load	100	100	100	100	100	100	100	100	100	100	100	100
Brake torque (ft.lbf)	218.25	211.00	198.25	213.00	208.25	203.25	217.25	209.25	196.00	215.25	214.00	208.25
Time (sec.)	900.44	900.77	900.68	900.73	900.69	900.66	900.74	904.74	900.75	900.88	900.97	900.83
Fuel weight (kg)	2.44	2.47	2.37	2.41	2.41	2.43	2.45	2.45	2.35	2.43	2.47	2.49
Coolant counts	107076	106417	98290	104584	103197	101659	102349	98896	90663	102188	101267	99237
Ambient air T. (F)	76	76	76	76	76	76	75	75	75	73	73	73
Patm (mmHg)	740.0	740.0	740.0	740.0	740.0	740.0	742.0	742.0	742.0	737.0	737.0	737.0
1. Inlet air T. (F)	76	84	83	84	84	85	80	81	80	79	83	85
2. Inlet air wet bulb T. (F)	62	64	65	65	66	66	62	63	63	69	71	72
3. Inlet manifold T. (F)	140	142	138	144	143	141	142	141	136	141	143	142
4. Fuel T. (F)	105	104	104	103	104	106	106	103	107	105	102	105
5. Oil T. (F)	179	179	177	210	215	214	154	166	165	209	214	212
6. Cooling water inlet T. (F)	160	159	156	159	158	158	159	157	156	158	158	157
7. Cooling water outlet T. (F)	181	181	179	181	180	180	181	180	179	181	180	180
8. Exhaust manifold T. (F)	901	903	866	907	896	876	907	898	821	920	903	882
9. Exhaust T. shielded (F)	935	922	888	934	918	901	939	917	878	936	929	909
10.Thermocouple shield T. (F)	927	915	881	927	911	895	931	910	872	927	921	901
11. Exhaust T. unshielded (F)	944	930	894	942	926	907	948	926	884	943	936	915
13.Building cooling water inlet T. (F)	62	62	62	62	62	62	62	62	62	63	63	63
14.Building cooling water outlet T. (F)	83	82	81	82	83	82	81	81	81	82	82	81
Pressure difference of LFE (in H2O)	2.11	2.11	2.09	2.13	2.12	2.10	2.12	2.10	2.09	2.12	2.12	2.12
Boost pressure (Psi)	3.2	3.2	3.0	3.2	3.2	3.0	3.3	3.2	3.0	3.3	3.2	3.2
Oil pressure (Psi)	47.0	47.0	47.0	47.0	47.0	47.0	47.0	47.0	47.0	47.0	47.0	47.0
Exhaust gas pressure (Psi)	3.2	3.2	3.0	3.2	3.2	3.0	3.2	3.2	3.0	3.2	3.2	3.1
Static pressure of 1st dilution tunnel (Psi)												
1st Dilution pressure transducer volt (mV)	2.75	2.74	2.75	2.76	2.75	2.76	2.75	2.76	2.76	2.77	2.78	2.76
15. Static T. of 1st dilution tunnel(F)	69	69	69	69	69	70	69	69	69	68	68	68
17. Filter chamber T. (F)	115	119	115	117	117	117	109	110	115	110	110	110
18. Sample T. at Roots (F)	110	113	113	117	116	112	94	110	110	95	97	99
19. Diluted exhaust gas T. at point 1 (F)	129	128	125	129	128	127	129	128	124	131	130	129
20. Diluted exhaust gas T. at point 2 (F)	154	141	138	145	143	141	146	145	144	149	148	145
Total sample volume (Ft^3)	105.46	105.41	105.07	105.27	105.27	105.44	105.39	105.58	105.78	105.78	105.66	105.87
CO (ppm)	346.24	309.80	419.13	461.89	428.99	360.25	367.70	352.43	303.39	411.45	330.00	285.04
NO (ppm)	1953.35	2060.39	1933.91	1931.23	2032.72	2011.97	1902.01	1933.42	1939.35	1971.88	1855.43	1872.79
NOx (ppm)	2393.80	2486.54	2489.71	2376.22	2607.23	2594.38	2349.47	2391.33	2405.94	2288.35	2218.76	2340.93
HC (ppm)	55.33	44.83	36.85	47.20	35.34	29.66	43.13	30.95	32.99	36.38	42.11	36.28
CO2 %	14.12	13.62	12.88	13.57	13.06	13.05	15.58	14.06	12.91	15.17	16.22	14.62
O2 %	7.97	7.87	8.67	7.79	7.95	8.02	8.04	8.45	8.55	7.88	7.73	7.97
Filter A serial No.	A/D/1400/1002	A/IP20/1400/1002	A/IP50/1400/1002	A/D/1400/1004	A/IP20/1400/1004	A/IP50/1400/1004	A/D/1400/1006	A/IP20/1400/1006	A/IP50/1400/1006	A/D/1400/N1	A/M20/1400/N1	A/M50/1400/N1
Filter B serial No.	B/D/1400/1002	B/IP20/1400/1002	B/IP50/1400/1002	B/D/1400/1004	B/IP20/1400/1004	B/IP50/1400/1004	B/D/1400/1006	B/IP20/1400/1006	B/IP50/1400/1006	B/D/1400/N1	B/M20/1400/N1	B/M50/1400/N1
Filter A weight before sampling (mg)	319.62	319.27	320.57	324.37	315.33	316.21	318.87	313.74	323.85	328.95	325.64	325.65
Filter B weight before sampling (mg)	318.00	319.04	323.24	320.21	317.90	316.01	324.47	320.69	319.66	319.74	326.39	324.12
Filter A weight after sampling(mg)(24hr)	341.23	338.21	335.20	346.54	332.60	331.00	343.40	330.73	339.36	353.96	347.20	343.95
Filter B weight after sampling(mg) (24hr)	318.18	319.50	323.65	320.44	318.21	316.29	324.86	320.99	320.23	319.99	326.80	324.64
Filter A weight after sampling(mg)(48hr)	341.09	338.20	335.24	346.52	332.63	330.91	343.41	330.69	339.07	353.86	347.16	343.90
Filter B weight after sampling(mg) (48hr)	318.19	319.49	323.67	320.41	318.27	316.44	324.74	320.97	320.15	319.98	326.71	324.59
Wt. of filter A w/ thimble B. extraction (g)	23.222595	22.865750	22.530590	22.406650	23.230865	22.861325	23.286430	22.514485	23.237235	22.537580	22.998655	23.286320
Wt. of filter A w/ thimble A. extraction (g)	23.219275	22.862110	22.523295	22.403335	23.227710	22.855195	23.282625	22.511370	23.229540	22.534190	22.994645	23.280835
Extraction time	4hr1'	4hr1'	4hr6'	4hr6'	4hr1'	4hr1'	4hr10'	4hr10'	4hr2'	4hr16'	4hr16'	5hr4'
Emission and pressure data file names	1R.100	1R12.100	1R15.100	2R.100	2R12.100	2R15.100	3R.100	3R12.100	3R15.100	1R.N	1RM2.N	1RM5.N
	1E1.100	1E112.100	1E115.100	2E1.100	2E112.100	2E115.100	3E1.100	3E112.100	3E115.100	1E1.N	1E1M2.N	1E1M5.N
	1E2.100	1E212.100	1E215.100	2E2.100	2E212.100	2E215.100	3E2.100	3E212.100	3E215.100	1E2.N	1E2M2.N	1E2M5.N
	1P.100	1P12.100	1P15.100	2P.100	2P12.100	2P15.100	3P.100	3P12.100	3P15.100	1P.N	1PM2.N	1PM5.N
	1PG.100	1PG12.100	1PG15.100	2PG.100	2PG12.100	2PG15.100	3PG.100	3PG12.100	3PG15.100	1PG.N	1PGM2.N	1PGM5.N

Date	9/5/94	9/5/94	9/5/94	9/5/94	9/5/94	9/5/94	10/15/94	10/15/94	10/15/94	10/15/94	10/15/94	10/15/94
Fuel	Diesel	20%MS+DL	50%MS+DL	Diesel	20%MS+DL	50%MS+DL	Diesel	20%WMS+DL	50%WMS+DL	Diesel	20%WMS+DL	50%WMS+DL
Engine speed (rpm)	1400	1400	1400	1400	1400	1400	1400.0000	1400.0000	1400.0000	1400.0000	1400.0000	1400.0000
% of rated load	100	100	100	100	100	100	100.0000	100.0000	100.0000	100.0000	100.0000	100.0000
Brake torque (ft.lbf)	215.50	212.75	206.75	214.75	212.50	207.25	218.2500	215.2500	209.0000	218.0000	214.0000	209.0000
Time (sec)	900.62	900.11	905.99	901.86	900.17	900.64	901.9200	899.5200	900.9700	903.1900	900.6900	900.8900
Fuel weight (kg)	2.42	2.45	2.50	2.42	2.45	2.49	2.4767	2.4900	2.5300	2.4800	2.4900	2.5200
Coolant counts	103314	103083	101273	104835	103086	100940	109627	106352	103198	106896	105496	102230
Ambient air T. (F)	73	73	73	73	73	73	77.0000	77.0000	77.0000	77.0000	77.0000	77.0000
Patm (mmHg)	737.0	737.0	737.0	737.0	737.0	737.0	736.0000	736.0000	736.0000	736.0000	736.0000	736.0000
1. Inlet air T. (F)	89	89	88	95	89	82	79.5000	81.0000	85.0000	86.0000	84.0000	89.0000
3. Inlet air wet bulb T. (F)	72	71	70	71	69	69	64.0000	64.5000	66.5000	66.5000	66.0000	67.0000
3. Inlet manifold T. (F)	150	151	148	154	149	144	139.5000	139.0000	137.0000	140.5000	138.0000	138.0000
4. Fuel T. (F)	106	105	105	105	105	103	104.5000	103.3000	105.0500	104.9500	105.9500	104.0500
5. Oil T. (F)	217	217	213	206	206	206	215.5000	215.0000	213.0500	215.0000	214.5000	213.5000
6. Cooling water inlet T. (F)	159	159	157	159	158	157	159.0000	157.0000	156.0000	157.0000	156.0000	156.0000
7. Cooling water outlet T. (F)	181	181	180	182	180	180	180.0000	179.0000	178.0000	179.0000	178.5000	178.0000
8. Exhaust manifold T. (F)	921	913	889	931	910	891	892.5000	878.5000	858.0000	890.5000	876.5000	855.5000
9. Exhaust T. shielded (F)	947	939	917	953	935	911	942.0000	931.0000	911.0000	945.5000	930.0000	912.0000
10.Thermocouple shield T. (F)	939	931	910	945	927	904	933.0000	923.0000	902.5000	937.0000	922.0000	904.5000
11.Exhaust T. unshielded (F)	956	948	926	963	943	920	951.5000	940.0000	918.5000	955.0000	939.5000	921.0000
13.Building cooling water inlet T. (F)	63	63	63	63	62	62	60.0000	60.0000	60.0000	60.0000	60.0000	60.0000
14.Building cooling water outlet T. (F)	81	81	81	82	81	81	81.0000	80.0000	79.0000	78.5000	78.0000	78.0000
Pressure difference of LFE (in H2O)	2.15	2.15	2.14	2.17	2.15	2.12	2.1270	2.1219	2.1172	2.1378	2.1197	2.1237
Boost pressure (Psi)	3.30	3.20	3.10	3.30	3.20	3.10	3.4000	3.2000	3.2000	3.3000	3.2000	3.2000
Oil pressure (Psi)	47.00	47.00	47.00	47.00	47.00	47.00	47.0000	47.0000	47.0000	47.0000	47.0000	47.0000
Exhaust gas pressure (Psi)	3.20	3.20	3.00	3.20	3.20	3.20	3.3000	3.2000	3.2000	3.3000	3.2000	3.2000
Static pressure of 1st dilution tunnel (Psi)				28.50		32.50						
1st Dilution pressure transducer volt (mV)	2.75	2.74	2.73	2.76	2.76	2.75	2.7600	2.7600	2.7700	2.7900	2.7950	2.7850
15. Static T. of 1st dilution tunnel(F)	68	68	68	68	68	68	68.0000	68.0000	68.0000	67.0000	68.0000	67.0000
17. Filter chamber T. (F)	114	112	113	113	111	112	109.5000	109.2500	106.0600	107.5000	105.5900	108.5000
18. Sample T. at Roots (F)	103	106	104	106	108	102	95.5900	101.0000	95.7500	98.0000	97.7500	96.2500
19. Diluted exhaust gas T. at point 1 (F)	132	130	129	131	130	128	130.0000	129.0000	126.0000	130.0000	129.0000	127.0000
20. Diluted exhaust gas T. at point 2 (F)	145	142	142	143	145	144	149.0000	149.5000	142.0000	150.0000	149.0000	144.0000
Total sample volume (Ft^3)	105.86	105.95	106.83	106.18	105.63	105.81	105.2240	105.1148	105.6111	105.9481	106.2222	105.9148
CO (ppm)	330.59	328.93	268.55	332.12	287.18	242.31	505.0711	474.1151	449.7797	515.5451	501.6269	458.2632
NO (ppm)	2008.79	1970.75	1958.33	1965.25	2021.43	1959.60	1933.6280	1964.4710	1894.8810	2006.5350	1901.3030	1805.3170
NOx (ppm)	2411.87	2430.85	2447.65	2442.28	2517.87	2415.82	2311.3690	2347.9210	2394.2200	2278.6840	2320.8190	2359.7780
HC (ppm)	45.27	41.23	37.34	37.61	36.89	31.93	57.5925	52.7127	44.6315	57.8289	53.2710	45.9944
CO2 %	15.12	14.86	15.53	15.23	16.08	14.80	9.5219	9.1454	8.9349	9.7372	8.2159	8.5420
O2 %	7.29	7.33	7.80	7.39	7.62	8.02	8.2556	8.1838	8.3000	7.9074	8.0273	8.0130
Filter A serial No.	A/D/1400/N2	A/M20/1400/N2	A/M50/1400/N2	A/D/1400/N3	A/M20/1400/N3	A/M50/1400/N3	A/D/1400/1	A/WM20/1400/1	A/WM50/1400/1	A/D/1400/2	A/WM20/1400/2	A/WM50/1400/2
Filter B serial No.	B/D/1400/N2	B/M20/1400/N2	B/M50/1400/N2	B/D/1400/N3	B/M20/1400/N3	B/M50/1400/N3	B/D/1400/1	B/WM20/1400/1	B/WMS50/1400/1	B/D/1400/2	B/WMS20/1400/2	B/WMS50/1400/2
Filter A weight before sampling (mg)	321.95	319.99	321.03	320.99	323.09	325.11	315.6650	319.4400	322.4500	325.7150	328.9150	320.6700
Filter B weight before sampling (mg)	320.11	322.63	321.35	322.54	319.78	322.88	322.6250	321.0350	316.1450	324.2050	314.2600	320.8000
Filter A weight after sampling(mg)(24hr)	343.84	341.37	338.79	343.00	341.44	341.07	344.9400	344.3600	345.1050	353.1050	354.4000	344.4500
Filter B weight after sampling(mg)(24hr)	320.39	323.13	321.94	342.58	319.99	323.38	322.9000	321.4900	316.9800	324.4350	314.7400	321.6150
Filter A weight after sampling(mg)(48hr)	343.81	341.40	321.85	342.97	341.39	341.07	344.88	344.31	344.97	353.10	353.34	344.22
Filter B weight after sampling(mg)(48hr)	320.38	323.04	338.66	322.63	323.31	323.31	322.84	321.40	316.90	324.38	314.68	321.50
Wt of filter A w/ thimble B. extraction (g)	22.536590	22.222865	22.990275	23.224540	22.401320	23.239195	22.997395	23.243260	22.537650	22.537220	23.298055	23.225965
Wt of filter A w/ thimble A. extraction (g)	22.532860	23.219010	22.984905	23.221110	22.398010	23.234735	22.993880	23.239060	22.529790	22.533770	23.293985	23.218025
Extraction time	4hr1'	4hr1'	4hr2'	4hr2'	4hr2'	4hr4'	4hr5'	4hr5'	4hr21'	4hr5'	4hr5'	4hr5'
Emission and pressure data file names	2R.N	2RM2.N	2RM5.N	3R.N	3RM2.N	3RM5.N	1R.100	1RW2.100	1RW5.100	2R.100	2RW2.100	2RW5.100
	2E1.N	2E1M2.N	2E1M5.N	3E1.N	3E1M2.N	3E1M5.N	1E1.100	1E1W2.100	1E1W5.100	2E1.100	2E1W2.100	2E1W5.100
	2E2.N	2E2M2.N	2E2M5.N	3E2.N	3E2M2.N	3E2M5.N	1E2.100	1E2W2.100	1E2W5.100	2E2.100	2E2W2.100	2E2W5.100
	2P.N	2PM2.N	2PM5.N	3P.N	3PM2.N	3PM5.N	1P.100	1PW2.100	1PW5.100	2P.100	2PW2.100	2PW5.100
	2PG.N	2PGM2.N	2PGM5.N	3PG.N	3PGM2.N	3PGM5.N	1PG.100	1PGW2.100	1PGW5.100	2PG.100	2PGW2.100	2PGW5.100

Date	10/15/94	10/15/94	10/15/94
Fuel	Diesel	20%WMS+DL	50%WMS+DL
Engine speed (rpm)	1400	1400	1400
% of rated load	100	100	100
Brake torque (ft.lbf)	217.25	213.75	208.75
Time (sec.)	900.16	900.56	900.61
Fuel weight (kg)	2.47	2.49	2.52
Coolant counts	107287	106936	103812
Ambient air T. (F)	77	77	77
Patm (mmHg)	736.0	736.0	736.0
1. Inlet air T. (F)	87	91	88
2. Inlet air wet bulb T. (F)	68	68	68
3. Inlet manifold T. (F)	142	141	138
4. Fuel T. (F)	105	104	106
5. Oil T. (F)	216	215	214
6. Cooling water inlet T. (F)	158	158	156
7. Cooling water outlet T. (F)	180	179	178
8. Exhaust manifold T. (F)	895	882	858
9. Exhaust T. shielded (F)	948	935	914
10.Thermocouple shield T. (F)	939	928	906
11.Exhaust T. unshielded (F)	957	945	922
13.Building cooling water inlet T. (F)	60	60	60
14.Building cooling water outlet T. (F)	79	79	79
Pressure difference of LFE (in H2O)	2.14	2.14	2.12
Boost pressure (Psi)	3.3	3.2	3.2
Oil pressure (Psi)	47.0	47.0	47.0
Exhaust gas pressure (Psi)	3.3	3.2	3.2
Static pressure of 1st dilution tunnel (Psi)			
1st Dilution pressure transducer volt.(mV)	2.79	2.79	2.79
15. Static T. of 1st dilution tunnel(F)	68	68	68
17. Filter chamber T. (F)	115	109	110
18. Sample T. at Roots (F)	110	103	99
19. Diluted exhaust gas T. at point 1 (F)	130	129	127
20.Diluted exhaust gas T. at point 2 (F)	147	145	144
Total sample volume (Ft^3)	105.58	105.54	105.90
CO (ppm)	575.47	517.21	466.96
NO (ppm)	1990.09	1962.35	2022.84
NOx (ppm)	2324.49	2390.76	2530.58
HC (ppm)	53.91	46.46	38.93
CO2 %	8.37	8.30	7.99
O2 %	7.67	7.81	8.02
Filter A serial No.	A/D/1400/3	A/WM20/1400/3	A/WM50/1400/3
Filter B serial No.	B/D/1400/3	B/WM20/1400/3	B/WM50/1400/3
Filter A weight before sampling (mg)	323.61	326.29	326.89
Filter B weight before sampling (mg)	330.34	325.15	326.72
Filter A weight after sampling(mg)(24hr)	353.35	351.75	349.93
Filter B weight after sampling(mg) (24hr)	330.67	325.73	327.49
Filter A weight after sampling(mg)(48hr)	353.31	351.64	349.91
Filter B weight after sampling(mg) (48hr)	330.64	325.66	327.35
Wt. of filter A w/ thimble B. extraction (g)	22.413530	22.882735	23.002080
Wt. of filter A w/ thimble A. extraction (g)	22.409975	22.878510	23.994580
Extraction time	4hr2'	4hr5'	4hr3'
Emission and pressure data file names	3R.100	3RW2.100	3RW5.100
	3E1.100	3E1W2.100	3E1W5.100
	3E2.100	3E2W2.100	3E2W5.100
	3P.100	3PW2.100	3PW5.100
	3PG.100	3PGW2.100	3PGW5.100